Composite Structures 96 (2013) 799–823

Contents lists available at SciVerse ScienceDirect

Composite Structures

journal homepage: www.elsevier.com/locate/compstruct

Free vibration response of functionally graded thick plates with shear and normal deformations effects

D.K. Jha [a], Tarun Kant [b,*], R.K. Singh [c]

[a] Arch. & Civil Engg. Division, Bhabha Atomic Research Centre, Mumbai 400 085, India
[b] Department of Civil Engineering, Indian Institute of Technology Bombay, Powai, Mumbai 400 076, India
[c] Reactor Safety Division, Bhabha Atomic Research Centre, Mumbai 400 085, India

ARTICLE INFO

Article history:
Available online 8 October 2012

Keywords:
Higher order shear and normal deformations theory
Functionally graded plates
Material gradient index
Navier solution
Free vibration
Natural frequency

ABSTRACT

Free vibration response of functionally graded (FG) elastic, rectangular, and simply (diaphragm) supported plates is presented based on higher order shear/shear-normal deformations theories (HOSTs/HOSNTs). The theoretical models are based on Taylor's series expansion of in-plane and transverse displacements in thickness coordinate defining the plate deformations. Some of these advanced models account for the effects of transverse shear deformations, transverse normal deformation and non-linear variation of in-plane displacements through plate's thickness. Functionally graded materials (FGMs) are idealized as continua with mechanical properties changing smoothly with respect to spatial coordinates. The material properties of FG plates are assumed here to be varying through thickness of plate in a continuous manner. Poisson's ratios of FG plates are assumed constant, but their Young's modulii and material densities vary continuously in thickness direction according to the volume fraction of constituents which is modeled as exponential and power law functions. The equations of motion are derived using Hamilton's principle on the basis of HOSTs/HOSNTs. Numerical solutions are obtained using Navier solution method. The accuracy of numerical solutions is first established through comparison with the exact three dimensional (3D) elasticity solutions and then compared with available other models' solutions. New solutions are then provided for future use.

1. Introduction

Functionally graded materials (FGMs) are the advanced materials in the family of engineering composites made of two or more constituent phases with smoothly varying composition in continuous manner [1]. Because of the continuous changes in the composition, microstructure, porosity, etc. of these advanced materials, the mechanical properties such as Young's modulus of elasticity, Poisson's ratio, shear modulus of elasticity, material density, etc. vary smoothly and continuously in preferred directions in FGMs. These advanced materials with engineered gradients of composition, structure and/or specific properties in the preferred direction/orientation are superior to homogeneous material composed of similar constituents. These materials are gaining wide applications in various branches of engineering and technology with a view to make suitable use of potential properties of the available materials in the best possible way. This has been possible through research and development in the area of mechanics of FGMs for the present day modern technologies of special nuclear components, spacecraft structural members, ceramics, composites and high temperature thermal barrier coatings, etc. These materials possess numerous advantages that make them appropriate in potential applications. It includes a potential reduction of in-plane and through-the thickness transverse stresses, improved thermal properties, high toughness, etc. FGMs consisting of metallic and ceramic components are well-known to enhance the properties of thermal-barrier systems, because cracking or de-lamination, which are often observed in conventional multi-layer systems are avoided due to the smooth transition between the properties of the components. By varying percentage contents of volume fractions of two or more materials spatially, FGMs can be formed which will have desired property gradation in spatial directions.

Suresh and Mortensen [2] furnished an excellent introduction to the fundamentals of FGMs. They published a very detailed literature review in FGM technology. Since then, numerous investigators have attempted variety of analytical, numerical methods for studying the mechanical, thermal and dynamic responses of

* Corresponding author. Tel.: +91 022 2576 7310; fax: +91 022 2576 7302.
E-mail address: tkant@civil.iitb.ac.in (T. Kant).

0263-8223/$ - see front matter © 2012 Elsevier Ltd. All rights reserved.
http://dx.doi.org/10.1016/j.compstruct.2012.09.034

structures made of FGMs. Birman and Byrd [3] have documented an exhaustive literature review of developments in FGM research addressing some recent progress in the characterization, modeling, and analysis of FGMs. Recently, Jha et al. [4] have presented a critical literature review of the recent research studies on functionally graded (FG) plates addressing thermo-elastic, vibration and stability analyses.

Pagano [5,6], Srinivas and Rao [7] and Srinivas et al. [8] developed the exact solutions of simply supported laminated plates by using 3D elasticity theory. Their benchmark solutions have proved to be very useful in assessing two-dimensional (2D) approximate plate theories by various researchers [9–11]. Their methods are valid for laminated plates and shells, where the material properties are piecewise constant, but not applicable for finding solutions of plate problems with continuous in-homogeneity of material properties such as FGMs. Cheng and Batra [12] have studied the buckling and steady-state vibrations of a simply supported FG polygonal plate resting on an elastic foundation based on Reddy's C^1 third order shear deformations theory (TSDT). Kim [13] has also developed a theoretical method based on TSDT to investigate the vibration characteristics of initially stressed FG rectangular plates in thermal environment. Vel and Batra [14] extended their previous exact 3D thermo-static analysis to the problem of free and forced vibrations of simply supported rectangular FG plates with an arbitrary variation of properties in the thickness direction. The exact solutions using the 3D elasticity solutions are then used to assess the accuracy of the results obtained by 2D plate theories, viz., classical plate theory (CPT), first order shear deformation theory (FOST) and TSDT for FG plates. They observed that there are substantial differences between the exact solutions and results obtained from the CPT even when the transverse shear and the transverse normal stresses of the plates are computed by integrating the 3D elasticity equations. These exact solutions presented by them may be considered as the benchmark results which can be used to assess the adequacy of different plate theories and other approximate methods such as the finite element method. Buckling and free vibrations of simply supported FG sandwich ceramic–metal panels were presented by Zenkour [15] extending his previous work of static analysis on such panels. Ferreira et al. [16] used the global collocation method to analyze the free vibrations of FG plates. The plate is modeled using the FOST and TSDT. They have compared their numerical solutions with the exact 3D elasticity solutions given by Vel and Batra [14], and the numerical solutions presented by Qian et al. [17]. Prakash and Ganapathi [18] have investigated the asymmetric free vibration characteristics and thermo-elastic stability of circular FG plates using a three-noded shear flexible plate finite element based on the field-consistency principle. Other recent studies on free vibration of FG plates using the 2D models of plates may be found in Bhangale and Ganesan [19], Matsunaga [20], Ebrahimi and Rastgoo [21], and Liu et al. [22]. Shahrjerdi et al. [23] have also studied the free vibration of rectangular simply supported FG plates using second order shear deformation theory (SSDT). Kumar et al. [24] have carried out the free vibration analysis of FG plates using higher order theory without enforcing zero transverse shear stress conditions on the top and bottom surfaces of the plate. Benachour et al. [25] have evaluated the natural frequency of plates made of FGMs by using a four variable refined plate theory with an arbitrary gradient considering only the four numbers of unknown functions taking account of transverse shear effects and parabolic distribution of the transverse shear strains through the thickness of the plate. Free vibration analysis of FG and composite sandwich plates are carried out by Xiang et al. [26] using a displacement model consisting of n-order polynomial satisfying zero transverse shear stress boundary conditions at the top and bottom surfaces of the plate. Neves et al. [27,28] have developed the quasi-3D sinusoidal and hyperbolic shear deformation theories for the bending and free vibration analysis of FG plates accounting for thickness deformations as well.

New methodologies need to be developed to characterize FGMs with their increase in applications in various fields, and also to analyze and design structural components, viz., beams, plates and shells made of these advanced materials with reasonably high accuracy and computational efforts. Due to the special properties exhibited by FGMs, such as high degree of anisotropy, higher load carrying capacity due to membrane–flexure coupling for preferential structural performance, the analysis based on CPT which neglects the effect of out-of-plane (transverse) stresses/strains become inadequate. FOST assumes constant states of transverse shear stresses and requires the use of shear correction coefficients to simplify the shear stresses/strains through the plate thickness in an approximate manner, which at times may become unrealistic. These limitations of the FOST necessitate the development of higher order refined theories, in which no such coefficients are required. These refined theories consider the realistic parabolic variation of transverse shear stresses through the plate thickness and warping of the transverse cross-section which is definitely essential for the analysis of FG plates. In the present article, free vibration of simply (diaphragm) supported FG plates has been carried out using a set of higher-order shear/shear-normal deformations theories. Hamilton's principle is used to obtain the governing equations of motion for the free vibration of FG plates. The Navier solution method is used as the solution technique for the free vibration problem of FG plate. The objective of present study is to study the influence of the higher order terms in the shear deformation theories of FG plate on its natural frequencies. The effect of constituent volume fraction (material grading) of FGMs on free vibration of FG plates is also captured. Natural frequencies evaluated by the present theories are presented in this article. These results are validated first with 3D elasticity solutions and then are compared with the other models' solutions available in the literature.

2. Problem description and governing equations

A linearly-elastic rectangular simply (diaphragm) supported FG plate of side dimensions a, b and uniform thickness h is considered as shown in Fig. 1.

2.1. Displacement-field

The membrane–flexure coupling phenomenon exhibited by a FG plate necessitates the use of a displacement field containing both, membrane as well as flexural deformation terms which contribute to the overall response of the plate. The displacements u, v and w of a general point (x,y,z) in the plate domain in 'X', 'Y' and 'Z' directions, respectively are given by:

$$\begin{aligned} u(x,y,z) &= u_o(x,y) + z\theta_x(x,y) + z^2 u_o^*(x,y) + z^3\theta_x^*(x,y) \\ v(x,y,z) &= v_o(x,y) + z\theta_y(x,y) + z^2 v_o^*(x,y) + z^3\theta_y^*(x,y) \\ w(x,y,z) &= w_o(x,y) + \xi_1 z\theta_z(x,y) + \xi_2 z^2 w_o^*(x,y) + \xi_3 z^3\theta_z^*(x,y) \end{aligned} \quad (1)$$

Here, the parameters u_o, v_o are the in-plane tangential displacements and w_o is the transverse displacement of a point (x,y) on the plate's middle surface. θ_x, θ_y are the rotations of the normals to the plate's middle surface ($z = 0$) about 'Y' and 'X' axes

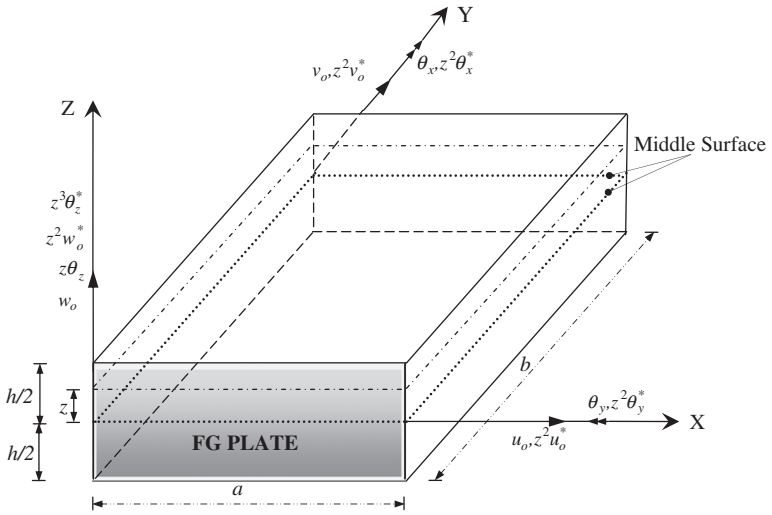

Fig. 1. Geometry of FG plate with positive set of reference axes and displacement components.

respectively. u_o^*, v_o^*, w_o^*, θ_x^*, θ_y^*, θ_z^* and θ_z are the higher order terms in the Taylor's series expansion and represent the higher order transverse cross-sectional deformation modes. The various models with their nomenclatures formulated in the present study based on higher order theories are given in Table 1.

In addition to the above higher order models, the FOST and CPT models reported in the literature are also considered for free vibration of isotropic, orthotropic and FG plates.

Model-7 'FOST' [29]

$$\begin{aligned} u(x,y,z) &= u_o(x,y) + z\theta_x(x,y) \\ v(x,y,z) &= v_o(x,y) + z\theta_y(x,y) \\ w(x,y,z) &= w_o(x,y) \end{aligned} \tag{2}$$

The FOST model has five middle surface parameters with zero transverse normal strain, and is also known as constant shear deformation theory.

Model-8 'CPT' [30]

$$\begin{aligned} u(x,y,z) &= u_o(x,y) - z\frac{\partial w_o}{\partial x}(x,y) \\ v(x,y,z) &= v_o(x,y) - z\frac{\partial w_o}{\partial y}(x,y) \\ w(x,y,z) &= w_o(x,y) \end{aligned} \tag{3}$$

This displacements definition is called CPT model, and has three middle surface parameters. The shear and normal deformations are completely ignored in this model.

2.2. Strain–displacement relations

The general linear strain–displacement relations [31] at any point within a plate are:

$$\varepsilon_x = \frac{\partial u}{\partial x}, \quad \varepsilon_y = \frac{\partial v}{\partial y}, \quad \gamma_{xy} = \frac{\partial u}{\partial y} + \frac{\partial v}{\partial x}, \quad \varepsilon_z = \frac{\partial w}{\partial z}, \quad \gamma_{yz} = \frac{\partial v}{\partial z} + \frac{\partial w}{\partial y}, \quad \gamma_{xz} = \frac{\partial u}{\partial z} + \frac{\partial w}{\partial x} \tag{4}$$

Table 1
List of displacement models based on higher order refined theories.

Model	Theory	DOF	Nomenclature	Displacement field	Transverse shear deformations (γ_{xz} and γ_{yz})	Transverse normal deformation (ε_z)
1	HOSNT	12	HOSNT12	As defined in Eq. (1) with $\xi_1 = \xi_2 = \xi_3 = 1$	Cubic	Parabolic
2	HOSNT	11	HOSNT11	As defined in Eq. (1) with $\xi_1 = \xi_2 = 1$; $\xi_3 = 0$	Parabolic	Linear
3	HOSNT	11	HOSNT11M	As defined in Eq. (1) with $\xi_1 = \xi_3 = 1$; $\xi_2 = 0$	Cubic	Parabolic
4	HOSNT	10	HOSNT10B	As defined in Eq. (1) with $\xi_1 = \xi_3 = 0$; $\xi_2 = 1$	Parabolic	Linear
5	HOSNT	10	HOSNT10M	As defined in Eq. (1) with $\xi_1 = 1$; $\xi_2 = \xi_3 = 0$	Parabolic	Constant
6	HOST	9	HOST9	As defined in Eq. (1) with $\xi_1 = \xi_2 = \xi_3 = 0$	Parabolic	Not considered

DOF: Degrees of freedom considered in the model.

Table 2
Non-dimensionalization of natural frequency.

Dependent quantity (non-dimensional parameter)	Type	Isotropic	Orthotropic	Functionally graded
Natural frequency	1	$\hat{\omega}_{mn} = \omega_{mn}(h)\sqrt{\rho/G}$	$\bar{\omega}_{mn} = \omega_{mn}(h)\sqrt{\rho/Q_{11}}$	$\tilde{\omega}_{mn} = \omega_{mn}(h)\sqrt{\rho_c/G_c}$
	2	–	–	$\tilde{\bar{\omega}}_{mn} = \omega_{mn}\left(\frac{a^2}{h}\right)\sqrt{\rho_c/E_c}$
	3	–	–	$\hat{\omega}_{mn} = \omega_{mn}(h)\sqrt{\rho_m/E_m}$
	4	–	–	$\hat{\bar{\omega}}_{mn} = \omega_{mn}\left(\frac{a^2}{h}\right)\sqrt{\rho_m/E_m}$
	5	–	–	$\omega_{mn} = \omega_{mn}(h)\sqrt{\rho_b/G_b}$

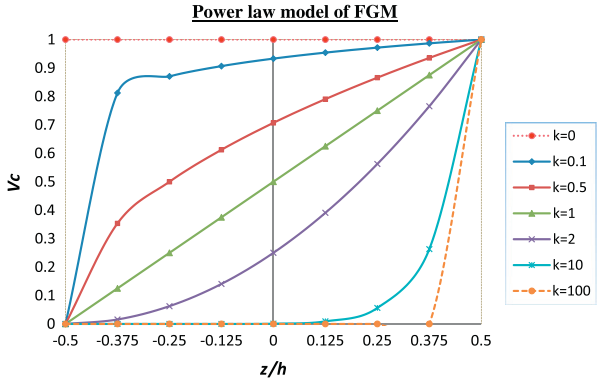

Fig. 2. Variation of ceramic volume fraction with respect to non-dimensional thickness of FG plate with different material grading index (k).

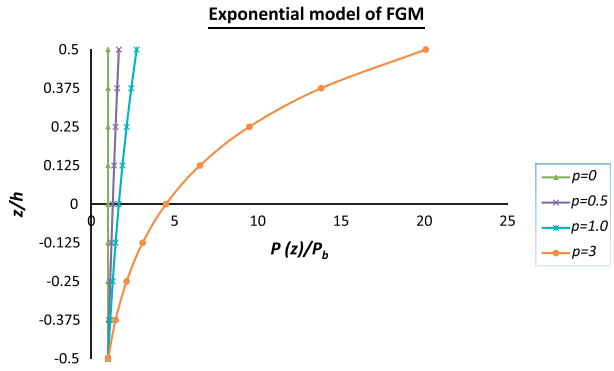

Fig. 3. Variation of material property with respect to non-dimensional thickness of FG plate with different material grading index (p).

The six quantities: three elongations $(\varepsilon_x, \varepsilon_y, \varepsilon_z)$ in three perpendicular directions and three shear strains $(\gamma_{xy}, \gamma_{yz}, \gamma_{xz})$ related to the three orthogonal planes are called components of strain at a point. The strain expressions at a point $P(x,y,z)$ corresponding to a typical displacement model 'HOSNT12' can be written as below. The strain vector $\boldsymbol{\varepsilon}^z$ is split into two parts, $\boldsymbol{\varepsilon}^z_{\mathrm{MB}}$ and $\boldsymbol{\varepsilon}^z_{\mathrm{S}}$. The former corresponds to membrane-bending part while the latter corresponds to transverse shear part. A superscript z signifies that the parameters are defined at a general point 'P' located at a distance z from the reference surface of FG plate.

$$\boldsymbol{\varepsilon}^z_{\mathrm{MB}} = \begin{Bmatrix} \varepsilon_x \\ \varepsilon_y \\ \varepsilon_z \\ \gamma_{xy} \end{Bmatrix}^z = \begin{Bmatrix} \varepsilon_{xo} \\ \varepsilon_{yo} \\ \varepsilon_{zo} \\ \varepsilon_{xyo} \end{Bmatrix} + z\begin{Bmatrix} \kappa_x \\ \kappa_y \\ \kappa^*_z \\ \kappa_{xy} \end{Bmatrix} + z^2\begin{Bmatrix} \varepsilon^*_{xo} \\ \varepsilon^*_{yo} \\ \varepsilon^*_{zo} \\ \varepsilon^*_{xyo} \end{Bmatrix} + z^3\begin{Bmatrix} \kappa^*_x \\ \kappa^*_y \\ 0 \\ \kappa^*_{xy} \end{Bmatrix}$$
$$= \boldsymbol{\varepsilon}_o + z\boldsymbol{\kappa} + z^2\boldsymbol{\varepsilon}^*_{\mathbf{o}} + z^3\boldsymbol{\kappa}^* \tag{5a}$$

$$\boldsymbol{\varepsilon}^z_{\mathrm{S}} = \begin{Bmatrix} \gamma_{yz} \\ \gamma_{xz} \end{Bmatrix}^z = \begin{Bmatrix} \varphi_y \\ \varphi_x \end{Bmatrix} + z\begin{Bmatrix} \kappa_{yz} \\ \kappa_{xz} \end{Bmatrix} + z^2\begin{Bmatrix} \varphi^*_y \\ \varphi^*_x \end{Bmatrix} + z^3\begin{Bmatrix} \kappa^*_{yz} \\ \kappa^*_{xz} \end{Bmatrix}$$
$$= \boldsymbol{\varphi}_{\mathbf{o}} + z\boldsymbol{\kappa}_{\mathbf{x}} + z^2\boldsymbol{\varphi}^*_{\mathbf{o}} + z^3\boldsymbol{\kappa}^*_{\mathbf{x}} \tag{5b}$$

where

$$(\varepsilon_{xo}, \varepsilon_{yo}, \varepsilon_{xyo}) = \left(\frac{\partial u_o}{\partial x}, \frac{\partial v_o}{\partial y}, \frac{\partial u_o}{\partial y} + \frac{\partial v_o}{\partial x}\right)$$
$$(\varepsilon^*_{xo}, \varepsilon^*_{yo}, \varepsilon^*_{xyo}) = \left(\frac{\partial u^*_o}{\partial x}, \frac{\partial v^*_o}{\partial y}, \frac{\partial u^*_o}{\partial y} + \frac{\partial v^*_o}{\partial x}\right)$$
$$(\varepsilon_{zo}, \varepsilon^*_{zo}) = (\theta_z, 3\theta^*_z)$$
$$(\kappa_{xz}, \kappa_{yz}) = \left(2u^*_o + \frac{\partial \theta_z}{\partial x}, 2v^*_o + \frac{\partial \theta_z}{\partial y}\right)$$
$$\left(\kappa^*_{xz}, \kappa^*_{yz}\right) = \left(\frac{\partial \theta^*_z}{\partial x}, \frac{\partial \theta^*_z}{\partial y}\right)$$
$$\left(\kappa_x, \kappa_y, \kappa^*_z, \kappa_{xy}\right) = \left(\frac{\partial \theta_x}{\partial x}, \frac{\partial \theta_y}{\partial y}, 2w^*_o, \frac{\partial \theta_x}{\partial y} + \frac{\partial \theta_y}{\partial x}\right)$$
$$\left(\kappa^*_x, \kappa^*_y, \kappa^*_{xy}\right) = \left(\frac{\partial \theta^*_x}{\partial x}, \frac{\partial \theta^*_y}{\partial y}, \frac{\partial \theta^*_x}{\partial y} + \frac{\partial \theta^*_y}{\partial x}\right)$$
$$\left(\varphi_x, \varphi^*_x, \varphi_y, \varphi^*_y\right) = \left(\theta_x + \frac{\partial w_o}{\partial x}, 3\theta^*_x + \frac{\partial w^*_o}{\partial x}, \theta_y + \frac{\partial w_o}{\partial y}, 3\theta^*_y + \frac{\partial w^*_o}{\partial y}\right) \tag{5c}$$

2.3. Stress–strain relations

A FG plate is modeled as an inhomogeneous plate. The material is assumed to be isotropic/orthotropic with varying material properties along plate thickness direction. For an orthotropic FG plate in a 3D state of stress/strain, the material constitutive relations from linear elasticity theory (generalized Hooke's law for an orthotropic material) at a point located at a distance z with reference to the principal material axes (1,2,3) can be written as [11]:

$$\begin{Bmatrix} \sigma_1 \\ \sigma_2 \\ \sigma_3 \\ \tau_{12} \\ \tau_{23} \\ \tau_{13} \end{Bmatrix}^z = \begin{bmatrix} C_{11} & C_{12} & C_{13} & 0 & 0 & 0 \\ C_{12} & C_{22} & C_{23} & 0 & 0 & 0 \\ C_{13} & C_{23} & C_{33} & 0 & 0 & 0 \\ 0 & 0 & 0 & C_{44} & 0 & 0 \\ 0 & 0 & 0 & 0 & C_{55} & 0 \\ 0 & 0 & 0 & 0 & 0 & C_{66} \end{bmatrix}^z \begin{Bmatrix} \varepsilon_1 \\ \varepsilon_2 \\ \varepsilon_3 \\ \gamma_{12} \\ \gamma_{23} \\ \gamma_{13} \end{Bmatrix}^z \tag{6a}$$

or,

$$\boldsymbol{\sigma}' = \mathbf{C}\boldsymbol{\varepsilon}' \tag{6b}$$

in which,

$$C_{11} = \frac{E_1(1-\upsilon_{23}\upsilon_{32})}{\Delta}; \quad C_{12} = \frac{E_1(\upsilon_{21}+\upsilon_{31}\upsilon_{23})}{\Delta} = C_{21}$$
$$C_{22} = \frac{E_2(1-\upsilon_{13}\upsilon_{31})}{\Delta}; \quad C_{13} = \frac{E_1(\upsilon_{31}+\upsilon_{21}\upsilon_{32})}{\Delta} = C_{31}$$
$$C_{33} = \frac{E_3(1-\upsilon_{12}\upsilon_{21})}{\Delta}; \quad C_{23} = \frac{E_2(\upsilon_{32}+\upsilon_{12}\upsilon_{31})}{\Delta} = C_{32}$$
$$C_{44} = G_{12}; \quad C_{55} = G_{23}; \quad C_{66} = G_{13}$$

where

$$\Delta = (1 - \upsilon_{12}\upsilon_{21} - \upsilon_{23}\upsilon_{32} - \upsilon_{31}\upsilon_{13} - 2\upsilon_{12}\upsilon_{23}\upsilon_{31}) \tag{6c}$$

Here, E_1, E_2, E_3 are the Young's modulii and G_{12}, G_{23}, G_{13} are the shear modulii for an orthotropic plate in the three orthogonal planes. υ_{ij} is Poisson's ratio giving the strain in the 'jth' direction caused by a strain in the 'ith' direction. In Eq. (6a), the superscript z is introduced to designate a point located at a distance z from the reference middle surface of FG plate. The relations given by Eqs. 6a, 6b and 6c are the stress–strain constitutive relations for FG plates with reference to the material principle axes (1,2,3) for a homogeneous orthotropic layer in a general 3D state of stress. It is assumed here that the structural reference axes (x,y,z) coincide with the principal material axes (1,2,3).

Table 3
Comparison of non-dimensional natural frequencies $\bar{\omega}_{mn}$ of simply (diaphragm) supported isotropic square plate ($h/a = 0.1, a/b = 1$).

Mode	m	n	Exact [8]	HOSNT12	HOSNT11	HOSNT10B	HOSNT11M/ HOSNT10M	HOST9	Mindlin's FOST[a]	Mindlin's FOST$^{k_s=5/6}$	Kirchhoff's CPT[a]	Reddy's TSDT [35]	Senthilnathan et al. [33]	RPT [35]
1	1	1	0.0932	0.0932 (0.00)	0.0932 (0.00)	0.0932 (0.00)	0.1024 (9.87)	0.093 (−0.21)	0.0934 (0.21)	0.093 (−0.21)	0.0955 (2.47)	0.093 (−0.21)	0.093 (−0.21)	0.093 (−0.21)
2	1	2	0.2226	0.2226 (0.00)	0.2226 (0.00)	0.2226 (0.00)	0.2425 (8.94)	0.222 (−0.27)	0.2241 (0.67)	0.2219 (−0.28)	0.236 (6.02)	0.222 (−0.27)	0.222 (−0.27)	0.222 (−0.27)
3	2	2	0.3421	0.3421 (0.00)	0.3421 (0.00)	0.3421 (0.00)	0.3701 (8.18)	0.3406 (−0.44)	0.3454 (0.96)	0.3406 (−0.44)	0.3732 (9.09)	0.3406 (−0.44)	0.3406 (−0.44)	0.3406 (−0.44)
4	1	3	0.4171	0.4172 (0.02)	0.4172 (0.02)	0.4172 (0.02)	0.4495 (7.77)	0.4151 (−0.48)	0.422 (1.17)	0.4149 (−0.53)	0.4629 (10.98)	0.4151 (−0.48)	0.415 (−0.50)	0.4151 (−0.48)
5	2	3	0.5239	0.524 (0.02)	0.524 (0.02)	0.524 (0.02)	0.5616 (7.20)	0.5208 (−0.59)	0.5312 (1.39)	0.5206 (−0.63)	0.5951 (13.59)	0.5208 (−0.59)	0.5208 (−0.59)	0.5208 (−0.59)
6	1	4	–	0.6573	0.6573	0.6573	0.7002	0.6525	0.668	0.652	0.7668	0.6525	0.6524	0.6525
7	3	3	0.6889	0.6892 (0.04)	0.6892 (0.04)	0.6892 (0.04)	0.7332 (6.43)	0.6839 (−0.73)	0.7008 (1.73)	0.6834 (−0.80)	0.809 (17.43)	0.6839 (−0.73)	0.6839 (−0.73)	0.684 (−0.71)
8	2	4	0.7511	0.7515 (0.05)	0.7515 (0.05)	0.7515 (0.05)	0.7974 (6.16)	0.7454 (−0.76)	0.7649 (1.84)	0.7447 (−0.85)	0.8926 (18.84)	0.7454 (−0.76)	0.7453 (−0.77)	0.7454 (−0.76)
9	3	4	–	0.8992	0.8992	0.8992	0.9488	0.8908	0.9172	0.8896	1.0965	0.8908	0.8908	0.8908
10	1	5	0.9268	0.9275 (0.08)	0.9275 (0.08)	0.9275 (0.08)	0.9777 (5.49)	0.9187 (−0.87)	0.9465 (2.13)	0.9174 (−1.01)	1.1365 (22.63)	0.9187 (−0.87)	0.9186 (−0.88)	0.9187 (−0.87)
11	2	5	–	1.0102	1.0102	1.0102	1.062	1	1.0321	0.9984	1.2549	1	1	1.0001
12	4	4	1.0889	1.0899 (0.09)	1.0899 (0.09)	1.0899 (0.09)	1.1429 (4.96)	1.0784 (−0.96)	1.1146 (2.36)	1.0764 (−0.96)	1.3716 (25.96)	1.0784 (−0.96)	1.0784 (−0.96)	1.0785 (−0.96)
13	3	5	–	1.1416	1.1416	1.1416	1.1951	1.1291	1.1681	1.1269	1.4475	1.1291	1.1292	1.1292

Numbers inside the bracket ( ) is the % error computed. k_s(=5/6) is the shear correction factor used in FOST. – Against an entry indicates that the results/data are not available.
[a] Results using these theories are computed independently and are found same as reported in various references.

Table 4
Comparison of non-dimensional natural frequencies $\bar{\omega}_{mn}$ of simply (diaphragm) supported orthotropic square plate ($h/a = 0.1, a/b = 1$).

Mode	m	n	Exact [8]	HOSNT12	HOSNT11	HOSNT10B	HOSNT11M/ HOSNT10M	HOST9	Mindlin's FOST[a]	Kirchhoff's CPT[a]	Reddy's TSDT [34]	Senthilnathan et al. [33]	RPT [34]
1	1	1	0.0474	0.0474	0.0467	0.0467	0.0520	0.0474	0.0476	0.0497	0.0476	0.0478	0.0477
	% error		*nil*	*0.00*	−1.50	−1.50	*9.80*	*0.02*	*0.42*	*4.85*	*0.42*	*0.84*	*0.63*
2	1	2	0.1033	0.1032	0.1030	0.1030	0.1125	0.1032	0.1041	0.1120	0.1041	0.1049	0.1040
	% error		*nil*	−0.11	−0.28	−0.28	*8.90*	−0.11	*0.77*	*8.42*	*0.77*	*1.55*	*0.68*
3	2	1	0.1188	0.1188	0.1157	0.1157	0.1283	0.1188	0.1188	0.1354	0.1189	0.1198	0.1198
	% error		*nil*	−0.03	−2.63	−2.63	*8.00*	−0.02	*0.00*	*13.97*	*0.08*	*0.84*	*0.84*
4	2	2	0.1694	0.1693	0.1679	0.1679	0.1821	0.1693	0.1698	0.1987	0.1698	0.1726	0.1722
	% error		*nil*	−0.08	−0.89	−0.89	*7.50*	−0.07	*0.24*	*17.30*	*0.24*	*1.89*	*1.65*
5	1	3	0.1888	0.1884	0.1884	0.1884	0.2024	0.1885	0.1905	0.2154	0.1906	0.1919	0.1898
	% error		*nil*	−0.20	−0.19	−0.19	*7.20*	−0.19	*0.90*	*14.09*	*0.95*	*1.64*	*0.53*
6	3	1	0.2180	0.2180	0.2133	0.2133	0.2333	0.2180	0.2178	0.2779	0.2181	0.2197	0.2197
	% error		*nil*	*0.00*	−2.15	−2.15	*7.00*	*0.01*	−0.09	*27.48*	*0.05*	*0.78*	*0.78*
7	2	3	0.2475	0.2471	0.2468	0.2468	0.2636	0.2471	0.2485	0.3029	0.2487	0.2533	0.2520
	% error		*nil*	−0.18	−0.30	−0.30	*6.50*	−0.16	*0.40*	*22.38*	*0.48*	*2.34*	*1.82*
8	3	2	0.2624	0.2622	0.2597	0.2597	0.2787	0.2623	0.2623	0.3418	0.2626	0.2677	0.2675
	% error		*nil*	−0.07	−1.02	−1.02	*6.20*	−0.05	−0.04	*30.26*	*0.08*	*2.02*	*1.94*
9	1	4	0.2969	0.2960	0.2960	0.2960	0.3147	0.2961	0.2994	0.3599	0.2995	0.3012	0.2980
	% error		*nil*	−0.31	−0.29	−0.29	*6.00*	−0.29	*0.84*	*21.22*	*0.88*	*1.45*	*0.37*
10	4	1	0.3319	0.3318	0.3273	0.3273	0.3502	0.3320	0.3340	0.4773	0.3320	0.3340	0.3340
	% error		*nil*	−0.02	−1.38	−1.38	*5.50*	*0.02*	*0.63*	*43.81*	*0.03*	*0.63*	*0.63*
11	3	3	0.3320	0.3314	0.3307	0.3307	0.3489	0.3315	0.3321	0.4470	0.3326	0.3414	0.3407
	% error		*nil*	−0.17	−0.39	−0.39	*5.10*	−0.14	*0.03*	*34.64*	*0.18*	*2.83*	*2.62*
12	2	4	0.3476	0.3465	0.3466	0.3466	0.3643	0.3467	0.3491	0.4480	0.3495	0.3558	0.3534
	% error		*nil*	−0.31	−0.28	−0.28	*4.80*	−0.27	*0.43*	*28.88*	*0.55*	*2.36*	*1.67*
13	4	2	0.3707	0.3704	0.3679	0.3679	0.3863	0.3706	0.3698	0.5415	0.3708	0.3775	0.3774
	% error		*nil*	−0.08	−0.76	−0.76	*4.20*	−0.04	−0.24	*46.07*	*0.03*	*1.83*	*1.81*

[a] Results using these theories are computed independently and are found same as reported in various references.

Table 5
Comparison of non-dimensional fundamental natural frequency $[\bar{\omega}_{mn}(m=n=1)]$ of simply (diaphragm) supported FG plates (Material set-1; $a/h = 10$,$b/a = 1$ and $\sqrt{2}$).

Aspect ratio and side-to-thickness ratio	Theory	Material gradient index (k)						
		0 (Ceramic)	0.1	0.5	1	2	10	100 (Metal)
$b/a = 1$; $a/h = 10$	Exact [8]	0.0932	–	–	–	–	–	–
	CPT1[a]	0.0955 (2.47)	–	–	–	–	–	–
	CPT2[a]	0.0963 (3.33)	0.0936	0.0866	0.0825	0.0797	0.0754	0.0701
	FOST[a]	0.0934 (0.21)	0.0908	0.0841	0.0802	0.0774	0.0731	0.0680
	FOST[a] ($k_s = 5/6$)	0.0930 (−0.21)	0.0904	0.0837	0.0798	0.0770	0.0727	0.0677
	HOSNT12	0.0932 (0.00)	0.0906	0.0839	0.0799	0.0770	0.0727	0.0678
	HOSNT11	0.0932 (0.00)	0.0906	0.0839	0.0799	0.0770	0.0727	0.0678
	HOSNT11M	0.1024 (9.84)	0.0995	0.0920	0.0876	0.0844	0.0796	0.0745
	HOSNT10B	0.0932 (0.00)	0.0906	0.0840	0.0802	0.0774	0.0728	0.0678
	HOSNT10M	0.1024 (9.84)	0.0996	0.0922	0.0879	0.0846	0.0798	0.0745
	HOST9	0.0930 (−0.21)	0.0905	0.0838	0.0798	0.0769	0.0726	0.0677
$b/a = \sqrt{2}$; $a/h = 10$	Exact [36]	0.0704	–	–	–	–	–	–
	CPT1[a]	0.0718 (1.99)	–	–	–	–	–	–
	CPT2[a]	0.0722 (2.56)	0.0702	0.0649	0.0619	0.0598	0.0566	0.0526
	FOST[a]	0.0706 (0.28)	0.0686	0.0635	0.0606	0.0585	0.0552	0.0514
	FOST[a] ($k_s = 5/6$)	0.0704 (0.00)	0.0684	0.0633	0.0604	0.0582	0.0550	0.0512
	HOSNT12	0.0704 (0.00)	0.0685	0.0634	0.0604	0.0583	0.0550	0.0512
	HOSNT11	0.0704 (0.00)	0.0685	0.0634	0.0604	0.0583	0.0550	0.0512
	HOSNT11M	0.0775 (10.09)	0.0754	0.0697	0.0663	0.0639	0.0604	0.0564
	HOSNT10B	0.0704 (0.00)	0.0685	0.0635	0.0607	0.0585	0.0551	0.0512
	HOSNT10M	0.0775 (10.09)	0.0754	0.0698	0.0665	0.0641	0.0605	0.0564
	HOST9	0.0704 (0.00)	0.0684	0.0633	0.0604	0.0582	0.0549	0.0512

Numbers inside the bracket ( ) is the % error computed. k_s(=5/6) is the shear correction factor used in FOST. – Against an entry indicates that the results/data are not available.
[a] Results using these theories are computed independently and found same as in various references.

2.4. Equations of motion and natural boundary conditions

The governing equations of motion appropriate for a displacement model can be derived using the Hamilton's principle [31]. For a typical model 'HOSNT12' the equations of motion is represented as;

$$\delta u_o: \quad \frac{\partial N_x}{\partial x}+\frac{\partial N_{xy}}{\partial y}=i_1\ddot{u}_o+i_2\ddot{\theta}_x+i_3\ddot{u}_o^*+i_4\ddot{\theta}_x^*$$

$$\delta v_o: \quad \frac{\partial N_y}{\partial y}+\frac{\partial N_{xy}}{\partial x}=i_1\ddot{v}_o+i_2\ddot{\theta}_y+i_3\ddot{v}_o^*+i_4\ddot{\theta}_y^*$$

$$\delta w_o: \quad \frac{\partial Q_x}{\partial x}+\frac{\partial Q_y}{\partial y}=i_1\ddot{w}_o+i_2\ddot{\theta}_z+i_3\ddot{w}_o^*+i_4\ddot{\theta}_z^*$$

$$\delta\theta_x: \quad \frac{\partial M_x}{\partial x}+\frac{\partial M_{xy}}{\partial y}-Q_x=i_2\ddot{u}_o+i_3\ddot{\theta}_x+i_4\ddot{u}_o^*+i_5\ddot{\theta}_x^*$$

$$\delta\theta_y: \quad \frac{\partial M_y}{\partial y}+\frac{\partial M_{xy}}{\partial x}-Q_y=i_2\ddot{v}_o+i_3\ddot{\theta}_y+i_4\ddot{v}_o^*+i_5\ddot{\theta}_y^*$$

$$\delta\theta_z: \quad \frac{\partial S_x}{\partial x}+\frac{\partial S_y}{\partial y}-N_z=i_2\ddot{w}_o+i_3\ddot{\theta}_z+i_4\ddot{w}_o^*+i_5\ddot{\theta}_z^*$$

$$\delta u_o^*: \quad \frac{\partial N_x^*}{\partial x}+\frac{\partial N_{xy}^*}{\partial y}-2S_x=i_3\ddot{u}_o+i_4\ddot{\theta}_x+i_5\ddot{u}_o^*+i_6\ddot{\theta}_x^*$$

$$\delta v_o^*: \quad \frac{\partial N_y^*}{\partial y}+\frac{\partial N_{xy}^*}{\partial x}-2S_y=i_3\ddot{v}_o+i_4\ddot{\theta}_y+i_5\ddot{v}_o^*+i_6\ddot{\theta}_y^*$$

$$\delta w_o^*: \quad \frac{\partial Q_x^*}{\partial x}+\frac{\partial Q_y^*}{\partial y}-2M_z^*=i_3\ddot{w}_o+i_4\ddot{\theta}_z+i_5\ddot{w}_o^*+i_6\ddot{\theta}_z^*$$

$$\delta\theta_x^*: \quad \frac{\partial M_x^*}{\partial x}+\frac{\partial M_{xy}^*}{\partial y}-3Q_x^*=i_4\ddot{u}_o+i_5\ddot{\theta}_x+i_6\ddot{u}_o^*+i_7\ddot{\theta}_x^*$$

$$\delta\theta_y^*: \quad \frac{\partial M_y^*}{\partial y}+\frac{\partial M_{xy}^*}{\partial x}-3Q_y^*=i_4\ddot{v}_o+i_5\ddot{\theta}_y+i_6\ddot{v}_o^*+i_7\ddot{\theta}_y^*$$

$$\delta\theta_z^*: \quad \frac{\partial S_x^*}{\partial x}+\frac{\partial S_y^*}{\partial y}-3N_z^*=i_4\ddot{w}_o+i_5\ddot{\theta}_z+i_6\ddot{w}_o^*+i_7\ddot{\theta}_z^* \tag{7}$$

Here, superposed dot on displacement quantities denotes its differentiation with respect to time. N_x, N_y, N_{xy}, N_z, M_x, M_y, M_{xy}, Q_x, Q_y, S_x, S_y, N_x^*, N_y^*, N_{xy}^*, N_z^*, M_x^*, M_y^*, M_{xy}^*, M_z^*, Q_x^*, Q_y^*, S_x^*, S_y^* represents 'stress resultants', which are the 'stresses' defined in terms of equivalent forces (axial force, shear, or bending moment imposed) acting on the middle surface of plate. The inertia terms i_1, i_2, i_3, i_4, i_5, i_6, i_7 in Eq. (7) are defined as;

$$i_1,i_2,i_3,i_4,i_5,i_6,i_7=\int_{-h/2}^{h/2}\rho(z)(1,z,z^2,z^3,z^4,z^5,z^6)dz \tag{8}$$

Table 6
Non-dimensional fundamental natural frequency $[\bar{\omega}_{mn}(m=n=1)]$ of FG (Material set-1) square and rectangular thin and thick plates using FOST and HOSNT12.

Aspect ratio (b/a)	Theory	Side-to-thickness ratio (a/h)	Material gradient index (k)						
			0 (Ceramic)	0.1	0.5	1	2	10	100 (Metal)
1	FOST (k_s = 5/6)	2	1.5597	1.5212	1.4163	1.3480	1.2883	1.1959	1.1300
		5	0.3454	0.3361	0.3116	0.2969	0.2857	0.2686	0.2511
		10	0.0934	0.0908	0.0841	0.0802	0.0774	0.0731	0.0680
		20	0.0239	0.0232	0.0215	0.0205	0.0198	0.0187	0.0174
		50	0.0038	0.0037	0.0035	0.0033	0.0032	0.0030	0.0028
		100	0.0010	0.0009	0.0009	0.0008	0.0008	0.0008	0.0007
	HOSNT12	2	1.5185	1.4836	1.3851	1.3162	1.2482	1.1481	1.0990
		5	0.3421	0.3331	0.3091	0.2942	0.2823	0.2646	0.2485
		10	0.0932	0.0906	0.0839	0.0799	0.0770	0.0727	0.0678
		20	0.0239	0.0232	0.0215	0.0205	0.0198	0.0187	0.0174
		50	0.0038	0.0037	0.0035	0.0033	0.0032	0.0030	0.0028
		100	0.0010	0.0009	0.0009	0.0008	0.0008	0.0008	0.0007
$\sqrt{2}$	FOST (k_s = 5/6)	2	1.2590	1.2274	1.1418	1.0869	1.0401	0.9678	0.9127
		5	0.2655	0.2583	0.2393	0.2280	0.2196	0.2068	0.1930
		10	0.0706	0.0686	0.0635	0.0606	0.0585	0.0552	0.0514
		20	0.0180	0.0174	0.0161	0.0154	0.0149	0.0141	0.0131
		50	0.0029	0.0028	0.0026	0.0025	0.0024	0.0023	0.0021
		100	0.0007	0.0007	0.0006	0.0006	0.0006	0.0006	0.0005
	HOSNT12	2	1.2292	1.2002	1.1192	1.0638	1.0108	0.9330	0.8902
		5	0.2634	0.2564	0.2378	0.2264	0.2175	0.2043	0.1915
		10	0.0704	0.0685	0.0634	0.0604	0.0583	0.0550	0.0512
		20	0.0179	0.0174	0.0161	0.0154	0.0149	0.0140	0.0131
		50	0.0029	0.0028	0.0026	0.0025	0.0024	0.0023	0.0021
		100	0.0007	0.0007	0.0006	0.0006	0.0006	0.0006	0.0005

k_s(=5/6) is the shear correction factor used in FOST.

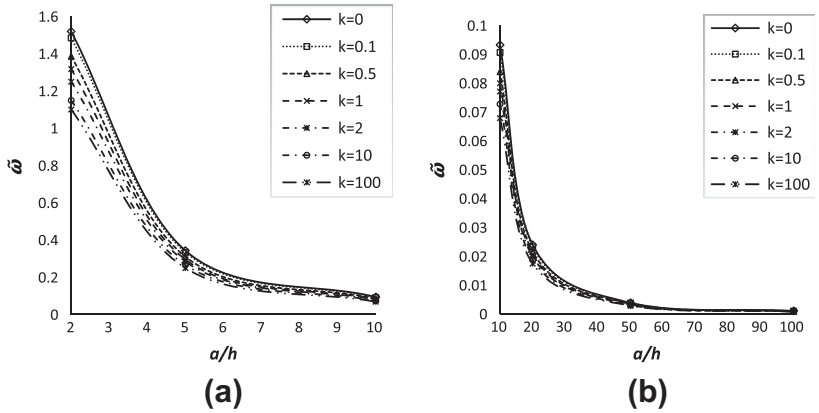

Fig. 4. Non-dimensional fundamental natural frequency $\bar{\omega}_{mn}(m=n=1)$ of simply (diaphragm) supported FG square plates ($b = a$) as a function of side-to thickness ratio (a/h) for different k using HOSNT12 (a) for a/h = 2 to 10; (b) for a/h = 10 to 100.

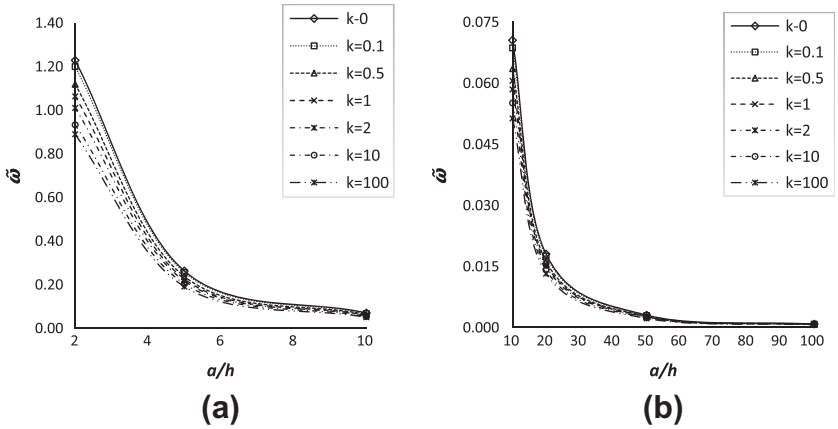

Fig. 5. Non-dimensional fundamental natural frequency $\bar{\omega}_{mn}(m=n=1)$ of simply (diaphragm) supported FG rectangular plates ($b = \sqrt{2}a$) as a function of side-to-thickness ratio (a/h) for different k using HOSNT12 (a) for a/h = 2–10; (b) for a/h = 10–100.

Table 7
Comparison of non-dimensional fundamental natural frequencies $\bar{\omega}_{mn}$ and $\tilde{\bar{\omega}}_{mn}$ of square and rectangular FG (material set-2) thin and thick plates using HOSNT12.

Aspect ratio (b/a)	Side-to-thickness ratio (a/h)	Material gradient index (k)							
		k = 0 (Ceramic)		k = 1		k = 10		k = 100 (Metal)	
		$\bar{\omega}_{mn}$	$\tilde{\bar{\omega}}_{mn}$	$\bar{\omega}_{mn}$	$\tilde{\bar{\omega}}_{mn}$	$\bar{\omega}_{mn}$	$\tilde{\bar{\omega}}_{mn}$	$\bar{\omega}_{mn}$	$\tilde{\bar{\omega}}_{mn}$
1	2	1.5185	3.7670	1.3160	3.2650	1.1481	2.8482	1.0990	2.7264
	5	0.3421	5.3042	0.2943	4.5621	0.2646	4.1022	0.2485	3.8535
	10	0.0932	5.7713	0.0799	4.9573	0.0727	4.5067	0.0678	4.2029
	20	0.0239	5.9219	0.0205	5.0780	0.0187	4.6332	0.0174	4.3104
	50	0.0038	5.9650	0.0033	5.1138	0.0030	4.6710	0.0028	4.3424
	100	0.0010	5.9713	0.0008	5.1190	0.0008	4.6765	0.0007	4.3470
$\sqrt{2}$	2	1.2292	3.0493	1.0638	2.6389	0.9330	2.3144	0.8902	2.2083
	5	0.2634	4.0845	0.2264	3.5107	0.2043	3.1668	0.1915	2.9686
	10	0.0704	4.3679	0.0604	3.7472	0.0550	3.4106	0.0512	3.1782
	20	0.0179	4.4510	0.0154	3.8164	0.0140	3.4832	0.0131	3.2398
	50	0.0029	4.4753	0.0025	3.8367	0.0023	3.5046	0.0021	3.2579
	100	0.0007	4.4788	0.0006	3.8396	0.0006	3.5077	0.0005	3.2605

Table 8
Natural frequencies of rectangular FG plates (material set-2; b/a = 2, a/h = 10).

Mode	$m \times n$	Non-dimensional natural frequencies, $\tilde{\bar{\omega}}_{mn} = \omega_{mn}\left(\frac{a^2}{h}\right)\sqrt{\rho_c/E_c}$							
		k = 0		k = 0.5		k = 1		k = 2	
		SSDT [23]	HOSNT12	SSDT [23]	HOSNT12	SSDT [23]	HOSNT12	SSDT [23]	HOSNT12
1	1 × 1	3.6983	3.6911	3.3713	3.3664	3.2225	3.2179	3.1354	3.1291
2	1 × 2	5.8498	5.8323	5.3359	5.3238	5.1002	5.0886	4.9594	4.9434
3	2 × 1	12.0345	11.965	10.9940	10.946	10.5062	10.461	10.1985	10.137
4	2 × 2	14.0144	13.921	12.8103	12.745	12.2421	12.180	11.8784	11.794
5	2 × 3	17.2325	17.096	15.7660	15.668	15.0670	14.973	14.6092	14.481
6	3 × 2	26.3462	26.051	24.1494	23.941	23.0749	22.876	22.3273	22.059
7	3 × 3	29.2257	28.871	26.8100	26.554	25.6184	25.372	24.7781	24.446

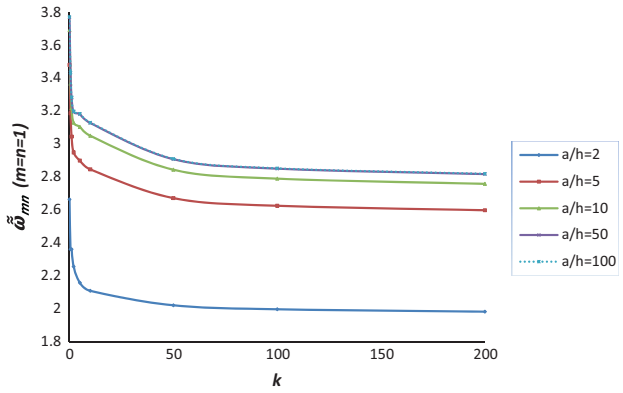

Fig. 6. Non-dimensional fundamental natural frequency $\tilde{\bar{\omega}}_{mn}$ $(m = n = 1)$ of simply (diaphragm) supported FG rectangular plates ($b = 2a$) as a function of k for different a/h.

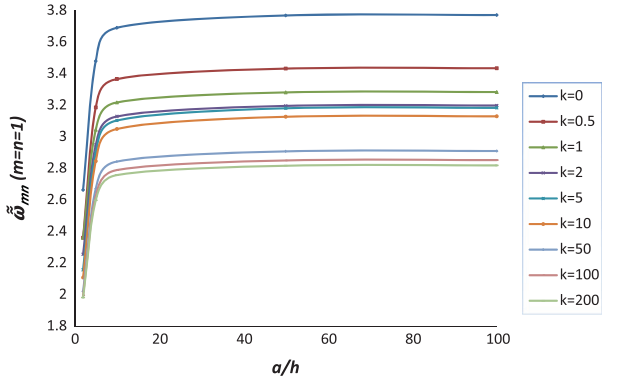

Fig. 7. Non-dimensional fundamental natural frequency $\tilde{\bar{\omega}}_{mn}$ $(m = n = 1)$ of simply (diaphragm) supported FG rectangular plates ($b = 2a$) as a function of a/h for different k.

and, the boundary conditions are on the edge x = constant,

$$u_o = \bar{u}_o \text{ or, } N_x = \overline{N}_x \quad v_o = \bar{v}_o \text{ or, } N_{xy} = \overline{N}_{xy} \quad w_o = \bar{w}_o \text{ or, } Q_x = \overline{Q}_x$$
$$\theta_x = \bar{\theta}_x \text{ or, } M_x = \overline{M}_x \quad \theta_y = \bar{\theta}_y \text{ or, } M_{xy} = \overline{M}_{xy} \quad \theta_z = \bar{\theta}_z \text{ or, } S_x = \overline{S}_x$$
$$u_o^* = \bar{u}_o^* \text{ or, } N_x^* = \overline{N}_x^* \quad v_o^* = \bar{v}_o^* \text{ or, } N_{xy}^* = \overline{N}_{xy}^* \quad w_o^* = \bar{w}_o^* \text{ or, } Q_x^* = \overline{Q}_x^*$$
$$\theta_x^* = \bar{\theta}_x^* \text{ or, } M_x^* = \overline{M}_x^* \quad \theta_y^* = \bar{\theta}_y^* \text{ or, } M_{xy}^* = \overline{M}_{xy}^* \quad \theta_z^* = \bar{\theta}_z^* \text{ or, } S_x^* = \overline{S}_x^* \tag{9a}$$

on the edge y = constant,

$$u_o = \bar{u}_o \text{ or, } N_{xy} = \overline{N}_{xy} \quad v_o = \bar{v}_o \text{ or, } N_y = \overline{N}_y \quad w_o = \bar{w}_o \text{ or, } Q_y = \overline{Q}_y$$
$$\theta_x = \bar{\theta}_x \text{ or, } M_{xy} = \overline{M}_{xy} \quad \theta_y = \bar{\theta}_y \text{ or, } M_y = \overline{M}_y \quad \theta_z = \bar{\theta}_z \text{ or, } S_y = \overline{S}_y$$
$$u_o^* = \bar{u}_o^* \text{ or, } N_{xy}^* = \overline{N}_{xy}^* \quad v_o^* = \bar{v}_o^* \text{ or, } N_y^* = \overline{N}_y^* \quad w_o^* = \bar{w}_o^* \text{ or, } Q_y^* = \overline{Q}_y^*$$
$$\theta_x^* = \bar{\theta}_x^* \text{ or, } M_{xy}^* = \overline{M}_{xy}^* \quad \theta_y^* = \bar{\theta}_y^* \text{ or, } M_y^* = \overline{M}_y^* \quad \theta_z^* = \bar{\theta}_z^* \text{ or, } S_y^* = \overline{S}_y^* \tag{9b}$$

The governing equations of motion using other displacement models (Model-2 to Model-8) considered in the present study are listed in Appendix A.

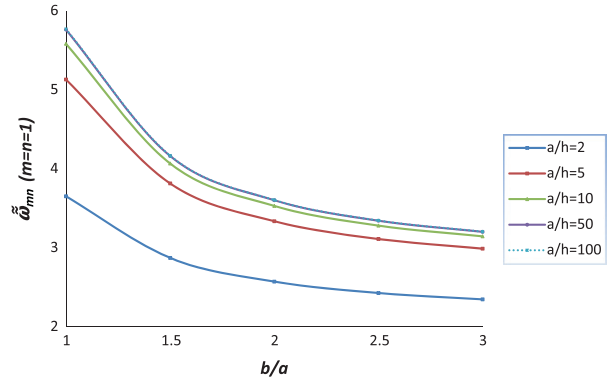

Fig. 8. Non-dimensional fundamental natural frequency $\bar{\tilde{\omega}}_{mn}$ $(m = n = 1)$ of simply (diaphragm) supported FG plates as a function of b/a for different a/h with $k = 0.2$.

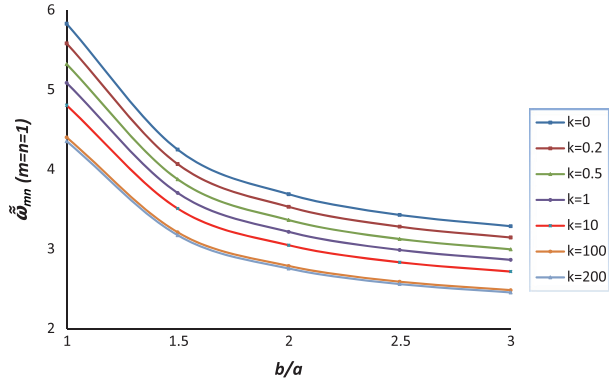

Fig. 9. Non-dimensional fundamental natural frequency $\bar{\tilde{\omega}}_{mn}$ $(m = n = 1)$ of simply (diaphragm) supported FG plates as a function of b/a for different k for $a/h = 10$.

2.5. Relationship between stress-resultants and middle surface displacements

Since, stresses in plate vary through its thickness; it is always convenient to define 'stresses' in terms of equivalent forces acting at plate's middle surfaces. This definition of stresses (i.e., 'stress resultants') considering a typical displacement model 'HOSNT12' for FG plate are:

$$\begin{bmatrix} N_x & N_x^* \\ N_y & N_y^* \\ N_z & N_z^* \\ N_{xy} & N_{xy}^* \end{bmatrix} = \int_{-h/2}^{h/2} \begin{Bmatrix} \sigma_x \\ \sigma_y \\ \sigma_z \\ \tau_{xy} \end{Bmatrix} \begin{bmatrix} 1 & z^2 \end{bmatrix} dz$$

$$\begin{bmatrix} M_x & M_x^* \\ M_y & M_y^* \\ M_z^* & 0 \\ M_{xy} & M_{xy}^* \end{bmatrix} = \int_{-h/2}^{h/2} \begin{Bmatrix} \sigma_x \\ \sigma_y \\ \sigma_z \\ \tau_{xy} \end{Bmatrix} \begin{bmatrix} z & z^3 \end{bmatrix} dz \tag{10}$$

$$\begin{bmatrix} Q_x & Q_x^* \\ Q_y & Q_y^* \end{bmatrix} = \int_{-h/2}^{h/2} \begin{Bmatrix} \tau_{xz} \\ \tau_{yz} \end{Bmatrix} \begin{bmatrix} 1 & z^2 \end{bmatrix} dz$$

$$\begin{bmatrix} S_x & S_x^* \\ S_y & S_y^* \end{bmatrix} = \int_{-h/2}^{h/2} \begin{Bmatrix} \tau_{xz} \\ \tau_{yz} \end{Bmatrix} \begin{bmatrix} z & z^3 \end{bmatrix} dz$$

In terms of displacement components, we obtain the following relations between 'stress resultants' and middle surface displacement quantities (typical for model 'HOSNT12');

$$\begin{Bmatrix} N_x \\ N_y \\ N_x^* \\ N_y^* \\ N_z \\ N_z^* \\ M_x \\ M_y \\ M_x^* \\ M_y^* \\ M_z^* \end{Bmatrix}_{11\times1} = [\mathbf{A}]_{11\times11} \begin{Bmatrix} \frac{\partial u_o}{\partial x} \\ \frac{\partial v_o}{\partial y} \\ \frac{\partial u_o^*}{\partial x} \\ \frac{\partial v_o^*}{\partial y} \\ \theta_z \\ \theta_z^* \\ \frac{\partial \theta_x}{\partial x} \\ \frac{\partial \theta_y}{\partial y} \\ \frac{\partial \theta_x^*}{\partial x} \\ \frac{\partial \theta_y^*}{\partial y} \\ w_o^* \end{Bmatrix}_{11\times1} + [\mathbf{A}']_{11\times8} \begin{Bmatrix} \frac{\partial u_o}{\partial y} \\ \frac{\partial v_o}{\partial x} \\ \frac{\partial u_o^*}{\partial y} \\ \frac{\partial v_o^*}{\partial x} \\ \frac{\partial \theta_x}{\partial y} \\ \frac{\partial \theta_y}{\partial x} \\ \frac{\partial \theta_x^*}{\partial y} \\ \frac{\partial \theta_y^*}{\partial x} \end{Bmatrix}_{8\times1}$$

$$\begin{Bmatrix} N_{xy} \\ N_{xy}^* \\ M_{xy} \\ M_{xy}^* \end{Bmatrix}_{4\times1} = [\mathbf{B}']_{4\times11} \begin{Bmatrix} \frac{\partial u_o}{\partial x} \\ \frac{\partial v_o}{\partial y} \\ \frac{\partial u_o^*}{\partial x} \\ \frac{\partial v_o^*}{\partial y} \\ \theta_z \\ \theta_z^* \\ \frac{\partial \theta_x}{\partial x} \\ \frac{\partial \theta_y}{\partial y} \\ \frac{\partial \theta_x^*}{\partial x} \\ \frac{\partial \theta_y^*}{\partial y} \\ w_o^* \end{Bmatrix}_{11\times1} + [\mathbf{B}]_{4\times8} \begin{Bmatrix} \frac{\partial u_o}{\partial y} \\ \frac{\partial v_o}{\partial x} \\ \frac{\partial u_o^*}{\partial y} \\ \frac{\partial v_o^*}{\partial x} \\ \frac{\partial \theta_x}{\partial y} \\ \frac{\partial \theta_y}{\partial x} \\ \frac{\partial \theta_x^*}{\partial y} \\ \frac{\partial \theta_y^*}{\partial x} \end{Bmatrix}_{8\times1} \tag{11}$$

$$\begin{Bmatrix} Q_x \\ Q_x^* \\ S_x \\ S_x^* \end{Bmatrix}_{4\times1} = [\mathbf{D}]_{4\times7} \begin{Bmatrix} \theta_x \\ \frac{\partial w_o}{\partial x} \\ \theta_x^* \\ \frac{\partial w_o^*}{\partial x} \\ u_o^* \\ \frac{\partial \theta_z}{\partial x} \\ \frac{\partial \theta_z^*}{\partial x} \end{Bmatrix}_{7\times1} + [\mathbf{D}']_{4\times7} \begin{Bmatrix} \theta_y \\ \frac{\partial w_o}{\partial y} \\ \theta_y^* \\ \frac{\partial w_o^*}{\partial y} \\ v_o^* \\ \frac{\partial \theta_z}{\partial y} \\ \frac{\partial \theta_z^*}{\partial y} \end{Bmatrix}_{7\times1}$$

$$\begin{Bmatrix} Q_y \\ Q_y^* \\ S_y \\ S_y^* \end{Bmatrix}_{4\times1} = [\mathbf{E}']_{4\times7} \begin{Bmatrix} \theta_x \\ \frac{\partial w_o}{\partial x} \\ \theta_x^* \\ \frac{\partial w_o^*}{\partial x} \\ u_o^* \\ \frac{\partial \theta_z}{\partial x} \\ \frac{\partial \theta_z^*}{\partial x} \end{Bmatrix}_{7\times1} + [\mathbf{E}]_{4\times7} \begin{Bmatrix} \theta_y \\ \frac{\partial w_o}{\partial y} \\ \theta_y^* \\ \frac{\partial w_o^*}{\partial y} \\ v_o^* \\ \frac{\partial \theta_z}{\partial y} \\ \frac{\partial \theta_z^*}{\partial y} \end{Bmatrix}_{7\times1}$$

Here, the matrices [**A**], [**A**′], [**B**], [**B**′], [**D**], [**D**′], [**E**], [**E**′] are the sub matrices of plate rigidity matrix, and their elements are defined in Appendix B.

3. Analytical solution

Among all the analytical methods available the Navier solution technique is very simple and easy to use when the plate is of rectangular geometry with simply (diaphragm) supported edge conditions. This method of solution for Kirchhoff plate problems of rectangular geometry is well documented [11].

3.1. Solution technique

Navier solution technique using the double Fourier series is adopted for solving the equations of motion for free vibration of FG plates. The boundary conditions for the simply (diaphragm) supported FG plate using a typical model 'HOSNT12' are:

At edges $x = 0$ and $x = a$:

$$\begin{array}{llllll} v_o = 0; & w_o = 0; & \theta_y = 0; & \theta_z = 0; & M_x = 0; & N_x = 0 \\ v_o^* = 0; & w_o^* = 0; & \theta_y^* = 0; & \theta_z^* = 0; & M_x^* = 0; & N_x^* = 0 \end{array} \tag{12a}$$

At edges $y = 0$ and $y = b$:

$$\begin{array}{llllll} u_o = 0; & w_o = 0; & \theta_x = 0; & \theta_z = 0; & M_y = 0; & N_y = 0 \\ u_o^* = 0; & w_o^* = 0; & \theta_x^* = 0; & \theta_z^* = 0; & M_y^* = 0; & N_y^* = 0 \end{array} \tag{12b}$$

Table 9
Comparison of non-dimensional fundamental frequency of simply (diaphragm) supported square FG (material set-3) thin and thick plates using various models.

Theory	h/a = 0.05	h/a = 0.1	h/a = 0.2			
	k = 1	k = 1	k = 1	k = 2	k = 3	k = 5
Non-dimensional fundamental natural frequency $\hat{\omega}_{mn} = \omega_{mn}(h)\sqrt{\rho_m/E_m}$						
Exact [14]	0.0153	0.0596	0.2192	0.2197	0.2211	0.2225
HOSNDPT [17]	0.0149	0.0584	0.2152	0.2153	0.2172	0.2194
TSDT [16]	0.0147	0.0592	0.2188	0.2188	0.2202	0.2215
HOSNT12	0.0153	0.0598	0.2219	0.2220	0.2227	0.2237
HOSNT11	0.0153	0.0598	0.2219	0.2220	0.2227	0.2237
HOSNT10B	0.0154	0.0599	0.2239	0.2239	0.2244	0.2250
HOSNT11M	0.0167	0.0655	0.2402	0.2403	0.2406	0.2413
HOSNT10M	0.0167	0.0655	0.2402	0.2403	0.2406	0.2413
HOST9	0.0153	0.0599	0.2211	0.2212	0.2218	0.2227
FOST (k_s = 5/6)	0.0154	0.0601	0.2217	0.2219	0.2231	0.2246
FOST	0.0156	0.0610	0.2248	0.2250	0.2264	0.2280
CPT	0.0162	0.0656	0.2500	0.2502	0.2529	0.2561

k_s(=5/6) is the shear correction factor used in FOST.

Table 10
Comparison of "thickness mode non-dimensional natural frequency" of a simply (diaphragm) supported square FG (Material set-3) thick plates, a/h = 5, and $m = n$ = 1.

Theory	Thickness mode	Non-dimensional natural frequency $\hat{\bar{\omega}}_{mn} = \omega_{mn}\left(\frac{a^2}{h}\right)\sqrt{\rho_m/E_m}$ Material gradient index, k						
		0 (Ceramic)	0.5	2	3	5	10	∞ (Metal)
Exact[14]	1	–	–	5.4923	5.5285	5.5632	–	–
	2	–	–	14.278	14.150	14.026	–	–
	3	–	–	23.909	23.696	23.494	–	–
	4	–	–	50.376	48.825	47.687	–	–
	5	–	–	54.685	53.179	52.068	–	–
HOSNT12	1	6.0519	5.7351	5.5507	5.5666	5.5919	5.5709	5.2002
	2	15.7188	15.3185	14.6780	14.4543	14.1930	13.9140	13.5067
	3	26.3977	25.7398	24.6471	24.2568	23.8030	23.3302	22.6827
	4	57.7694	57.8370	52.4375	50.0819	47.9768	47.2074	49.6394
	5	62.5433	62.3364	56.8427	54.5505	52.5115	51.7124	53.7415
HOSNT11	1	6.0519	5.7351	5.5510	5.5669	5.5922	5.5709	5.2002
	2	15.7188	15.3186	14.6780	14.4543	14.1930	13.9140	13.5067
	3	26.4023	25.7431	24.6508	24.2616	23.8092	23.3370	22.6866
	4	57.7694	57.8373	52.4375	50.0819	47.9768	47.2074	49.6394
	5	62.5433	62.3451	56.8689	54.5728	52.5257	51.7181	53.7415
HOSNT10B	1	6.0519	5.7528	5.5976	5.6106	5.6245	5.5867	5.2002
	2	15.7188	15.3185	14.6780	14.4543	14.1930	13.9140	13.5067
	3	29.4072	28.5589	27.2066	26.8059	26.3770	25.9423	25.2686
	4	57.7694	57.8370	52.4375	50.0819	47.9768	47.2074	49.6394
	5	62.5433	62.3610	56.8978	54.6002	52.5476	51.7304	53.7415
HOSNT11M/HOSNT10M	1	6.5466	6.2130	6.0063	6.0148	6.0321	6.0061	5.6253
	2	15.7188	15.3185	14.6780	14.4543	14.1930	13.9140	13.5067
	3	26.4023	25.7434	24.6531	24.2644	23.8118	23.3382	22.6866
	4	57.7694	57.8370	52.4375	50.0819	47.9768	47.2074	49.6394
	5	64.1354	63.8116	58.2307	55.9659	53.9725	53.1940	55.1095
HOST9	1	6.0258	5.7122	5.5293	5.5439	5.5672	5.5449	5.1777
	2	15.7188	15.3185	14.6780	14.4543	14.1930	13.9140	13.5067
	3	26.5696	25.8909	24.7997	24.4200	23.9796	23.5129	22.8304
	4	57.7694	57.8370	52.4375	50.0819	47.9768	47.2074	49.6394
	5	62.9358	62.7110	57.1924	54.8964	52.8556	52.0559	54.0787
FOST (k_s = 5/6)	1	6.0245	5.7058	5.5481	5.5786	5.6149	5.5844	5.1767
	2	15.7188	15.3185	14.6784	14.4549	14.1935	13.9141	13.5067
	3	26.5696	25.8910	24.8015	24.4225	23.9820	23.5137	22.8304
	4	58.1068	57.8397	54.2537	52.5794	50.8175	49.5509	49.9293
	5	63.2840	62.7310	59.0283	57.3967	55.6839	54.3978	54.3779
FOST	1	6.1109	5.7830	5.6254	5.6595	5.7006	5.6722	5.2509
	2	15.7188	15.3187	14.6793	14.4559	14.1944	13.9147	13.5067
	3	26.5696	25.8919	24.8059	24.4275	23.9864	23.5163	22.8304
	4	63.2633	62.9966	59.0760	57.2355	55.2975	53.9084	54.3602
	5	68.3436	67.7975	63.7630	61.9630	60.0712	58.6613	58.7255
CPT	1	6.8154	6.4094	6.2544	6.3213	6.4032	6.3928	5.8563
	2	31.4373	30.6392	29.3676	28.9225	28.3980	27.8343	27.0137
	3	53.1392	51.8059	49.6863	48.9314	48.0363	47.0667	45.6608

– Against an entry indicates that the results/data are not available. k_s(=5/6) is the shear correction factor used in FOST.

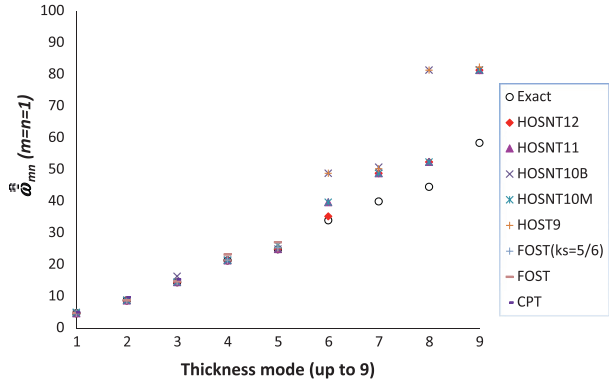

Fig. 10. First nine "thickness mode natural frequencies" of homogeneous (Al) square plates ($a/h = \sqrt{10}$) using various models.

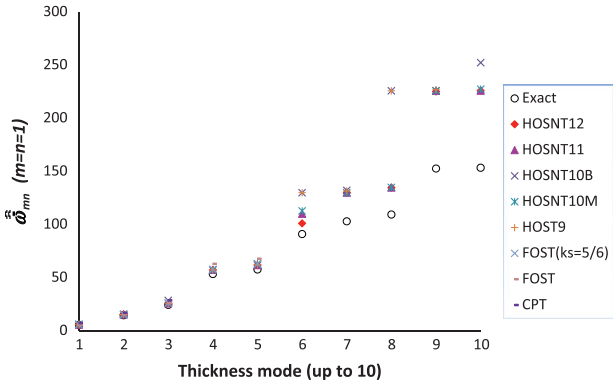

Fig. 11. First ten "thickness mode natural frequencies" of FG (Al/ZrO_2) square plates ($a/h = 5$, $k = 1$) using various models.

The generalized displacement field for a typical model 'HOSNT12' to satisfy the above boundary conditions is expanded in double Fourier series as:

$$
\begin{aligned}
u_o &= \sum_{m=1}^{\infty}\sum_{n=1}^{\infty} u_{o_{mn}} \cos\alpha_m x \sin\beta_n y e^{-i\omega_{mn}t} & u_o^* &= \sum_{m=1}^{\infty}\sum_{n=1}^{\infty} u^*_{o_{mn}} \cos\alpha_m x \sin\beta_n y e^{-i\omega_{mn}t} \\
v_o &= \sum_{m=1}^{\infty}\sum_{n=1}^{\infty} v_{o_{mn}} \sin\alpha_m x \cos\beta_n y e^{-i\omega_{mn}t} & v_o^* &= \sum_{m=1}^{\infty}\sum_{n=1}^{\infty} v^*_{o_{mn}} \sin\alpha_m x \cos\beta_n y e^{-i\omega_{mn}t} \\
w_o &= \sum_{m=1}^{\infty}\sum_{n=1}^{\infty} w_{o_{mn}} \sin\alpha_m x \sin\beta_n y e^{-i\omega_{mn}t} & w_o^* &= \sum_{m=1}^{\infty}\sum_{n=1}^{\infty} w^*_{o_{mn}} \sin\alpha_m x \sin\beta_n y e^{-i\omega_{mn}t} \\
\theta_x &= \sum_{m=1}^{\infty}\sum_{n=1}^{\infty} \theta_{x_{mn}} \cos\alpha_m x \sin\beta_n y e^{-i\omega_{mn}t} & \theta_x^* &= \sum_{m=1}^{\infty}\sum_{n=1}^{\infty} \theta^*_{x_{mn}} \cos\alpha_m x \sin\beta_n y e^{-i\omega_{mn}t} \\
\theta_y &= \sum_{m=1}^{\infty}\sum_{n=1}^{\infty} \theta_{y_{mn}} \sin\alpha_m x \cos\beta_n y e^{-i\omega_{mn}t} & \theta_y^* &= \sum_{m=1}^{\infty}\sum_{n=1}^{\infty} \theta^*_{y_{mn}} \sin\alpha_m x \cos\beta_n y e^{-i\omega_{mn}t} \\
\theta_z &= \sum_{m=1}^{\infty}\sum_{n=1}^{\infty} \theta_{z_{mn}} \sin\alpha_m x \sin\beta_n y e^{-i\omega_{mn}t} & \theta_z^* &= \sum_{m=1}^{\infty}\sum_{n=1}^{\infty} \theta^*_{z_{mn}} \sin\alpha_m x \sin\beta_n y e^{-i\omega_{mn}t}
\end{aligned}
\tag{13}
$$

where $\alpha_m = \frac{m\pi}{a}$ and $\beta_n = \frac{n\pi}{b}$ in which $m, n = 1,2,3,\ldots$

Using the above generalized displacement field and following the standard steps described in previous section for collecting the coefficients of the twelve displacement degrees of freedom in a (12×12) system of simultaneous equations, we obtain the following eigenvalue problem for any fixed values of m and n:

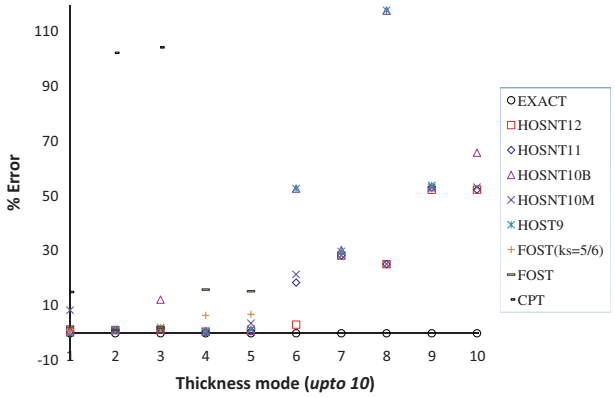

Fig. 12. Errors (%) in the first ten "thickness mode natural frequencies" of thick FG plates ($b/a = 1$, $a/h = 5$, $k = 1$) using various models.

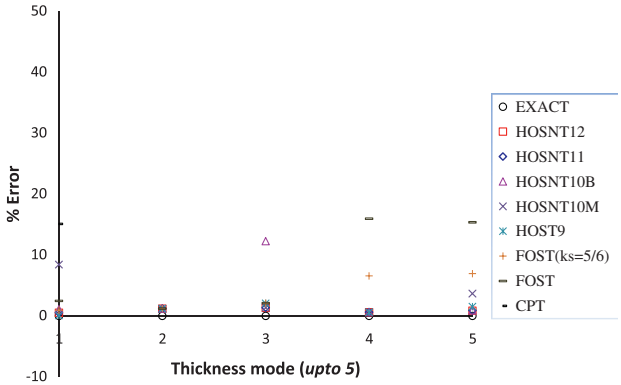

Fig. 13. Errors (%) in the first five "thickness mode natural frequencies" of thick FG plates ($b/a = 1$, $a/h = 5$, $k = 1$) using various models.

$$
([\mathbf{X}]_{12\times12} - \omega_{mn}^2[\mathbf{M}]_{12\times12})
\begin{Bmatrix}
u_{o_{mn}} \\ v_{o_{mn}} \\ w_{o_{mn}} \\ \theta_{x_{mn}} \\ \theta_{y_{mn}} \\ \theta_{z_{mn}} \\ u^*_{o_{mn}} \\ v^*_{o_{mn}} \\ w^*_{o_{mn}} \\ \theta^*_{x_{mn}} \\ \theta^*_{y_{mn}} \\ \theta^*_{z_{mn}}
\end{Bmatrix}_{12\times1}
= \{\mathbf{0}\}
\tag{14}
$$

Here, $[\mathbf{X}]$ is the coefficient matrix using displacement Model-1 (HOSNT12) whose elements are presented in Appendix C. $[\mathbf{M}]$ is the mass matrix using Model-1(HOSNT12) whose elements are provided in Appendix D. ω_{mn} is the circular natural frequency of vibration of the system associated with mth mode in x-direction and nth mode in y-direction. $u_{o_{mn}}$, $v_{o_{mn}}$, $w_{o_{mn}}$, $\theta_{x_{mn}}$, $\theta_{y_{mn}}$, $\theta_{z_{mn}}$, $u^*_{o_{mn}}$, $v^*_{o_{mn}}$, $w^*_{o_{mn}}$, $\theta^*_{x_{mn}}$, $\theta^*_{y_{mn}}$, and $\theta^*_{z_{mn}}$ are the twelve unknown coefficients. The above eigenvalue problem can be solved for the various eigen-

Table 11
Comparison of "thickness mode non-dimensional natural frequency" of a simply (diaphragm) supported square thick homogeneous and FG (Material set-3) plates, $m = n = 1$.

Theory	Thickness mode	Non-dimensional natural frequency $\hat{\bar{\omega}}_{mn} = \omega_{mn}\left(\frac{a^2}{h}\right)\sqrt{\rho_m/E_m}$				
		Homogeneous (Al) Plate		FG (Al/ZrO_2) Plate; $k = 1$		
		$a/h = \sqrt{10}$	$a/h = 10$	$a/h = 5$	$a/h = 10$	$a/h = 20$
Exact[14]	1	4.6582	5.7769	5.4806	5.9609	6.1076
	2	8.7132	27.554	14.558	29.123	58.250
	3	14.463	46.503	24.381	49.013	98.145
	4	21.343	196.77	53.366	207.50	823.92
	5	24.830	201.34	57.620	212.22	828.78
HOSNT12	1	4.6605	5.7770	5.7130	6.1933	6.3390
	2	8.7132	27.554	15.341	30.686	61.374
	3	14.463	46.503	25.776	51.795	103.71
	4	21.348	196.83	57.243	222.94	885.64
	5	24.918	201.47	61.725	227.89	890.73
HOSNT11	1	4.6605	5.7770	5.7132	6.1933	6.3390
	2	8.7132	27.554	15.341	30.686	61.374
	3	14.481	46.503	25.779	51.795	103.71
	4	21.348	196.83	57.243	222.94	885.64
	5	24.918	201.47	61.746	227.91	890.75
HOSNT10B	1	4.6605	5.7770	5.7495	6.2362	6.3841
	2	8.7132	27.554	15.341	30.686	61.374
	3	16.301	51.548	28.498	57.000	114.00
	4	21.348	196.83	57.243	222.94	885.64
	5	24.918	201.47	61.772	227.94	890.78
HOSNT11M/HOSNT10M	1	4.9452	6.3487	6.1899	6.8101	7.0038
	2	8.7132	27.554	15.341	30.686	61.374
	3	14.481	46.503	25.780	51.796	103.71
	4	21.348	196.83	57.243	222.94	885.64
	5	26.137	203.01	63.162	229.48	892.37
HOST9	1	4.6224	5.7694	5.6911	6.1862	6.3371
	2	8.7132	27.554	15.341	30.686	61.374
	3	14.728	46.574	25.925	51.866	103.74
	4	21.348	196.83	57.243	222.94	885.64
	5	25.245	201.83	62.095	228.27	891.11
FOST ($k_s = 5/6$)	1	4.6181	5.7693	5.6908	6.1864	6.3372
	2	8.7132	27.554	15.341	30.686	61.374
	3	14.728	46.574	25.925	51.866	103.74
	4	21.460	198.04	57.812	225.25	894.89
	5	25.367	203.05	62.691	230.60	900.39
FOST	1	4.7436	5.7944	5.7672	6.2113	6.3439
	2	8.7132	27.554	15.341	30.686	61.375
	3	14.728	46.574	25.928	51.867	103.74
	4	23.183	216.59	62.968	246.37	979.92
	5	27.053	221.47	67.758	251.59	985.27
CPT	1	4.9436	5.9944	7.1331	7.1416	7.1436
	2	9.7010	28.500	16.859	33.718	67.437
	3	15.346	47.765	28.542	57.016	114.00

Numbers inside the bracket ( ) is the % error computed. – Against an entry indicates that the results/data are not available. k_s(=5/6) is the shear correction factor used in FOST.

values and associated eigenvectors. To obtain non-trivial solution, we must set $|[\mathbf{X}] - \omega_{mn}^2[\mathbf{M}]| = 0$. The real positive roots of Eq. (14) yield the circular natural frequency ω_{mn} corresponding to vibration modes (m,n). The lowest eigenvalue gives the square of the fundamental natural frequency of vibration of FG plate.

4. Numerical investigations

The various displacement models considered in the present study as presented in Table 1, viz., HOSNT12, HOSNT11, HOSNT11M, HOSNT10B, HOSNT10M, HOST9, FOST and CPT have been used to analyze the free vibration responses of simply (diaphragm) supported isotropic, orthotropic and FG plates. A set of computer programs are developed in MATLAB 7.0 based on the present theoretical formulations for the free vibration of FG plates. Additional modules are also developed for the free vibration of isotropic and orthotropic plates. The natural frequencies for the simply (diaphragm) supported isotropic, orthotropic and FG plates are evaluated using these computer programs. In order to validate the accuracy, the numerical results using present formulations are compared with the other models' solutions and the exact 3D elasticity solutions available in the literature. The comparisons of the results are presented in tabular form. The errors in the solutions are computed as follows:

$$\% \text{ Error} = \left(\frac{\text{Value obtained by a theory}}{\text{Corresponding value by exact solution}} - 1\right) \times 100.$$

The results are presented in the non-dimensional form, and the various kinds of non-dimensionalizations of the natural frequencies are given in Table 2. The following material properties are used in the analysis:

- Isotropic material

Table 12
Comparison of non-dimensional natural frequencies of FG plates (Material set-4).

a/h	a/b	Theory	Non-dimensional natural frequency $\omega_{mn} = \omega_{mn}(h)\sqrt{\rho_b/G_b}$ (m,n)						
			(1, 1)	(1, 2)	(2, 1)	(2, 2)	(1, 3)	(2, 3)	(3, 3)
4	1	3D Elasticity [37]	0.4275	0.9199	0.9199	1.3174	1.5493	1.8621	2.3175
		HOSNT12	0.4277	0.9207	0.9207	1.3188	1.5511	1.8648	2.3221
	2	3D Elasticity [37]	0.9199	2.2317	1.3174	2.4825	3.6442	3.8188	4.0958
		HOSNT12	0.9207	2.2359	1.3188	2.4880	3.6637	3.8418	4.1255
	5	3D Elasticity [37]	2.9342	6.5089	3.1406	6.6160	10.1169	10.1891	10.3082
		HOSNT12	2.9434	6.6538	3.1522	6.7684	10.5869	10.6666	10.7984
	10	3D Elasticity [37]	6.5089	13.7403	6.6160	13.7947	21.0055	21.0418	21.1022
		HOSNT12	6.6538	14.6110	6.7684	14.6715	22.6831	22.7234	22.7902
5	1	3D Elasticity [37]	0.2865	0.6400	0.6400	0.9373	1.1142	1.3560	1.7123
		HOSNT12	0.2865	0.6404	0.6404	0.9381	1.1153	1.3574	1.7146
	2	3D Elasticity [37]	0.6400	1.6449	0.9373	1.8424	2.7663	2.9058	3.1272
		HOSNT12	0.6404	1.6470	0.9381	1.8450	2.7739	2.9147	3.1386
	5	3D Elasticity [37]	2.2003	5.0572	2.3645	5.1428	7.9386	7.9962	8.0914
		HOSNT12	2.2043	5.1202	2.3694	5.2095	8.1962	8.2589	8.3625
	10	3D Elasticity [37]	5.0572	10.8326	5.1428	10.8760	16.6390	16.6681	16.7164
		HOSNT12	5.1202	11.3790	5.2095	11.4270	17.8370	17.8700	17.9230
10	1	3D Elasticity [37]	0.0769	0.1852	0.1852	0.2865	0.3506	0.4431	0.5857
		HOSNT12	0.0769	0.1852	0.1852	0.2865	0.3507	0.4427	0.5860
	2	3D Elasticity [37]	0.1852	0.5580	0.2865	0.6400	1.0495	1.1142	1.2180
		HOSNT12	0.1852	0.5583	0.2865	0.6404	1.0505	1.1153	1.2192
	5	3D Elasticity [37]	0.7942	2.1578	0.8670	2.2003	3.5941	3.6228	3.6703
		HOSNT12	0.7948	2.1616	0.8677	2.2043	3.6126	3.6419	3.6902
	10	3D Elasticity [37]	2.1578	5.0356	2.2003	5.0572	7.9242	7.9386	7.9627
		HOSNT12	2.1616	5.0977	2.2043	5.1202	8.1805	8.1962	8.2224
100	1	3D Elasticity [37]	0.0008	0.0020	0.0020	0.0032	0.0039	0.0051	0.0071
		HOSNT12	0.0008	0.0020	0.0020	0.0032	0.0039	0.0051	0.0071
	2	3D Elasticity [37]	0.0020	0.0067	0.0032	0.0079	0.0145	0.0157	0.0177
		HOSNT12	0.0020	0.0067	0.0032	0.0079	0.0145	0.0157	0.0177
	5	3D Elasticity [37]	0.0102	0.0393	0.0114	0.0405	0.0866	0.0877	0.0895
		HOSNT12	0.0102	0.0393	0.0114	0.0405	0.0866	0.0877	0.0895
	10	3D Elasticity [37]	0.0393	0.1503	0.0405	0.1514	0.3192	0.3201	0.3217
		HOSNT12	0.0393	0.1503	0.0405	0.1514	0.3193	0.3202	0.3218

$\upsilon = 0.3$.

- Orthotropic material

$$E_2/E_1 = 0.5250, \quad \upsilon_{12} = 0.4405, \quad \upsilon_{21} = 0.2312$$
$$G_{12}/E_1 = 0.2629, \quad G_{13}/E_1 = 0.1599, \quad G_{23}/E_1 = 0.2688$$

- Functionally Graded Material (FGM)

The free vibration response of FG plates is investigated using following two FGM models.

(a) Power-law model of FGM The material properties of the FG plate are assumed to be graded in the thickness direction and the volume fractions of its constituent materials, i.e., ceramic and metal are assumed to follow the power law distribution [32] expressed as:

$$V_c = \left(\frac{z}{h} + \frac{1}{2}\right)^k, \qquad V_m = 1 - V_c \tag{15}$$

in which, subscripts m and c indicate the metal and ceramic constituents of FGM, respectively; z represents the thickness coordinate ($-h/2 \leqslant z \leqslant h/2$); and k is the material gradient index ($k \geqslant 0$). The variation of the composition of ceramic and metal is linear for $k = 1$. The value of k equal to zero represents a fully ceramic plate. The variation of the ceramic volume fraction function V_c versus non-dimensional thickness of a FG plate z/h with different material gradient index k is plotted in Fig. 2. The mechanical properties of FGM are determined from the volume fraction of the material constituents. The Young's modulus, E and density of material, ρ are assumed to vary in the thickness direction based on the Voigt's rule [32] over the whole range of the volume fraction. The Poisson's ratio υ is assumed to be constant. The effective material properties of FGM with two constituents can be expressed as;

$$\begin{aligned} E(z) &= E_c V_c + E_m V_m = E_m + (E_c - E_m)\left(\frac{z}{h} + \frac{1}{2}\right)^k \\ &= E_b + (E_t - E_b)\left(\frac{z}{h} + \frac{1}{2}\right)^k \\ \rho(z) &= \rho_c V_c + \rho_m V_m = \rho_m + (\rho_c - \rho_m)\left(\frac{z}{h} + \frac{1}{2}\right)^k \\ &= \rho_b + (\rho_t - \rho_b)\left(\frac{z}{h} + \frac{1}{2}\right)^k \end{aligned} \tag{16}$$

Here subscripts b and t refer to the bottom ($z = -h/2$) and top ($z = +h/2$) surfaces of FG plate. It is clear from the assumed variation expression that the bottom surface of the FG plate is "metal rich" and the top is "ceramic rich" in constituents. Following material properties are used in the numerical exercises pertaining to free vibration of FG plates.

- Material set-1

$$\text{Metal (Aluminum)}: E_m = 70\,\text{GPa}, \quad \upsilon = 0.3, \quad \rho_m = 2707\,\text{kg/m}^3$$

$$\text{Ceramic (Zirconia)}: E_c = 151\,\text{GPa}, \quad \upsilon = 0.3, \quad \rho_c = 3000\,\text{kg/m}^3$$

Table C.1
Model-1 'HOSNT12'.

Disp. $\mathbf{X}_{12\times12}$	u_0 1	v_0 2	w_0 3	θ_x 4	θ_y 5	θ_z 6	u_0^* 7	v_0^* 8	w_0^* 9	θ_x^* 10	θ_y^* 11	θ_z^* 12
1	$+A_{1,1}\alpha_m^2$ $+B_{1,1}\beta_n^2$	$+A_{1,2}\alpha_m\beta_n$ $+B_{1,2}\alpha_m\beta_n$	0	$+A_{1,7}\alpha_m^2$ $+B_{1,5}\beta_n^2$	$+A_{1,8}\alpha_m\beta_n$ $+B_{1,6}\alpha_m\beta_n$	$-A_{1,5}\alpha_m$	$+A_{1,3}\alpha_m^2$ $+B_{1,3}\beta_n^2$	$+A_{1,4}\alpha_m\beta_n$ $+B_{1,4}\alpha_m\beta_n$	$-A_{1,11}\alpha_m$	$+A_{1,9}\alpha_m^2$ $+B_{1,7}\beta_n^2$	$+A_{1,10}\alpha_m\beta_n$ $+B_{1,8}\alpha_m\beta_n$	$-A_{1,6}\alpha_m$
2	$+A_{2,1}\alpha_m\beta_n$ $+B_{1,1}\alpha_m\beta_n$	$+A_{2,2}\beta_n^2$ $+B_{1,2}\alpha_m^2$	0	$+A_{2,7}\alpha_m\beta_n$ $+B_{1,5}\alpha_m\beta_n$	$+A_{2,8}\beta_n^2$ $+B_{1,6}\alpha_m^2$	$-A_{2,5}\beta_n$	$+A_{2,3}\alpha_m\beta_n$ $+B_{1,3}\alpha_m\beta_n$	$+A_{2,4}\beta_n^2$ $+B_{1,4}\alpha_m^2$	$-A_{2,11}\beta_n$	$+A_{2,9}\alpha_m\beta_n$ $+B_{1,7}\alpha_m\beta_n$	$+A_{2,10}\beta_n^2$ $+B_{1,8}\alpha_m^2$	$-A_{2,6}\beta_n$
3	0	0	$+D_{1,2}\alpha_m^2$ $+E_{1,2}\beta_n^2$	$+D_{1,1}\alpha_m$	$+E_{1,1}\beta_n$	$+D_{1,6}\alpha_m^2$ $+E_{1,6}\beta_n^2$	$+D_{1,5}\alpha_m$	$+E_{1,5}\beta_n$	$+D_{1,4}\alpha_m^2$ $+E_{1,4}\beta_n^2$	$+D_{1,3}\alpha_m$	$+E_{1,3}\beta_n$	$+D_{1,7}\alpha_m^2$ $+E_{1,7}\beta_n^2$
4	$+A_{7,1}\alpha_m^2$ $+B_{3,1}\beta_n^2$	$+A_{7,2}\alpha_m\beta_n$ $+B_{3,2}\alpha_m\beta_n$	$+D_{1,2}\alpha_m$	$+A_{7,7}\alpha_m^2$ $+B_{3,5}\beta_n^2$ $+D_{1,1}$	$+A_{7,8}\alpha_m\beta_n$ $+B_{3,6}\alpha_m\beta_n$	$-A_{7,5}\alpha_m$ $+D_{1,6}\alpha_m$	$+A_{7,3}\alpha_m^2$ $+B_{3,3}\beta_n^2$ $+D_{1,5}$	$+A_{7,4}\alpha_m\beta_n$ $+B_{3,4}\alpha_m\beta_n$	$-A_{7,11}\alpha_m$ $+D_{1,4}\alpha_m$	$+A_{7,9}\alpha_m^2$ $+B_{3,7}\beta_n^2$ $+D_{1,3}$	$+A_{7,10}\alpha_m\beta_n$ $+B_{3,8}\alpha_m\beta_n$	$-A_{7,6}\alpha_m$ $+D_{1,7}\alpha_m$
5	$+A_{8,1}\alpha_m\beta_n$ $+B_{3,1}\alpha_m\beta_n$	$+A_{8,2}\beta_n^2$ $+B_{3,2}\alpha_m^2$	$+E_{1,2}\beta_n$	$+A_{8,7}\alpha_m\beta_n$ $+B_{3,5}\alpha_m\beta_n$	$+A_{8,8}\beta_n^2$ $+B_{3,6}\alpha_m^2$ $+E_{1,1}$	$-A_{8,5}\beta_n$ $+E_{1,6}\beta_n$	$+A_{8,3}\alpha_m\beta_n$ $+B_{3,3}\alpha_m\beta_n$	$+A_{8,4}\beta_n^2$ $+B_{3,4}\alpha_m^2$ $+E_{1,5}$	$-A_{8,11}\beta_n$ $+E_{1,4}\beta_n$	$+A_{8,9}\alpha_m\beta_n$ $+B_{3,7}\alpha_m\beta_n$	$+A_{8,10}\beta_n^2$ $+B_{3,8}\alpha_m^2$ $+E_{1,3}$	$-A_{8,6}\beta_n$ $+E_{1,7}\beta_n$
6	$-A_{5,1}\alpha_m$	$-A_{5,2}\beta_n$	$+D_{3,2}\alpha_m^2$ $+E_{3,2}\beta_n^2$	$-A_{5,7}\alpha_m$ $+D_{3,1}\alpha_m$	$-A_{5,8}\beta_n$ $+E_{3,1}\beta_n$	$+A_{5,5}$ $+D_{3,6}\alpha_m^2$ $+E_{3,6}\beta_n^2$	$-A_{5,3}\alpha_m$ $+D_{3,5}\alpha_m$	$-A_{5,4}\beta_n$ $+E_{3,5}\beta_n$	$+A_{5,11}$ $+D_{3,4}\alpha_m^2$ $+E_{3,4}\beta_n^2$	$-A_{5,9}\alpha_m$ $+D_{3,3}\alpha_m$	$-A_{5,10}\beta_n$ $+E_{3,3}\beta_n$	$+A_{5,6}$ $+D_{3,7}\alpha_m^2$ $+E_{3,7}\beta_n^2$
7	$+A_{3,1}\alpha_m^2$ $+B_{2,1}\beta_n^2$	$+A_{3,2}\alpha_m\beta_n$ $+B_{2,2}\alpha_m\beta_n$	$+2D_{3,2}\alpha_m$	$+A_{3,7}\alpha_m^2$ $+B_{2,5}\beta_n^2$ $+2D_{3,1}$	$+A_{3,8}\alpha_m\beta_n$ $+B_{2,6}\alpha_m\beta_n$	$-A_{3,5}\alpha_m$ $+2D_{3,6}\alpha_m$	$+A_{3,3}\alpha_m^2$ $+B_{2,3}\beta_n^2$ $+2D_{3,5}$	$+A_{3,4}\alpha_m\beta_n$ $+B_{2,4}\alpha_m\beta_n$	$-A_{3,11}\alpha_m$ $+2D_{3,4}\alpha_m$	$+A_{3,9}\alpha_m^2$ $+B_{2,7}\beta_n^2$ $+2D_{3,3}$	$+A_{3,10}\alpha_m\beta_n$ $+B_{2,8}\alpha_m\beta_n$	$-A_{3,6}\alpha_m$ $+2D_{3,7}\alpha_m$
8	$+A_{4,1}\alpha_m\beta_n$ $+B_{2,1}\alpha_m\beta$	$+A_{4,2}\beta_n^2$ $+B_{2,2}\alpha_m^2$	$+2E_{3,2}\beta_n$	$+A_{4,7}\alpha_m\beta_n$ $+B_{2,5}\alpha_m\beta_n$	$+A_{4,8}\beta_n^2$ $+B_{2,6}\alpha_m^2$ $+2E_{3,1}$	$-A_{4,5}\beta_n$ $+2E_{3,6}\beta_n$	$+A_{4,3}\alpha_m\beta_n$ $+B_{2,3}\alpha_m\beta_n$	$+A_{4,4}\beta_n^2$ $+B_{2,4}\alpha_m^2$ $+2E_{3,5}$	$-A_{4,11}\beta_n$ $+2E_{3,4}\beta_n$	$+A_{4,9}\alpha_m\beta_n$ $+B_{2,7}\alpha_m\beta_n$	$+A_{4,10}\beta_n^2$ $+B_{2,8}\alpha_m^2$ $+2E_{3,3}$	$-A_{4,6}\beta_n$ $+2E_{3,7}\beta_n$
9	$-2A_{11,1}\alpha_m$	$-2A_{11,2}\beta_n$	$+D_{2,2}\alpha_m^2$ $+E_{2,2}\beta_n^2$	$-2A_{11,7}\alpha_m$ $+D_{2,1}\alpha_m$	$-2A_{11,8}\beta_n$ $+E_{2,1}\beta_n$	$+2A_{11,5}$ $+D_{2,6}\alpha_m^2$ $+E_{2,6}\beta_n^2$	$-2A_{11,3}\alpha_m$ $+D_{2,5}\alpha_m$	$-2A_{11,4}\beta_n$ $+E_{2,5}\beta_n$	$+2A_{11,11}$ $+D_{2,4}\alpha_m^2$ $+E_{2,4}\beta_n^2$	$-2A_{11,9}\alpha_m$ $+D_{2,3}\alpha_m$	$-2A_{11,10}\beta_n$ $+E_{2,3}\beta_n$	$+2A_{11,6}$ $+D_{2,7}\alpha_m^2$ $+E_{2,7}\beta_n^2$
10	$+A_{9,1}\alpha_m^2$ $+B_{4,1}\beta_n^2$	$+A_{9,2}\alpha_m\beta_n$ $+B_{4,2}\alpha_m\beta_n$	$+3D_{2,2}\alpha_m$	$+A_{9,7}\alpha_m^2$ $+B_{4,5}\beta_n^2$ $+3D_{2,1}$	$+A_{9,8}\alpha_m\beta_n$ $+B_{4,6}\alpha\beta_n$	$-A_{9,5}\alpha_m$ $+3D_{2,6}\alpha_m$	$+A_{9,3}\alpha_m^2$ $+B_{4,3}\beta_n^2$ $+3D_{2,5}$	$+A_{9,4}\alpha_m\beta_n$ $+B_{4,4}\alpha_m\beta_n$	$-A_{9,11}\alpha_m$ $+3D_{2,4}\alpha_m$	$+A_{9,9}\alpha_m^2$ $+B_{4,7}\beta_n^2$ $+3D_{2,3}$	$+A_{9,10}\alpha_m\beta_n$ $+B_{4,8}\alpha_m\beta_n$	$-A_{9,6}\alpha_m$ $+3D_{2,7}\alpha_m$
11	$+A_{10,1}\alpha_m\beta_n$ $+B_{4,1}\alpha_m\beta_n$	$+A_{10,2}\beta_n^2$ $+B_{4,2}\alpha_m^2$	$+3E_{2,2}\beta_n$	$+A_{10,7}\alpha_m\beta_n$ $+B_{4,5}\alpha_m\beta_n$	$+A_{10,8}\beta_n^2$ $+B_{4,6}\alpha_m^2$ $+3E_{2,1}$	$-A_{10,5}\beta_n$ $+3E_{2,6}\beta_n$	$+A_{10,3}\alpha_m\beta_n$ $+B_{4,3}\alpha_m\beta_n$	$+A_{10,4}\beta_n^2$ $+B_{4,4}\alpha_m^2$ $+3E_{2,5}$	$-A_{10,11}\beta_n$ $+3E_{2,4}\beta_n$	$+A_{10,9}\alpha_m\beta_n$ $+B_{4,7}\alpha_m\beta_n$	$+A_{10,10}\beta_n^2$ $+B_{4,8}\alpha_m^2$ $+3E_{2,3}$	$-A_{10,6}\beta_n$ $+3E_{2,7}\beta_n$
12	$-3A_{6,1}\alpha_m$	$-3A_{6,2}\beta_n$	$+D_{4,2}\alpha_m^2$ $+E_{4,2}\beta_n^2$	$-3A_{6,7}\alpha_m$ $+D_{4,1}\alpha_m$	$-3A_{6,8}\beta_n$ $+E_{4,1}\beta_n$	$+3A_{6,5}$ $+D_{4,6}\alpha_m^2$ $+E_{4,6}\beta_n^2$	$-3A_{6,3}\alpha_m$ $+D_{4,5}\alpha_m$	$-3A_{6,4}\beta_n$ $+E_{4,5}\beta_n$	$+3A_{6,11}$ $+D_{4,4}\alpha_m^2$ $+E_{4,4}\beta_n^2$	$-3A_{6,9}\alpha_m$ $+D_{4,3}\alpha_m$	$-3A_{6,10}\beta_n$ $+E_{4,3}\beta_n$	$+3A_{6,6}$ $+D_{4,7}\alpha_m^2$ $+E_{4,7}\beta_n^2$

- Material set-2 [23]

$$\text{Metal (Al)}: E_m = 68.9\ \text{GPa}, \quad \upsilon = 0.33, \quad \rho_m = 2700\ \text{kg/m}^3$$

$$\text{Ceramic}\ (ZrO_2): E_c = 211\ \text{GPa}, \quad \upsilon = 0.33, \quad \rho_c = 4500\ \text{kg/m}^3$$

- Material set-3 [14,16,17]

$$\text{Metal (Al)}: E_m = 70\ \text{GPa}, \quad \rho_m = 2702\ \text{kg/m}^3, \quad \upsilon = 0.30$$

$$\text{Ceramic (ZrO2)}: E_c = 200\ \text{GPa}, \quad \rho_c = 5700\ \text{kg/m}^3, \quad \upsilon = 0.30$$

(b) Exponential model of FGM

In this model, the material properties of the FG plate are assumed to be graded in the thickness direction according to an exponential law, expressed as:

$$E(z) = E_b e^{p\left(\frac{z}{h}+\frac{1}{2}\right)}; \qquad \rho(z) = \rho_b e^{p\left(\frac{z}{h}+\frac{1}{2}\right)} \tag{17}$$

Here E_b and ρ_b indicate the Young modulus and material density of the plate on its bottom surface ($z = -h/2$). $E(z)$ and $\rho(z)$ are Young modulus and material density respectively at a point located at a distance z form the plate middle surface ($z = 0$). p is the exponential index of material gradation along the thickness direction of the FG plate. Poisson's ratio is assumed to be constant. The variation of the mechanical properties versus non-dimensional thickness of plate z/h with different exponential index p is plotted in Fig. 3.

- Material set-4 [37]

$$E_b = 70\ \text{GPa}, \quad \rho_b = 2702\ \text{kg/m}^3, \quad \upsilon = 0.30, \quad p = 3$$

4.1. Free vibration of isotropic and orthotropic plates

Non-dimensional natural frequencies (bending frequencies predominantly) are evaluated using the various displacement models

Table C.2
Model-2 'HOSNT11'.

Disp.	u_0	v_0	w_0	θ_x	θ_y	θ_z	u_0^*	v_0^*	w_0^*	θ_x^*	θ_y^*
$\mathbf{X}_{11\times11}$	1	2	3	4	5	6	7	8	9	10	11
1	$+A_{1,1}\alpha_m^2$ $+B_{1,1}\beta_n^2$	$+A_{1,2}\alpha_m\beta_n$ $+B_{1,2}\alpha_m\beta_n$	0	$+A_{1,7}\alpha_m^2$ $+B_{1,5}\beta_n^2$	$+A_{1,8}\alpha_m\beta_n$ $+B_{1,6}\alpha_m\beta_n$	$-A_{1,5}\alpha_m$	$+A_{1,3}\alpha_m^2$ $+B_{1,3}\beta_n^2$	$+A_{1,4}\alpha_m\beta_n$ $+B_{1,4}\alpha_m\beta_n$	$-A_{1,11}\alpha_m$	$+A_{1,9}\alpha_m^2$ $+B_{1,7}\beta_n^2$	$+A_{1,10}\alpha_m\beta_n$ $+B_{1,8}\alpha_m\beta_n$
2	$+A_{2,1}\alpha_m\beta_n$ $+B_{1,1}\alpha_m\beta_n$	$+A_{2,2}\beta_n^2$ $+B_{1,2}\alpha_m^2$	0	$+A_{2,7}\alpha_m\beta_n$ $+B_{1,5}\alpha_m\beta_n$	$+A_{2,8}\beta_n^2$ $+B_{1,6}\alpha_m^2$	$-A_{2,5}\beta_n$	$+A_{2,3}\alpha_m\beta_n$ $+B_{1,3}\alpha_m\beta_n$	$+A_{2,4}\beta_n^2$ $+B_{1,4}\alpha_m^2$	$-A_{2,11}\beta_n$	$+A_{2,9}\alpha_m\beta_n$ $+B_{1,7}\alpha_m\beta_n$	$+A_{2,10}\beta_n^2$ $+B_{1,8}\alpha_m^2$
3	0	0	$+D_{1,2}\alpha_m^2$ $+E_{1,2}\beta_n^2$	$+D_{1,1}\alpha_m$	$+E_{1,1}\beta_n$	$+D_{1,6}\alpha_m^2$ $+E_{1,6}\beta_n^2$	$+D_{1,5}\alpha_m$	$+E_{1,5}\beta_n$	$+D_{1,4}\alpha_m^2$ $+E_{1,4}\beta_n^2$	$+D_{1,3}\alpha_m$	$+E_{1,3}\beta_n$
4	$+A_{7,1}\alpha_m^2$ $+B_{3,1}\beta_n^2$	$+A_{7,2}\alpha_m\beta_n$ $+B_{3,2}\alpha_m\beta_n$	$+D_{1,2}\alpha_m$	$+A_{7,7}\alpha_m^2$ $+B_{3,5}\beta_n^2$ $+D_{1,1}$	$+A_{7,8}\alpha_m\beta_n$ $+B_{3,6}\alpha_m\beta_n$	$-A_{7,5}\alpha_m$ $+D_{1,6}\alpha_m$	$+A_{7,3}\alpha_m^2$ $+B_{3,3}\beta_n^2$ $+D_{1,5}$	$+A_{7,4}\alpha_m\beta_n$ $+B_{3,4}\alpha_m\beta_n$	$-A_{7,11}\alpha_m$ $+D_{1,4}\alpha_m$	$+A_{7,9}\alpha_m^2$ $+B_{3,7}\beta_n^2$ $+D_{1,3}$	$+A_{7,10}\alpha_m\beta_n$ $+B_{3,8}\alpha_m\beta_n$
5	$+A_{8,1}\alpha_m\beta_n$ $+B_{3,1}\alpha_m\beta_n$	$+A_{8,2}\beta_n^2$ $+B_{3,2}\alpha_m^2$	$+E_{1,2}\beta_n$	$+A_{8,7}\alpha_m\beta_n$ $+B_{3,5}\alpha_m\beta_n$	$+A_{8,8}\beta_n^2$ $+B_{3,6}\alpha_m^2$ $+E_{1,1}$	$-A_{8,5}\beta_n$ $+E_{1,6}\beta_n$	$+A_{8,3}\alpha_m\beta_n$ $+B_{3,3}\alpha_m\beta_n$	$+A_{8,4}\beta_n^2$ $+B_{3,4}\alpha_m^2$ $+E_{1,5}$	$-A_{8,11}\beta_n$ $+E_{1,4}\beta_n$	$+A_{8,9}\alpha_m\beta_n$ $+B_{3,7}\alpha_m\beta_n$	$+A_{8,10}\beta_n^2$ $+B_{3,8}\alpha_m^2$ $+E_{1,3}$
6	$-A_{5,1}\alpha_m$	$-A_{5,2}\beta_n$	$+D_{3,2}\alpha_m^2$ $+E_{3,2}\beta_n^2$	$-A_{5,7}\alpha_m$ $+D_{3,1}\alpha_m$	$-A_{5,8}\beta_n$ $+E_{3,1}\beta_n$	$+A_{5,5}$ $+D_{3,6}\alpha_m^2$ $+E_{3,6}\beta_n^2$	$-A_{5,3}\alpha_m$ $+D_{3,5}\alpha_m$	$-A_{5,4}\beta_n$ $+E_{3,5}\beta_n$	$+A_{5,11}$ $+D_{3,4}\alpha_m^2$ $+E_{3,4}\beta_n^2$	$-A_{5,9}\alpha_m$ $+D_{3,3}\alpha_m$	$-A_{5,10}\beta_n$ $+E_{3,3}\beta_n$
7	$+A_{3,1}\alpha_m^2$ $+B_{2,1}\beta_n^2$	$+A_{3,2}\alpha_m\beta_n$ $+B_{2,2}\alpha_m\beta_n$	$+2D_{3,2}\alpha_m$	$+A_{3,7}\alpha_m^2$ $+B_{2,5}\beta_n^2$ $+2D_{3,1}$	$+A_{3,8}\alpha_m\beta_n$ $+B_{2,6}\alpha_m\beta_n$	$-A_{3,5}\alpha_m$ $+2D_{3,6}\alpha_m$	$+A_{3,3}\alpha_m^2$ $+B_{2,3}\beta_n^2$ $+2D_{3,5}$	$+A_{3,4}\alpha_m\beta_n$ $+B_{2,4}\alpha_m\beta_n$	$-A_{3,11}\alpha_m$ $+2D_{3,4}\alpha_m$	$+A_{3,9}\alpha_m^2$ $+B_{2,7}\beta_n^2$ $+2D_{3,3}$	$+A_{3,10}\alpha_m\beta_n$ $+B_{2,8}\alpha_m\beta_n$
8	$+A_{4,1}\alpha_m\beta_n$ $+B_{2,1}\alpha_m\beta_n$	$+A_{4,2}\beta_n^2$ $+B_{2,2}\alpha_m^2$	$+2E_{3,2}\beta_n$	$+A_{4,7}\alpha_m\beta_n$ $+B_{2,5}\alpha_m\beta_n$	$+A_{4,8}\beta_n^2$ $+B_{2,6}\alpha_m^2$ $+2E_{3,1}$	$-A_{4,5}\beta_n$ $+2E_{3,6}\beta_n$	$+A_{4,3}\alpha_m\beta_n$ $+B_{2,3}\alpha_m\beta_n$	$+A_{4,4}\beta_n^2$ $+B_{2,4}\alpha_m^2$ $+2E_{3,5}$	$-A_{4,11}\beta_n$ $+2E_{3,4}\beta_n$	$+A_{4,9}\alpha_m\beta_n$ $+B_{2,7}\alpha_m\beta_n$	$+A_{4,10}\beta_n^2$ $+B_{2,8}\alpha_m^2$ $+2E_{3,3}$
9	$-2A_{11,1}\alpha_m$	$-2A_{11,2}\beta_n$	$+D_{2,2}\alpha_m^2$ $+E_{2,2}\beta_n^2$	$-2A_{11,7}\alpha_m$ $+D_{2,1}\alpha_m$	$-2A_{11,8}\beta_n$ $+E_{2,1}\beta_n$	$+2A_{11,5}$ $+D_{2,6}\alpha_m^2$ $+E_{2,6}\beta_n^2$	$-2A_{11,3}\alpha_m$ $+D_{2,5}\alpha_m$	$-2A_{11,4}\beta_n$ $+E_{2,5}\beta_n$	$+2A_{11,11}$ $+D_{2,4}\alpha_m^2$ $+E_{2,4}\beta_n^2$	$-2A_{11,9}\alpha_m$ $+D_{2,3}\alpha_m$	$-2A_{11,10}\beta_n$ $+E_{2,3}\beta_n$
10	$+A_{9,1}\alpha_m^2$ $+B_{4,1}\beta_n^2$	$+A_{9,2}\alpha_m\beta_n$ $+B_{4,2}\alpha_m\beta_n$	$+3D_{2,2}\alpha_m$	$+A_{9,7}\alpha_m^2$ $+B_{4,5}\beta_n^2$ $+3D_{2,1}$	$+A_{9,8}\alpha_m\beta_n$ $+B_{4,6}\alpha_m\beta_n$	$-A_{9,5}\alpha_m$ $+3D_{2,6}\alpha_m$	$+A_{9,3}\alpha_m^2$ $+B_{4,3}\beta_n^2$ $+3D_{2,5}$	$+A_{9,4}\alpha_m\beta_n$ $+B_{4,4}\alpha_m\beta_n$	$-A_{9,11}\alpha_m$ $+3D_{2,4}\alpha_m$	$+A_{9,9}\alpha_m^2$ $+B_{4,7}\beta_n^2$ $+3D_{2,3}$	$+A_{9,10}\alpha_m\beta_n$ $+B_{4,8}\alpha_m\beta_n$
11	$+A_{10,1}\alpha_m\beta_n$ $+B_{4,1}\alpha_m\beta_n$	$+A_{10,2}\beta_n^2$ $+B_{4,2}\alpha_m^2$	$+3E_{2,2}\beta_n$	$+A_{10,7}\alpha_m\beta_n$ $+B_{4,5}\alpha_m\beta_n$	$+A_{10,8}\beta_n^2$ $+B_{4,6}\alpha_m^2$ $+3E_{2,1}$	$-A_{10,5}\beta_n$ $+3E_{2,6}\beta_n$	$+A_{10,3}\alpha_m\beta_n$ $+B_{4,3}\alpha_m\beta_n$	$+A_{10,4}\beta_n^2$ $+B_{4,4}\alpha_m^2$ $+3E_{2,5}$	$-A_{10,11}\beta_n$ $+3E_{2,4}\beta_n$	$+A_{10,9}\alpha_m\beta_n$ $+B_{4,7}\alpha_m\beta_n$	$+A_{10,10}\beta_n^2$ $+B_{4,8}\alpha_m^2$ $+3E_{2,3}$

considered in the present study for isotropic and orthotropic square plates, and are tabulated in Tables 3 and 4 respectively. These tables also show the exact 3D elasticity solutions [7,8] and the available solutions by other plate theories, viz., Reddy's TSDT, Mindlin's FOST, Kirchhoff's CPT (without accounting for the rotary inertias), Senthilnathan et al. [33], and refined plate theory (RPT) [34,35]. Present results are obtained using same values of m and n as those used for obtaining results using 3D elasticity exact theory [7,8].

4.2. Free vibration of FG plates

Example-1: Free vibration of FG plates using Material set-1.

The various displacement models are used here to evaluate the natural frequencies of simply (diaphragm) supported FG plates of several geometrical/material configurations, viz., aspect ratio (b/a), side-to-thickness ratio (a/h) and material gradient index (k). The FG Material set-1 is used for the numerical exercises. The exact solutions using 3D elasticity theory are available for $b/a = 1$ and $a/h = 10$ in [7], and for $b/a = \sqrt{2}$ and $a/h = 10$ in [36]. A comparison between these results and the present solutions is shown in Table 5. The comparison shows that HOSNT12, HOSNT11 and HOSNT10B solutions are in excellent agreement with the 3D elasticity solutions. In fact, these three models provide the zero error solutions in this particular case. HOSNT10M has 9.84% error, which is much more than even CPT and FOST solutions with the errors of 2.4% and 0.21% respectively. This particular model (HOSNT10M) has significant errors in computing free vibration parameters of plates, in general. The influence of constituents' volume fraction on natural frequencies of FG plate is studied by varying the material gradient index, k. As can be seen from the presented results, the natural frequencies decreased with increase k. The natural frequencies of rectangular plate with $b = \sqrt{2}a$ are smaller than the other one, $b = a$.

In Table 6, the free vibration parameters of square and rectangular FG plates are presented for different a/h ratios using the various displacement models considered in the present study. The results show that for thin plates ($a/h > 10$), all these models provide more or less the similar solutions. But, for thick plates ($a/h < 10$), the results are quite different. The effectiveness of higher order model HOSNT12 can be easily observed by the presented results for thick FG plates. Also, when the ratio a/h is small (thicker plates), the difference between the results are more. The natural frequency of simply (diaphragm) supported FG plates against k for various a/h and for $b/a = 1$ and $\sqrt{2}$ are plotted in Figs. 4 and 5 respectively based on the model 'HOSNT12'. The fundamental nat-

Table C.3
Model-3 'HOSNT11M'.

Disp. $\mathbf{X}_{11\times11}$	u_0 1	v_0 2	w_0 3	θ_x 4	θ_y 5	θ_z 6	u_0^* 7	v_0^* 8	θ_x^* 9	θ_y^* 10	θ_z^* 11
1	$+A_{1,1}\alpha_m^2$ $+B_{1,1}\beta_n^2$	$+A_{1,2}\alpha_m\beta_n$ $+B_{1,2}\alpha_m\beta_n$	0	$+A_{1,7}\alpha_m^2$ $+B_{1,5}\beta_n^2$	$+A_{1,8}\alpha_m\beta_n$ $+B_{1,6}\alpha_m\beta_n$	$-A_{1,5}\alpha_m$	$+A_{1,3}\alpha_m^2$ $+B_{1,3}\beta_n^2$	$+A_{1,4}\alpha_m\beta_n$ $+B_{1,4}\alpha_m\beta_n$	$+A_{1,9}\alpha_m^2$ $+B_{1,7}\beta_n^2$	$+A_{1,10}\alpha_m\beta_n$ $+B_{1,8}\alpha_m\beta_n$	$-A_{1,6}\alpha_m$
2	$+A_{2,1}\alpha_m\beta_n$ $+B_{1,1}\alpha_m\beta_n$	$+A_{2,2}\beta_n^2$ $+B_{1,2}\alpha_m^2$	0	$+A_{2,7}\alpha_m\beta_n$ $+B_{1,5}\alpha_m\beta_n$	$+A_{2,8}\beta_n^2$ $+B_{1,6}\alpha_m^2$	$-A_{2,5}\beta_n$	$+A_{2,3}\alpha_m\beta_n$ $+B_{1,3}\alpha_m\beta_n$	$+A_{2,4}\beta_n^2$ $+B_{1,4}\alpha_m^2$	$+A_{2,9}\alpha_m\beta_n$ $+B_{1,7}\alpha_m\beta_n$	$+A_{2,10}\beta_n^2$ $+B_{1,8}\alpha_m^2$	$-A_{2,6}\beta_n$
3	0	0	$+D_{1,2}\alpha_m^2$ $+E_{1,2}\beta_n^2$	$+D_{1,1}\alpha_m$	$+E_{1,1}\beta_n$	$+D_{1,6}\alpha_m^2$ $+E_{1,6}\beta_n^2$	$+D_{1,5}\alpha_m$	$+E_{1,5}\beta_n$	$+D_{1,3}\alpha_m$	$+E_{1,3}\beta_n$	$+D_{1,7}\alpha_m^2$ $+E_{1,7}\beta_n^2$
4	$+A_{7,1}\alpha_m^2$ $+B_{3,1}\beta_n^2$	$+A_{7,2}\alpha_m\beta_n$ $+B_{3,2}\alpha_m\beta_n$	$+D_{1,2}\alpha_m$	$+A_{7,7}\alpha_m^2$ $+B_{3,5}\beta_n^2$ $+D_{1,1}$	$+A_{7,8}\alpha_m\beta_n$ $+B_{3,6}\alpha_m\beta_n$	$-A_{7,5}\alpha_m$ $+D_{1,6}\alpha_m$	$+A_{7,3}\alpha_m^2$ $+B_{3,3}\beta_n^2$ $+D_{1,5}$	$+A_{7,4}\alpha_m\beta_n$ $+B_{3,4}\alpha_m\beta_n$	$+A_{7,9}\alpha_m^2$ $+B_{3,7}\beta_n^2$ $+D_{1,3}$	$+A_{7,10}\alpha_m\beta_n$ $+B_{3,8}\alpha_m\beta_n$	$-A_{7,6}\alpha_m$ $+D_{1,7}\alpha_m$
5	$+A_{8,1}\alpha_m\beta_n$ $+B_{3,1}\alpha_m\beta_n$	$+A_{8,2}\beta_n^2$ $+B_{3,2}\alpha_m^2$	$+E_{1,2}\beta_n$	$+A_{8,7}\alpha_m\beta_n$ $+B_{3,5}\alpha_m\beta_n$	$+A_{8,8}\beta_n^2$ $+B_{3,6}\alpha_m^2$ $+E_{1,1}$	$-A_{8,5}\beta_n$ $+E_{1,6}\beta_n$	$+A_{8,3}\alpha_m\beta_n$ $+B_{3,3}\alpha_m\beta_n$	$+A_{8,4}\beta_n^2$ $+B_{3,4}\alpha_m^2$ $+E_{1,5}$	$+A_{8,9}\alpha_m\beta_n$ $+B_{3,7}\alpha_m\beta_n$	$+A_{8,10}\beta_n^2$ $+B_{3,8}\alpha_m^2$ $+E_{1,3}$	$-A_{8,6}\beta_n$ $+E_{1,7}\beta_n$
6	$-A_{5,1}\alpha_m$	$-A_{5,2}\beta_n$	$+D_{3,2}\alpha_m^2$ $+E_{3,2}\beta_n^2$	$-A_{5,7}\alpha_m$ $+D_{3,1}\alpha_m$	$-A_{5,8}\beta_n$ $+E_{3,1}\beta_n$	$+A_{5,5}$ $+D_{3,6}\alpha_m^2$ $+E_{3,6}\beta_n^2$	$-A_{5,3}\alpha_m$ $+D_{3,5}\alpha_m$	$-A_{5,4}\beta_n$ $+E_{3,5}\beta_n$	$-A_{5,9}\alpha_m$ $+D_{3,3}\alpha_m$	$-A_{5,10}\beta_n$ $+E_{3,3}\beta_n$	$+A_{5,6}$ $+D_{3,7}\alpha_m^2$ $+E_{3,7}\beta_n^2$
7	$+A_{3,1}\alpha_m^2$ $+B_{2,1}\beta_n^2$	$+A_{3,2}\alpha_m\beta_n$ $+B_{2,2}\alpha_m\beta_n$	$+2D_{3,2}\alpha_m$	$+A_{3,7}\alpha_m^2$ $+B_{2,5}\beta_n^2$ $+2D_{3,1}$	$+A_{3,8}\alpha_m\beta_n$ $+B_{2,6}\alpha_m\beta_n$	$-A_{3,5}\alpha_m$ $+2D_{3,6}\alpha_m$	$+A_{3,3}\alpha_m^2$ $+B_{2,3}\beta_n^2$ $+2D_{3,5}$	$+A_{3,4}\alpha_m\beta_n$ $+B_{2,4}\alpha_m\beta_n$	$+A_{3,9}\alpha_m^2$ $+B_{2,7}\beta_n^2$ $+2D_{3,3}$	$+A_{3,10}\alpha_m\beta_n$ $+B_{2,8}\alpha_m\beta_n$	$-A_{3,6}\alpha_m$ $+2D_{3,7}\alpha_m$
8	$+A_{4,1}\alpha_m\beta_n$ $+B_{2,1}\alpha_m\beta_n$	$+A_{4,2}\beta_n^2$ $+B_{2,2}\alpha_m^2$	$+2E_{3,2}\beta_n$	$+A_{4,7}\alpha_m\beta_n$ $+B_{2,5}\alpha_m\beta_n$	$+A_{4,8}\beta_n^2$ $+B_{2,6}\alpha_m^2$ $+2E_{3,1}$	$-A_{4,5}\beta_n$ $+2E_{3,6}\beta_n$	$+A_{4,3}\alpha_m\beta_n$ $+B_{2,3}\alpha_m\beta_n$	$+A_{4,4}\beta_n^2$ $+B_{2,4}\alpha_m^2$ $+2E_{3,5}$	$+A_{4,9}\alpha_m\beta_n$ $+B_{2,7}\alpha_m\beta_n$	$+A_{4,10}\beta_n^2$ $+B_{2,8}\alpha_m^2$ $+2E_{3,3}$	$-A_{4,6}\beta_n$ $+2E_{3,7}\beta_n$
9	$+A_{9,1}\alpha_m^2$ $+B_{4,1}\beta_n^2$	$+A_{9,2}\alpha_m\beta_n$ $+B_{4,2}\alpha_m\beta_n$	$+3D_{2,2}\alpha_m$	$+A_{9,7}\alpha_m^2$ $+B_{4,5}\beta_n^2$ $+3D_{2,1}$	$+A_{9,8}\alpha_m\beta_n$ $+B_{4,6}\alpha_m\beta_n$	$-A_{9,5}\alpha_m$ $+3D_{2,6}\alpha_m$	$+A_{9,3}\alpha_m^2$ $+B_{4,3}\beta_n^2$ $+3D_{2,5}$	$+A_{9,4}\alpha_m\beta_n$ $+B_{4,4}\alpha_m\beta_n$	$+A_{9,9}\alpha_m^2$ $+B_{4,7}\beta_n^2$ $+3D_{2,3}$	$+A_{9,10}\alpha_m\beta_n$ $+B_{4,8}\alpha_m\beta_n$	$-A_{9,6}\alpha_m$ $+3D_{2,7}\alpha_m$
10	$+A_{10,1}\alpha_m\beta_n$ $+B_{4,1}\alpha_m\beta_n$	$+A_{10,2}\beta_n^2$ $+B_{4,2}\alpha_m^2$	$+3E_{2,2}\beta_n$	$+A_{10,7}\alpha_m\beta_n$ $+B_{4,5}\alpha_m\beta_n$	$+A_{10,8}\beta_n^2$ $+B_{4,6}\alpha_m^2$ $+3E_{2,1}$	$-A_{10,5}\beta_n$ $+3E_{2,6}\beta_n$	$+A_{10,3}\alpha_m\beta_n$ $+B_{4,3}\alpha_m\beta_n$	$+A_{10,4}\beta_n^2$ $+B_{4,4}\alpha_m^2$ $+3E_{2,5}$	$+A_{10,9}\alpha_m\beta_n$ $+B_{4,7}\alpha_m\beta_n$	$+A_{10,10}\beta_n^2$ $+B_{4,8}\alpha_m^2$ $+3E_{2,3}$	$-A_{10,6}\beta_n$ $+3E_{2,7}\beta_n$
11	$-3A_{6,1}\alpha_m$	$-3A_{6,2}\beta_n$	$+D_{4,2}\alpha_m^2$ $+E_{4,2}\beta_n^2$	$-3A_{6,7}\alpha_m$ $+D_{4,1}\alpha_m$	$-3A_{6,8}\beta_n$ $+E_{4,1}\beta_n$	$+3A_{6,5}$ $+D_{4,6}\alpha_m^2$ $+E_{4,6}\beta_n^2$	$-3A_{6,3}\alpha_m$ $+D_{4,5}\alpha_m$	$-3A_{6,4}\beta_n$ $+E_{4,5}\beta_n$	$-3A_{6,9}\alpha_m$ $+D_{4,3}\alpha_m$	$-3A_{6,10}\beta_n$ $+E_{4,3}\beta_n$	$+3A_{6,6}$ $+D_{4,7}\alpha_m^2$ $+E_{4,7}\beta_n^2$

ural frequency decreases significantly with increase of the metal percentage of FGM. It is basically due to the fact that the Young's modulus of ceramic is higher than metal. It is worth noting that, as a/h increases, the natural frequencies decreases because of the decrease in stiffness of the plate.

Example-2: Free vibration of FG plates using Material set-2.

There is one another kind of non-dimensionalization of natural frequency parameter available in the literature [23–26]. The non-dimensional frequency in these references is defined as $\tilde{\bar{\omega}}_{mn}$ (in Table 2). The FG Material set-2 is used for the numerical exercises. This kind of non-dimensional fundamental natural frequency $\tilde{\bar{\omega}}_{mn}(m=n=1)$ is also evaluated using HOSNT12 for various k, a/h and b/a, and presented in Table 7 along with $\bar{\omega}_{mn}(m=n=1)$ for making a comparison of the two different non-dimensional natural frequency parameters. It can be clearly seen from the presented results that this non-dimensional frequency parameter also decreases with increase of material gradient index (k). Here, it is interesting to note that this non-dimensional frequency increases with the increase of side-to-thickness ratio (a/h) of the plate. This is because of the fact that the a/h term is getting multiplied into the non-dimensional frequency parameter.

In Table 8, non-dimensional frequency $\tilde{\bar{\omega}}_{mn}$ of rectangular FG plates ($b/a = 2, a/h = 10$) with zirconia as upper-surface ceramic and aluminum as lower-surface metal is evaluated based on HOSNT12. The present solutions are compared with the SSDT solutions [23] taking the similar material properties (FG Material set-2). The non-dimensional fundamental natural frequency, $\tilde{\bar{\omega}}_{mn}(m=n=1)$ of simply (diaphragm) supported rectangular FG plates ($b/a = 2$) against material gradient index (k) for various values of side-to-thickness ratios (a/h) is plotted in Fig. 6 based on HOSNT12. The same parameter is plotted against side-to-thickness ratio (a/h) for different material gradient index (k) in Fig. 7. As can be seen, the frequency decreases significantly with the increase of k. It is basically due to the fact that the Young's modulus of ceramic is higher than metal. The variation of frequency parameter with aspect ratios (b/a) of FG plates using HOSNT12 is plotted in Figs. 8 and 9. As can be seen from the presented results, the natural frequencies decrease with increasing value of material gradient index, k for the same mode. For the same value of k, natural frequency increases for the higher modes. Actually, this kind of non-dimensionalization defies the physical characteristics of the frequency parameter, although mathematically it is all right. With the increase of side-to-thickness ratio (a/h) of the plate, the plates become thin, hence becomes more flexible, the fundamental natural frequency must decrease because of the reduced stiffness of plate.

Table C.4
Model-4 'HOSNT10B'.

Disp. $\mathbf{X}_{10\times10}$	u_0 1	v_0 2	w_0 3	θ_x 4	θ_y 5	u_0^* 6	v_0^* 7	w_0^* 8	θ_x^* 9	θ_y^* 10
1	$+A_{1,1}\alpha_m^2$ $+B_{1,1}\beta_n^2$	$+A_{1,2}\alpha_m\beta_n$ $+B_{1,2}\alpha_m\beta_n$	0	$+A_{1,7}\alpha_m^2$ $+B_{1,5}\beta_n^2$	$+A_{1,8}\alpha_m\beta_n$ $+B_{1,6}\alpha_m\beta_n$	$+A_{1,3}\alpha_m^2$ $+B_{1,3}\beta_n^2$	$+A_{1,4}\alpha_m\beta_n$ $+B_{1,4}\alpha_m\beta_n$	$-A_{1,11}\alpha_m$	$+A_{1,9}\alpha_m^2$ $+B_{1,7}\beta_n^2$	$+A_{1,10}\alpha_m\beta_n$ $+B_{1,8}\alpha_m\beta_n$
2	$+A_{2,1}\alpha_m\beta_n$ $+B_{1,1}\alpha_m\beta_n$	$+A_{2,2}\beta_n^2$ $+B_{1,2}\alpha_m^2$	0	$+A_{2,7}\alpha_m\beta_n$ $+B_{1,5}\alpha_m\beta_n$	$+A_{2,8}\beta_n^2$ $+B_{1,6}\alpha_m^2$	$+A_{2,3}\alpha_m\beta_n$ $+B_{1,3}\alpha_m\beta_n$	$+A_{2,4}\beta_n^2$ $+B_{1,4}\alpha_m^2$	$-A_{2,11}\beta_n$	$+A_{2,9}\alpha_m\beta_n$ $+B_{1,7}\alpha_m\beta_n$	$+A_{2,10}\beta_n^2$ $+B_{1,8}\alpha_m^2$
3	0	0	$+D_{1,2}\alpha_m^2$ $+E_{1,2}\beta_n^2$	$+D_{1,1}\alpha_m$	$+E_{1,1}\beta_n$	$+D_{1,5}\alpha_m$	$+E_{1,5}\beta_n$	$+D_{1,4}\alpha_m^2$ $+E_{1,4}\beta_n^2$	$+D_{1,3}\alpha_m$	$+E_{1,3}\beta_n$
4	$+A_{7,1}\alpha_m^2$ $+B_{3,1}\beta_n^2$	$+A_{7,2}\alpha_m\beta_n$ $+B_{3,2}\alpha_m\beta_n$	$+D_{1,2}\alpha_m$	$+A_{7,7}\alpha_m^2$ $+B_{3,5}\beta_n^2$ $+D_{1,1}$	$+A_{7,8}\alpha_m\beta_n$ $+B_{3,6}\alpha_m\beta_n$	$+A_{7,3}\alpha_m^2$ $+B_{3,3}\beta_n^2$ $+D_{1,5}$	$+A_{7,4}\alpha_m\beta_n$ $+B_{3,4}\alpha_m\beta_n$	$-A_{7,11}\alpha_m$ $+D_{1,4}\alpha_m$	$+A_{7,9}\alpha_m^2$ $+B_{3,7}\beta_n^2$ $+D_{1,3}$	$+A_{7,10}\alpha_m\beta_n$ $+B_{3,8}\alpha_m\beta_n$
5	$+A_{8,1}\alpha_m\beta_n$ $+B_{3,1}\alpha_m\beta_n$	$+A_{8,2}\beta_n^2$ $+B_{3,2}\alpha_m^2$	$+E_{1,2}\beta_n$	$+A_{8,7}\alpha_m\beta_n$ $+B_{3,5}\alpha_m\beta_n$	$+A_{8,8}\beta_n^2$ $+B_{3,6}\alpha_m^2$ $+E_{1,1}$	$+A_{8,3}\alpha_m\beta_n$ $+B_{3,3}\alpha_m\beta_n$	$+A_{8,4}\beta_n^2$ $+B_{3,4}\alpha_m^2$ $+E_{1,5}$	$-A_{8,11}\beta_n$ $+E_{1,4}\beta_n$	$+A_{8,9}\alpha_m\beta_n$ $+B_{3,7}\alpha_m\beta_n$	$+A_{8,10}\beta_n^2$ $+B_{3,8}\alpha_m^2$ $+E_{1,3}$
6	$+A_{3,1}\alpha_m^2$ $+B_{2,1}\beta_n^2$	$+A_{3,2}\alpha_m\beta_n$ $+B_{2,2}\alpha_m\beta_n$	$+2D_{3,2}\alpha_m$	$+A_{3,7}\alpha_m^2$ $+B_{2,5}\beta_n^2$ $+2D_{3,1}$	$+A_{3,8}\alpha_m\beta_n$ $+B_{2,6}\alpha_m\beta_n$	$+A_{3,3}\alpha_m^2$ $+B_{2,3}\beta_n^2$ $+2D_{3,5}$	$+A_{3,4}\alpha_m\beta_n$ $+B_{2,4}\alpha_m\beta_n$	$-A_{3,11}\alpha_m$ $+2D_{3,4}\alpha_m$	$+A_{3,9}\alpha_m^2$ $+B_{2,7}\beta_n^2$ $+2D_{3,3}$	$+A_{3,10}\alpha_m\beta_n$ $+B_{2,8}\alpha_m\beta_n$
7	$+A_{4,1}\alpha_m\beta_n$ $+B_{2,1}\alpha_m\beta_n$	$+A_{4,2}\beta_n^2$ $+B_{2,2}\alpha_m^2$	$+2E_{3,2}\beta_n$	$+A_{4,7}\alpha_m\beta_n$ $+B_{2,5}\alpha_m\beta_n$	$+A_{4,8}\beta_n^2$ $+B_{2,6}\alpha_m^2$ $+2E_{3,1}$	$+A_{4,3}\alpha_m\beta_n$ $+B_{2,3}\alpha_m\beta_n$	$+A_{4,4}\beta_n^2$ $+B_{2,4}\alpha_m^2$ $+2E_{3,5}$	$-A_{4,11}\beta_n$ $+2E_{3,4}\beta_n$	$+A_{4,9}\alpha_m\beta_n$ $+B_{2,7}\alpha_m\beta_n$	$+A_{4,10}\beta_n^2$ $+B_{2,8}\alpha_m^2$ $+2E_{3,3}$
8	$-2A_{11,1}\alpha_m$	$-2A_{11,2}\beta_n$	$+D_{2,2}\alpha_m^2$ $+E_{2,2}\beta_n^2$	$-2A_{11,7}\alpha_m$ $+D_{2,1}\alpha_m$	$-2A_{11,8}\beta_n$ $+E_{2,1}\beta_n$	$-2A_{11,3}\alpha_m$ $+D_{2,5}\alpha_m$	$-2A_{11,4}\beta_n$ $+E_{2,5}\beta_n$	$+2A_{11,11}$ $+D_{2,4}\alpha_m^2$ $+E_{2,4}\beta_n^2$	$-2A_{11,9}\alpha_m$ $+D_{2,3}\alpha_m$	$-2A_{11,10}\beta_n$ $+E_{2,3}\beta_n$
9	$+A_{9,1}\alpha_m^2$ $+B_{4,1}\beta_n^2$	$+A_{9,2}\alpha_m\beta_n$ $+B_{4,2}\alpha_m\beta_n$	$+3D_{2,2}\alpha_m$	$+A_{9,7}\alpha_m^2$ $+B_{4,5}\beta_n^2$ $+3D_{2,1}$	$+A_{9,8}\alpha_m\beta_n$ $+B_{4,6}\alpha_m\beta_n$	$+A_{9,3}\alpha_m^2$ $+B_{4,3}\beta_n^2$ $+3D_{2,5}$	$+A_{9,4}\alpha_m\beta_n$ $+B_{4,4}\alpha_m\beta_n$	$-A_{9,11}\alpha_m$ $+3D_{2,4}\alpha_m$	$+A_{9,9}\alpha_m^2$ $+B_{4,7}\beta_n^2$ $+3D_{2,3}$	$+A_{9,10}\alpha_m\beta_n$ $+B_{4,8}\alpha_m\beta_n$
10	$+A_{10,1}\alpha_m\beta_n$ $+B_{4,1}\alpha_m\beta_n$	$+A_{10,2}\beta_n^2$ $+B_{4,2}\alpha_m^2$	$+3E_{2,2}\beta_n$	$+A_{10,7}\alpha_m\beta_n$ $+B_{4,5}\alpha_m\beta_n$	$+A_{10,8}\beta_n^2$ $+B_{4,6}\alpha_m^2$ $+3E_{2,1}$	$+A_{10,3}\alpha_m\beta_n$ $+B_{4,3}\alpha_m\beta_n$	$+A_{10,4}\beta_n^2$ $+B_{4,4}\alpha_m^2$ $+3E_{2,5}$	$-A_{10,11}\beta_n$ $+3E_{2,4}\beta_n$	$+A_{10,9}\alpha_m\beta_n$ $+B_{4,7}\alpha_m\beta_n$	$+A_{10,10}\beta_n^2$ $+B_{4,8}\alpha_m^2$ $+3E_{2,3}$

Example-3: Free vibration of FG plates using Material set-3.

The non-dimensional fundamental natural frequency using various displacement models considered in the present study are computed for FG plates comprised of aluminum and zirconia (FG Material set-3), mainly because exact solutions for a plate made of these materials are available in [14]. The same parameter has been evaluated based on various higher order plate theories by Ferreira et al. [16] and Qian et al. [17]. The comparisons of present results with these available solutions are presented in Table 9.

For an aluminum (Al)/zirconia (ZrO_2) FG plate, "thickness mode natural frequencies" $[\hat{\bar{\omega}}_{mn}(m=n=1)]$ using various models are presented along with the exact 3D elasticity solutions [14] in Tables 10 and 11. Here m and n define the in-plane mode shapes of vibration. Corresponding to each in-plane mode shape, there are as many natural frequencies (eigenvalues) as the degree of freedoms considered in the displacement model, each one of them representing a different thickness-mode. These thickness modes appear in symmetric and unsymmetric manner for the identical in-plane harmonic modes of the FG plate as has been reported by Vel and Batra [14]. The first eigenvalue is generally referred to the flexural mode eigenvalue. These parameters obtained from present models along with the exact solutions are plotted in Figs. 10 and 11. HOSNT12 and HOSNT11 models are in excellent agreement with the exact solutions. The % errors with respect to the exact solutions in the "thickness mode natural frequencies" of thick FG plates ($a/h = 5, k = 1$) using various models considered in the present study are plotted in Figs. 12 and 13. The results demonstrate that the HOSNT12 and HOSNT11 are highly accurate 2D models for studying the free vibration behavior of thick FG plates. CPT has very high errors of about 17%, and hence not suitable for modeling thick FG plates. FOST shows improved results than CPT, but the errors in the higher modes are quite significant (18% in the fifth mode). HOSNT12 and HOSNT11 have less than 5% errors in the "thickness mode natural frequencies" up-to fifth thickness modes.

Example-4: Free vibration of FG plates using Material set-4.

The non-dimensional natural frequency parameter using the most accurate Model-1 (HOSNT12) are computed for FG plates of different aspect and side-to-thickness ratios using FG Material set-4, and compared with the 3D elasticity solutions [37]. The comparison is presented in Table 12. The HOSNT12 model is in excellent agreement with the 3D elasticity solutions even for higher modes of vibration.

5. Conclusions

In this article, the displacement based higher order 2D plate theories for the free vibration of thick FG elastic, rectangular plates are presented. Some of these theories account for both the transverse shear and normal deformations of the plate. Free vibration of FG plates with simply (diaphragm) supported edge conditions are carried out assuming the variation of material properties of FG plates in its thickness direction to follow both power and expo-

Table C.5
Model-5 'HOSNT10M'.

Disp. $\mathbf{X}_{10\times10}$	u_0 1	v_0 2	w_0 3	θ_x 4	θ_y 5	θ_z 6	u_0^* 7	v_0^* 8	θ_x^* 9	θ_y^* 10
1	$+A_{1,1}\alpha_m^2$ $+B_{1,1}\beta_n^2$	$+A_{1,2}\alpha_m\beta_n$ $+B_{1,2}\alpha_m\beta_n$	0	$+A_{1,7}\alpha_m^2$ $+B_{1,5}\beta_n^2$	$+A_{1,8}\alpha_m\beta_n$ $+B_{1,6}\alpha_m\beta_n$	$-A_{1,5}\alpha_m$	$+A_{1,3}\alpha_m^2$ $+B_{1,3}\beta_n^2$	$+A_{1,4}\alpha_m\beta_n$ $+B_{1,4}\alpha_m\beta_n$	$+A_{1,9}\alpha_m^2$ $+B_{1,7}\beta_n^2$	$+A_{1,10}\alpha_m\beta_n$ $+B_{1,8}\alpha_m\beta_n$
2	$+A_{2,1}\alpha_m\beta_n$ $+B_{1,1}\alpha_m\beta_n$	$+A_{2,2}\beta_n^2$ $+B_{1,2}\alpha_m^2$	0	$+A_{2,7}\alpha_m\beta_n$ $+B_{1,5}\alpha_m\beta_n$	$+A_{2,8}\beta_n^2$ $+B_{1,6}\alpha_m^2$	$-A_{2,5}\beta_n$	$+A_{2,3}\alpha_m\beta_n$ $+B_{1,3}\alpha_m\beta_n$	$+A_{2,4}\beta_n^2$ $+B_{1,4}\alpha_m^2$	$+A_{2,9}\alpha_m\beta_n$ $+B_{1,7}\alpha_m\beta_n$	$+A_{2,10}\beta_n^2$ $+B_{1,8}\alpha_m^2$
3	0	0	$+D_{1,2}\alpha_m^2$ $+E_{1,2}\beta_n^2$	$+D_{1,1}\alpha_m$	$+E_{1,1}\beta_n$	$+D_{1,6}\alpha_m^2$ $+E_{1,6}\beta_n^2$	$+D_{1,5}\alpha_m$	$+E_{1,5}\beta_n$	$+D_{1,3}\alpha_m$	$+E_{1,3}\beta_n$
4	$+A_{7,1}\alpha_m^2$ $+B_{3,1}\beta_n^2$	$+A_{7,2}\alpha_m\beta_n$ $+B_{3,2}\alpha_m\beta_n$	$+D_{1,2}\alpha_m$	$+A_{7,7}\alpha_m^2$ $+B_{3,5}\beta_n^2$ $+D_{1,1}$	$+A_{7,8}\alpha_m\beta_n$ $+B_{3,6}\alpha_m\beta_n$	$-A_{7,5}\alpha_m$ $+D_{1,6}\alpha_m$	$+A_{7,3}\alpha_m^2$ $+B_{3,3}\beta_n^2$ $+D_{1,5}$	$+A_{7,4}\alpha_m\beta_n$ $+B_{3,4}\alpha_m\beta_n$	$+A_{7,9}\alpha_m^2$ $+B_{3,7}\beta_n^2$ $+D_{1,3}$	$+A_{7,10}\alpha_m\beta_n$ $+B_{3,8}\alpha_m\beta_n$
5	$+A_{8,1}\alpha_m\beta_n$ $+B_{3,1}\alpha_m\beta_n$	$+A_{8,2}\beta_n^2$ $+B_{3,2}\alpha_m^2$	$+E_{1,2}\beta_n$	$+A_{8,7}\alpha_m\beta_n$ $+B_{3,5}\alpha_m\beta_n$	$+A_{8,8}\beta_n^2$ $+B_{3,6}\alpha_m^2$ $+E_{1,1}$	$-A_{8,5}\beta_n$ $+E_{1,6}\beta_n$	$+A_{8,3}\alpha_m\beta_n$ $+B_{3,3}\alpha_m\beta_n$	$+A_{8,4}\beta_n^2$ $+B_{3,4}\alpha_m^2$ $+E_{1,5}$	$+A_{8,9}\alpha_m\beta_n$ $+B_{3,7}\alpha_m\beta_n$	$+A_{8,10}\beta_n^2$ $+B_{3,8}\alpha_m^2$ $+E_{1,3}$
6	$-A_{5,1}\alpha_m$	$-A_{5,2}\beta_n$	$+D_{3,2}\alpha_m^2$ $+E_{3,2}\beta_n^2$	$-A_{5,7}\alpha_m$ $+D_{3,1}\alpha_m$	$-A_{5,8}\beta_n$ $+E_{3,1}\beta_n$	$+A_{5,5}$ $+D_{3,6}\alpha_m^2$ $+E_{3,6}\beta_n^2$	$-A_{5,3}\alpha_m$ $+D_{3,5}\alpha_m$	$-A_{5,4}\beta_n$ $+E_{3,5}\beta_n$	$-A_{5,9}\alpha_m$ $+D_{3,3}\alpha_m$	$-A_{5,10}\beta_n$ $+E_{3,3}\beta_n$
7	$+A_{3,1}\alpha_m^2$ $+B_{2,1}\beta_n^2$	$+A_{3,2}\alpha_m\beta_n$ $+B_{2,2}\alpha_m\beta_n$	$+2D_{3,2}\alpha_m$	$+A_{3,7}\alpha_m^2$ $+B_{2,5}\beta_n^2$ $+2D_{3,1}$	$+A_{3,8}\alpha_m\beta_n$ $+B_{2,6}\alpha_m\beta_n$	$-A_{3,5}\alpha_m$ $+2D_{3,6}\alpha_m$	$+A_{3,3}\alpha_m^2$ $+B_{2,3}\beta_n^2$ $+2D_{3,5}$	$+A_{3,4}\alpha_m\beta_n$ $+B_{2,4}\alpha_m\beta_n$	$+A_{3,9}\alpha_m^2$ $+B_{2,7}\beta_n^2$ $+2D_{3,3}$	$+A_{3,10}\alpha_m\beta_n$ $+B_{2,8}\alpha_m\beta_n$
8	$+A_{4,1}\alpha_m\beta_n$ $+B_{2,1}\alpha_m\beta_n$	$+A_{4,2}\beta_n^2$ $+B_{2,2}\alpha_m^2$	$+2E_{3,2}\beta_n$	$+A_{4,7}\alpha_m\beta_n$ $+B_{2,5}\alpha_m\beta_n$	$+A_{4,8}\beta_n^2$ $+B_{2,6}\alpha_m^2$ $+2E_{3,1}$	$-A_{4,5}\beta_n$ $+2E_{3,6}\beta_n$	$+A_{4,3}\alpha_m\beta_n$ $+B_{2,3}\alpha_m\beta_n$	$+A_{4,4}\beta_n^2$ $+B_{2,4}\alpha_m^2$ $+2E_{3,5}$	$+A_{4,9}\alpha_m\beta_n$ $+B_{2,7}\alpha_m\beta_n$	$+A_{4,10}\beta_n^2$ $+B_{2,8}\alpha_m^2$ $+2E_{3,3}$
9	$+A_{9,1}\alpha_m^2$ $+B_{4,1}\beta_n^2$	$+A_{9,2}\alpha_m\beta_n$ $+B_{4,2}\alpha_m\beta_n$	$+3D_{2,2}\alpha_m$	$+A_{9,7}\alpha_m^2$ $+B_{4,5}\beta_n^2$ $+3D_{2,1}$	$+A_{9,8}\alpha_m\beta_n$ $+B_{4,6}\alpha_m\beta_n$	$-A_{9,5}\alpha_m$ $+3D_{2,6}\alpha_m$	$+A_{9,3}\alpha_m^2$ $+B_{4,3}\beta_n^2$ $+3D_{2,5}$	$+A_{9,4}\alpha_m\beta_n$ $+B_{4,4}\alpha_m\beta_n$	$+A_{9,9}\alpha_m^2$ $+B_{4,7}\beta_n^2$ $+3D_{2,3}$	$+A_{9,10}\alpha_m\beta_n$ $+B_{4,8}\alpha_m\beta_n$
10	$+A_{10,1}\alpha_m\beta_n$ $+B_{4,1}\alpha_m\beta_n$	$+A_{10,2}\beta_n^2$ $+B_{4,2}\alpha_m^2$	$+3E_{2,2}\beta_n$	$+A_{10,7}\alpha_m\beta_n$ $+B_{4,5}\alpha_m\beta_n$	$+A_{10,8}\beta_n^2$ $+B_{4,6}\alpha_m^2$ $+3E_{2,1}$	$-A_{10,5}\beta_n$ $+3E_{2,6}\beta_n$	$+A_{10,3}\alpha_m\beta_n$ $+B_{4,3}\alpha_m\beta_n$	$+A_{10,4}\beta_n^2$ $+B_{4,4}\alpha_m^2$ $+3E_{2,5}$	$+A_{10,9}\alpha_m\beta_n$ $+B_{4,7}\alpha\ \beta_n$	$+A_{10,10}\beta_n^2$ $+B_{4,8}\alpha_m^2$ $+3E_{2,3}$

nential law distributions. Navier solution technique employing double Fourier series is used to get the results with desired level of accuracy. The present numerical solutions are compared with the available exact 3D elasticity solutions and also with the solutions available using other 2D models in the literature under similar edge conditions and material grading through the thickness. The numerical solutions obtained using some of the higher order models (in particular, HOSNT12 and HOSNT11 models) used in the present study are in excellent agreement with the exact 3D elasticity solutions. These high accurate numerical solutions can be used as benchmark to assess any other analytical/computational model for FG plates. The results show that the natural frequencies decrease with increasing the material gradient index as well as side-to-thickness ratios.

The comparative study of HOSNT12 and HOSNT11 results with the other HOSNTs/HOSTs/FOST/CPT available in the literature (some of them are considered in the present study too) establish that these two models, HOSNT12 and HOSNT11 have the improved accuracy for thicker plates. The difference in the numerical solutions of higher order models HOSNT12 and HOSNT11 are only observed after the side-to-thickness ratios of plates become less than 5 (very thick plate). The difference occurs only at the second decimal place and hence is quite insignificant. The accuracy of the HOSNT11 solutions for free vibration problems is as good as HOSNT12, and therefore including the higher order membrane term (θ_z^*) in the theoretical formulation for defining the transverse displacement (w) has no significant contribution, as such. Thus, HOSNT11 may be treated as the most accurate and justified higher order displacement model for the analysis of both thick and thin FG plates. Although the presented formulation for FG plates using higher order models, viz., HOSNT12 and HOSNT11 involve large computations compared to FOST and CPT, but the obtained numerical results are very accurate when compared to 3D elasticity solutions. The benefit of this approach is that a 2D theory is able to predict solutions as good as 3D elasticity solutions.

Appendix A. Equations of motion for various displacement models other than Model-1

A.1. Model-2 'HOSNT11'

$$\delta u_o: \quad \frac{\partial N_x}{\partial x}+\frac{\partial N_{xy}}{\partial y}=i_1\ddot{u}_o+i_2\ddot{\theta}_x+i_3\ddot{u}_o^*+i_4\ddot{\theta}_x^*$$

$$\delta v_o: \quad \frac{\partial N_y}{\partial y}+\frac{\partial N_{xy}}{\partial x}=i_1\ddot{v}_o+i_2\ddot{\theta}_y+i_3\ddot{v}_o^*+i_4\ddot{\theta}_y^*$$

$$\delta w_o: \quad \frac{\partial Q_x}{\partial x}+\frac{\partial Q_y}{\partial y}=i_1\ddot{w}_o+i_2\ddot{\theta}_z+i_3\ddot{w}_o^*$$

$$\delta\theta_x: \quad \frac{\partial M_x}{\partial x}+\frac{\partial M_{xy}}{\partial y}-Q_x=i_2\ddot{u}_o+i_3\ddot{\theta}_x+i_4\ddot{u}_o^*+i_5\ddot{\theta}_x^*$$

Table C.6
Model-6 'HOST9'.

Disp. $\mathbf{X}_{9\times9}$	u_0 1	v_0 2	w_0 3	θ_x 4	θ_y 5	u_0^* 6	v_0^* 7	θ_x^* 8	θ_y^* 9
1	$+A_{1,1}\alpha_m^2$ $+B_{1,1}\beta_n^2$	$+A_{1,2}\alpha_m\beta_n$ $+B_{1,2}\alpha\beta_n$	0	$+A_{1,7}\alpha_m^2$ $+B_{1,5}\beta_n^2$	$+A_{1,8}\alpha_m\beta_n$ $+B_{1,6}\alpha\beta_n$	$+A_{1,3}\alpha_m^2$ $+B_{1,3}\beta_n^2$	$+A_{1,4}\alpha_m\beta_n$ $+B_{1,4}\alpha\beta_n$	$+A_{1,9}\alpha_m^2$ $+B_{1,7}\beta_n^2$	$+A_{1,10}\alpha_m\beta_n$ $+B_{1,8}\alpha_m\beta_n$
2	$+A_{2,1}\alpha_m\beta_n$ $+B_{1,1}\alpha_m\beta_n$	$+A_{2,2}\beta_n^2$ $+B_{1,2}\alpha_m^2$	0	$+A_{2,7}\alpha_m\beta_n$ $+B_{1,5}\alpha_m\beta_n$	$+A_{2,8}\beta_n^2$ $+B_{1,6}\alpha_m^2$	$+A_{2,3}\alpha_m\beta_n$ $+B_{1,3}\alpha_m\beta_n$	$+A_{2,4}\beta_n^2$ $+B_{1,4}\alpha_m^2$	$+A_{2,9}\alpha_m\beta_n$ $+B_{1,7}\alpha_m\beta_n$	$+A_{2,10}\beta_n^2$ $+B_{1,8}\alpha_m^2$
3	0	0	$+D_{1,2}\alpha_m^2$ $+E_{1,2}\beta_n^2$	$+D_{1,1}\alpha_m$	$+E_{1,1}\beta_n$	$+D_{1,5}\alpha_m$	$+E_{1,5}\beta_n$	$+D_{1,3}\alpha_m$	$+E_{1,3}\beta_n$
4	$+A_{7,1}\alpha_m^2$ $+B_{3,1}\beta_n^2$	$+A_{7,2}\alpha_m\beta_n$ $+B_{3,2}\alpha_m\beta_n$	$+D_{1,2}\alpha_m$	$+A_{7,7}\alpha_m^2$ $+B_{3,5}\beta_n^2$ $+D_{1,1}$	$+A_{7,8}\alpha_m\beta_n$ $+B_{3,6}\alpha_m\beta_n$	$+A_{7,3}\alpha_m^2$ $+B_{3,3}\beta_n^2$ $+D_{1,5}$	$+A_{7,4}\alpha_m\beta_n$ $+B_{3,4}\alpha_m\beta_n$	$+A_{7,9}\alpha_m^2$ $+B_{3,7}\beta_n^2$ $+D_{1,3}$	$+A_{7,10}\alpha_m\beta_n$ $+B_{3,8}\alpha_m\beta_n$
5	$+A_{8,1}\alpha_m\beta_n$ $+B_{3,1}\alpha_m\beta_n$	$+A_{8,2}\beta_n^2$ $+B_{3,2}\alpha_m^2$	$+E_{1,2}\beta_n$	$+A_{8,7}\alpha_m\beta_n$ $+B_{3,5}\alpha_m\beta_n$	$+A_{8,8}\beta_n^2$ $+B_{3,6}\alpha_m^2$ $+E_{1,1}$	$+A_{8,3}\alpha_m\beta_n$ $+B_{3,3}\alpha_m\beta_n$	$+A_{8,4}\beta_n^2$ $+B_{3,4}\alpha_m^2$ $+E_{1,5}$	$+A_{8,9}\alpha\ \beta_n$ $+B_{3,7}\alpha_m\beta_n$	$+A_{8,10}\beta_n^2$ $+B_{3,8}\alpha_m^2$ $+E_{1,3}$
6	$+A_{3,1}\alpha_m^2$ $+B_{2,1}\beta_n^2$	$+A_{3,2}\alpha_m\beta_n$ $+B_{2,2}\alpha_m\beta_n$	$+2D_{3,2}\alpha_m$	$+A_{3,7}\alpha_m^2$ $+B_{2,5}\beta_n^2$ $+2D_{3,1}$	$+A_{3,8}\alpha_m\beta_n$ $+B_{2,6}\alpha_m\beta_n$	$+A_{3,3}\alpha_m^2$ $+B_{2,3}\beta_n^2$ $+2D_{3,5}$	$+A_{3,4}\alpha_m\beta_n$ $+B_{2,4}\alpha_m\beta_n$	$+A_{3,9}\alpha_m^2$ $+B_{2,7}\beta_n^2$ $+2D_{3,3}$	$+A_{3,10}\alpha_m\beta_n$ $+B_{2,8}\alpha_m\beta_n$
7	$+A_{4,1}\alpha_m\beta_n$ $+B_{2,1}\alpha_m\beta_n$	$+A_{4,2}\beta_n^2$ $+B_{2,2}\alpha_m^2$	$+2E_{3,2}\beta_n$	$+A_{4,7}\alpha_m\beta_n$ $+B_{2,5}\alpha_m\beta_n$	$+A_{4,8}\beta_n^2$ $+B_{2,6}\alpha_m^2$ $+2E_{3,1}$	$+A_{4,3}\alpha_m\beta_n$ $+B_{2,3}\alpha_m\beta_n$	$+A_{4,4}\beta_n^2$ $+B_{2,4}\alpha_m^2$ $+2E_{3,5}$	$+A_{4,9}\alpha_m\beta_n$ $+B_{2,7}\alpha_m\beta_n$	$+A_{4,10}\beta_n^2$ $+B_{2,8}\alpha_m^2$ $+2E_{3,3}$
8	$+A_{9,1}\alpha_m^2$ $+B_{4,1}\beta_n^2$	$+A_{9,2}\alpha_m\beta_n$ $+B_{4,2}\alpha_m\beta_n$	$+3D_{2,2}\alpha_m$	$+A_{9,7}\alpha_m^2$ $+B_{4,5}\beta_n^2$ $+3D_{2,1}$	$+A_{9,8}\alpha_m\beta_n$ $+B_{4,6}\alpha_m\beta_n$	$+A_{9,3}\alpha_m^2$ $+B_{4,3}\beta_n^2$ $+3D_{2,5}$	$+A_{9,4}\alpha_m\beta_n$ $+B_{4,4}\alpha_m\beta_n$	$+A_{9,9}\alpha_m^2$ $+B_{4,7}\beta_n^2$ $+3D_{2,3}$	$+A_{9,10}\alpha_m\beta_n$ $+B_{4,8}\alpha_m\beta_n$
9	$+A_{10,1}\alpha_m\beta_n$ $+B_{4,1}\alpha_m\beta_n$	$+A_{10,2}\beta_n^2$ $+B_{4,2}\alpha_m^2$	$+3E_{2,2}\beta_n$	$+A_{10,7}\alpha_m\beta_n$ $+B_{4,5}\alpha_m\beta_n$	$+A_{10,8}\beta_n^2$ $+B_{4,6}\alpha_m^2$ $+3E_{2,1}$	$+A_{10,3}\alpha_m\beta_n$ $+B_{4,3}\alpha_m\beta_n$	$+A_{10,4}\beta_n^2$ $+B_{4,4}\alpha_m^2$ $+3E_{2,5}$	$+A_{10,9}\alpha_m\beta_n$ $+B_{4,7}\alpha_m\beta_n$	$+A_{10,10}\beta_n^2$ $+B_{4,8}\alpha_m^2$ $+3E_{2,3}$

$$
\begin{aligned}
\delta\theta_y:&\quad \frac{\partial M_y}{\partial y}+\frac{\partial M_{xy}}{\partial x}-Q_y=i_2\ddot{v}_o+i_3\ddot{\theta}_y+i_4\ddot{v}_o^*+i_5\ddot{\theta}_y^*\\
\delta\theta_z:&\quad \frac{\partial S_x}{\partial x}+\frac{\partial S_y}{\partial y}-N_z=i_2\ddot{w}_o+i_3\ddot{\theta}_z+i_4\ddot{w}_o^*\\
\delta u_o^*:&\quad \frac{\partial N_x^*}{\partial x}+\frac{\partial N_{xy}^*}{\partial y}-2S_x=i_3\ddot{u}_o+i_4\ddot{\theta}_x+i_5\ddot{u}_o^*+i_6\ddot{\theta}_x^*\\
\delta v_o^*:&\quad \frac{\partial N_y^*}{\partial y}+\frac{\partial N_{xy}^*}{\partial x}-2S_y=i_3\ddot{v}_o+i_4\ddot{\theta}_y+i_5\ddot{v}_o^*+i_6\ddot{\theta}_y^*\\
\delta w_o^*:&\quad \frac{\partial Q_x^*}{\partial x}+\frac{\partial Q_y^*}{\partial y}-2M_z^*=i_3\ddot{w}_o+i_4\ddot{\theta}_z+i_5\ddot{w}_o^*\\
\delta\theta_x^*:&\quad \frac{\partial M_x^*}{\partial x}+\frac{\partial M_{xy}^*}{\partial y}-3Q_x^*=i_4\ddot{u}_o+i_5\ddot{\theta}_x+i_6\ddot{u}_o^*+i_7\ddot{\theta}_x^*\\
\delta\theta_y^*:&\quad \frac{\partial M_y^*}{\partial y}+\frac{\partial M_{xy}^*}{\partial x}-3Q_y^*=i_4\ddot{v}_o+i_5\ddot{\theta}_y+i_6\ddot{v}_o^*+i_7\ddot{\theta}_y^*
\end{aligned}
\tag{A.1}
$$

A.2. Model-3 'HOSNT11M'

$$
\begin{aligned}
\delta u_o:&\quad \frac{\partial N_x}{\partial x}+\frac{\partial N_{xy}}{\partial y}=i_1\ddot{u}_o+i_2\ddot{\theta}_x+i_3\ddot{u}_o^*+i_4\ddot{\theta}_x^*\\
\delta v_o:&\quad \frac{\partial N_y}{\partial y}+\frac{\partial N_{xy}}{\partial x}=i_1\ddot{v}_o+i_2\ddot{\theta}_y+i_3\ddot{v}_o^*+i_4\ddot{\theta}_y^*\\
\delta w_o:&\quad \frac{\partial Q_x}{\partial x}+\frac{\partial Q_y}{\partial y}=i_1\ddot{w}_o+i_2\ddot{\theta}_z+i_4\ddot{\theta}_z^*\\
\delta\theta_x:&\quad \frac{\partial M_x}{\partial x}+\frac{\partial M_{xy}}{\partial y}-Q_x=i_2\ddot{u}_o+i_3\ddot{\theta}_x+i_4\ddot{u}_o^*+i_5\ddot{\theta}_x^*\\
\delta\theta_y:&\quad \frac{\partial M_y}{\partial y}+\frac{\partial M_{xy}}{\partial x}-Q_y=i_2\ddot{v}_o+i_3\ddot{\theta}_y+i_4\ddot{v}_o^*+i_5\ddot{\theta}_y^*\\
\delta\theta_z:&\quad \frac{\partial S_x}{\partial x}+\frac{\partial S_y}{\partial y}-N_z=i_2\ddot{w}_o+i_3\ddot{\theta}_z+i_5\ddot{\theta}_z^*\\
\delta u_o^*:&\quad \frac{\partial N_x^*}{\partial x}+\frac{\partial N_{xy}^*}{\partial y}-2S_x=i_3\ddot{u}_o+i_4\ddot{\theta}_x+i_5\ddot{u}_o^*+i_6\ddot{\theta}_x^*\\
\delta v_o^*:&\quad \frac{\partial N_y^*}{\partial y}+\frac{\partial N_{xy}^*}{\partial x}-2S_y=i_3\ddot{v}_o+i_4\ddot{\theta}_y+i_5\ddot{v}_o^*+i_6\ddot{\theta}_y^*\\
\delta\theta_x^*:&\quad \frac{\partial M_x^*}{\partial x}+\frac{\partial M_{xy}^*}{\partial y}-3Q_x^*=i_4\ddot{u}_o+i_5\ddot{\theta}_x+i_6\ddot{u}_o^*+i_7\ddot{\theta}_x^*\\
\delta\theta_y^*:&\quad \frac{\partial M_y^*}{\partial y}+\frac{\partial M_{xy}^*}{\partial x}-3Q_y^*=i_4\ddot{v}_o+i_5\ddot{\theta}_y+i_6\ddot{v}_o^*+i_7\ddot{\theta}_y^*\\
\delta\theta_z^*:&\quad \frac{\partial S_x^*}{\partial x}+\frac{\partial S_y^*}{\partial y}-3N_z^*=i_4\ddot{w}_o+i_5\ddot{\theta}_z+i_7\ddot{\theta}_z^*
\end{aligned}
\tag{A.2}
$$

Table C.7
Model-7 'FOST'.

Disp. $\mathbf{X}_{5\times5}$	u_0 1	v_0 2	w_0 3	θ_x 4	θ_y 5
1	$+D_{4,1}\alpha_m^2+D_{6,3}\beta_n^2$	$+D_{4,2}\alpha_m\beta_n$ $+D_{6,3}\alpha_m\beta_n$	0	$+D_{4,4}\alpha_m^2$ $+D_{6,6}\beta_n^2$	$+D_{4,5}\alpha_m\beta_n$ $+D_{6,6}\alpha_m\beta_n$
2	$+D_{5,1}\alpha_m\beta_n$ $+D_{6,3}\alpha_m\beta_n$	$+D_{5,2}\beta_n^2$ $+D_{6,3}\alpha_m^2$	0	$+D_{5,4}\alpha_m\beta_n$ $+D_{6,6}\alpha_m\beta_n$	$+D_{5,5}\beta_n^2$ $+D_{6,6}\alpha_m^2$
3	0	0	$+D_{7,7}\alpha_m^2$ $+D_{8,8}\beta_n^2$	$+D_{7,7}\alpha_m$	$+D_{8,8}\beta_n$
4	$+D_{1,1}\alpha_m^2$ $+D_{3,3}\beta_n^2$	$+D_{1,2}\alpha_m\beta_n$ $+D_{3,3}\alpha_m\beta_n$	$+D_{7,7}\alpha_m$	$+D_{1,4}\alpha_m^2$ $+D_{3,6}\beta_n^2$ $+D_{7,7}$	$+D_{1,5}\alpha_m\beta_n$ $+D_{3,6}\alpha_m\beta_n$
5	$+D_{2,1}\alpha_m\beta_n$ $+D_{3,3}\alpha_m\beta_n$	$+D_{2,2}\beta_n^2$ $+D_{3,3}\alpha_m^2$	$+D_{8,8}\beta_n$	$+D_{2,4}\alpha_m\beta_n$ $+D_{3,6}\alpha_m\beta_n$	$+D_{2,5}\beta_n^2$ $+D_{3,6}\alpha_m^2$ $+D_{8,8}$

Table C.8
Model-8 'CPT'.

Disp. $\mathbf{X}_{3\times3}$	u_0 1	v_0 2	w_0 3
1	$+D_{4,1}\alpha_m^2$ $+D_{6,3}\beta_n^2$	$+D_{4,2}\alpha_m\beta_n$ $+D_{6,3}\alpha_m\beta_n$	$+D_{4,4}\alpha_m^3$ $+D_{4,5}\alpha_m\beta_n^2$ $+2D_{6,6}\alpha_m\beta_n^2$
2	$+D_{5,1}\alpha_m\beta_n$ $+D_{6,3}\alpha_m\beta_n$	$+D_{5,2}\beta_n^2$ $+D_{6,3}\alpha_m^2$	$+D_{5,5}\beta_n^3$ $+D_{5,4}\alpha_m^2\beta_n$ $+2D_{6,6}\alpha_m^2\beta_n$
3	$+D_{1,1}\alpha_m^3$ $+D_{2,1}\alpha_m\beta_n^2$ $+2D_{3,3}\alpha_m\beta_n^2$	$+D_{2,2}\beta_n^3$ $+D_{1,2}\alpha_m^2\beta_n$ $+2D_{3,3}\alpha_m^2\beta_n$	$+D_{1,4}\alpha_m^4+D_{1,5}\alpha_m^2\beta_n^2$ $+D_{2,4}\alpha_m^2\beta_n^2+D_{2,5}\beta_n^4$ $+4D_{3,6}\alpha_m^2\beta_n^2$

Table D.1
Model-1 'HOSNT12'.

Disp. $[\mathbf{M}]_{12\times12}$	u_0 1	v_0 2	w_0 3	θ_x 4	θ_y 5	θ_z 6	u_0^* 7	v_0^* 8	w_0^* 9	θ_x^* 10	θ_y^* 11	θ_z^* 12
1	i_1	0	0	i_2	0	0	i_3	0	0	i_4	0	0
2	0	i_1	0	0	i_2	0	0	i_3	0	0	i_4	0
3	0	0	i_1	0	0	i_2	0	0	i_3	0	0	i_4
4	i_2	0	0	i_3	0	0	i_4	0	0	i_5	0	0
5	0	i_2	0	0	i_3	0	0	i_4	0	0	i_5	0
6	0	0	i_2	0	0	i_3	0	0	i_4	0	0	i_5
7	i_3	0	0	i_4	0	0	i_5	0	0	i_6	0	0
8	0	i_3	0	0	i_4	0	0	i_5	0	0	i_6	0
9	0	0	i_3	0	0	i_4	0	0	i_5	0	0	i_6
10	i_4	0	0	i_5	0	0	i_6	0	0	i_7	0	0
11	0	i_4	0	0	i_5	0	0	i_6	0	0	i_7	0
12	0	0	i_4	0	0	i_5	0	0	i_6	0	0	i_7

Table D.2
Model-2 'HOSNT11'.

Disp. $[\mathbf{M}]_{11\times11}$	u_0 1	v_0 2	w_0 3	θ_x 4	θ_y 5	θ_z 6	u_0^* 7	v_0^* 8	w_0^* 9	θ_x^* 10	θ_y^* 11
1	i_1	0	0	i_2	0	0	i_3	0	0	i_4	0
2	0	i_1	0	0	i_2	0	0	i_3	0	0	i_4
3	0	0	i_1	0	0	i_2	0	0	i_3	0	0
4	i_2	0	0	i_3	0	0	i_4	0	0	i_5	0
5	0	i_2	0	0	i_3	0	0	i_4	0	0	i_5
6	0	0	i_2	0	0	i_3	0	0	i_4	0	0
7	i_3	0	0	i_4	0	0	i_5	0	0	i_6	0
8	0	i_3	0	0	i_4	0	0	i_5	0	0	i_6
9	0	0	i_3	0	0	i_4	0	0	i_5	0	0
10	i_4	0	0	i_5	0	0	i_6	0	0	i_7	0
11	0	i_4	0	0	i_5	0	0	i_6	0	0	i_7

Table D.3
Model-3 'HOSNT11M'.

Disp. $[\mathbf{M}]_{11\times11}$	u_0 1	v_0 2	w_0 3	θ_x 4	θ_y 5	θ_z 6	u_0^* 7	v_0^* 8	θ_x^* 9	θ_y^* 10	θ_z^* 11
1	i_1	0	0	i_2	0	0	i_3	0	i_4	0	0
2	0	i_1	0	0	i_2	0	0	i_3	0	i_4	0
3	0	0	i_1	0	0	i_2	0	0	0	0	i_4
4	i_2	0	0	i_3	0	0	i_4	0	i_5	0	0
5	0	i_2	0	0	i_3	0	0	i_4	0	i_5	0
6	0	0	i_2	0	0	i_3	0	0	0	0	i_5
7	i_3	0	0	i_4	0	0	i_5	0	i_6	0	0
8	0	i_3	0	0	i_4	0	0	i_5	0	i_6	0
9	i_4	0	0	i_5	0	0	i_6	0	i_7	0	0
10	0	i_4	0	0	i_5	0	0	i_6	0	i_7	0
11	0	0	i_4	0	0	i_5	0	0	0	0	i_7

Table D.4
Model-4 'HOSNT10B'.

Disp. $[\mathbf{M}]_{10\times10}$	u_0 1	v_0 2	w_0 3	θ_x 4	θ_y 5	u_0^* 6	v_0^* 7	w_0^* 8	θ_x^* 9	θ_y^* 10
1	i_1	0	0	i_2	0	i_3	0	0	i_4	0
2	0	i_1	0	0	i_2	0	i_3	0	0	i_4
3	0	0	I_1	0	0	0	0	I_3	0	0
4	i_2	0	0	i_3	0	i_4	0	0	i_5	0
5	0	i_2	0	0	i_3	0	i_4	0	0	i_5
6	i_3	0	0	i_4	0	i_5	0	0	i_6	0
7	0	i_3	0	0	i_4	0	i_5	0	0	i_6
8	0	0	I_3	0	0	0	0	I_5	0	0
9	i_4	0	0	i_5	0	i_6	0	0	i_7	0
10	0	i_4	0	0	i_5	0	i_6	0	0	i_7

A.3. Model-4 'HOSNT10B'

$$
\begin{aligned}
\delta u_o:&\quad \frac{\partial N_x}{\partial x}+\frac{\partial N_{xy}}{\partial y}=i_1\ddot{u}_o+i_2\ddot{\theta}_x+i_3\ddot{u}_o^*+i_4\ddot{\theta}_x^*\\
\delta v_o:&\quad \frac{\partial N_y}{\partial y}+\frac{\partial N_{xy}}{\partial x}=i_1\ddot{v}_o+i_2\ddot{\theta}_y+i_3\ddot{v}_o^*+i_4\ddot{\theta}_y^*\\
\delta w_o:&\quad \frac{\partial Q_x}{\partial x}+\frac{\partial Q_y}{\partial y}=i_1\ddot{w}_o+i_3\ddot{w}_o^*\\
\delta\theta_x:&\quad \frac{\partial M_x}{\partial x}+\frac{\partial M_{xy}}{\partial y}-Q_x=i_2\ddot{u}_o+i_3\ddot{\theta}_x+i_4\ddot{u}_o^*+i_5\ddot{\theta}_x^*\\
\delta\theta_y:&\quad \frac{\partial M_y}{\partial y}+\frac{\partial M_{xy}}{\partial x}-Q_y=i_2\ddot{v}_o+i_3\ddot{\theta}_y+i_4\ddot{v}_o^*+i_5\ddot{\theta}_y^*\\
\delta u_o^*:&\quad \frac{\partial N_x^*}{\partial x}+\frac{\partial N_{xy}^*}{\partial y}-2S_x=i_3\ddot{u}_o+i_4\ddot{\theta}_x+i_5\ddot{u}_o^*+i_6\ddot{\theta}_x^*\\
\delta v_o^*:&\quad \frac{\partial N_y^*}{\partial y}+\frac{\partial N_{xy}^*}{\partial x}-2S_y=i_3\ddot{v}_o+i_4\ddot{\theta}_y+i_5\ddot{v}_o^*+i_6\ddot{\theta}_y^*\\
\delta w_o^*:&\quad \frac{\partial Q_x^*}{\partial x}+\frac{\partial Q_y^*}{\partial y}-2M_z^*=i_3\ddot{w}_o+i_5\ddot{w}_o^*\\
\delta\theta_x^*:&\quad \frac{\partial M_x^*}{\partial x}+\frac{\partial M_{xy}^*}{\partial y}-3Q_x^*=i_4\ddot{u}_o+i_5\ddot{\theta}_x+i_6\ddot{u}_o^*+i_7\ddot{\theta}_x^*\\
\delta\theta_y^*:&\quad \frac{\partial M_y^*}{\partial y}+\frac{\partial M_{xy}^*}{\partial x}-3Q_y^*=i_4\ddot{v}_o+i_5\ddot{\theta}_y+i_6\ddot{v}_o^*+i_7\ddot{\theta}_y^*
\end{aligned}
\tag{A.3}
$$

A.4. Model-5 'HOSNT10M'

$$
\begin{aligned}
\delta u_o:&\quad \frac{\partial N_x}{\partial x}+\frac{\partial N_{xy}}{\partial y}=i_1\ddot{u}_o+i_2\ddot{\theta}_x+i_3\ddot{u}_o^*+i_4\ddot{\theta}_x^*\\
\delta v_o:&\quad \frac{\partial N_y}{\partial y}+\frac{\partial N_{xy}}{\partial x}=i_1\ddot{v}_o+i_2\ddot{\theta}_y+i_3\ddot{v}_o^*+i_4\ddot{\theta}_y^*\\
\delta w_o:&\quad \frac{\partial Q_x}{\partial x}+\frac{\partial Q_y}{\partial y}=i_1\ddot{w}_o+i_2\ddot{\theta}_z\\
\delta\theta_x:&\quad \frac{\partial M_x}{\partial x}+\frac{\partial M_{xy}}{\partial y}-Q_x=i_2\ddot{u}_o+i_3\ddot{\theta}_x+i_4\ddot{u}_o^*+i_5\ddot{\theta}_x^*\\
\delta\theta_y:&\quad \frac{\partial M_y}{\partial y}+\frac{\partial M_{xy}}{\partial x}-Q_y=i_2\ddot{v}_o+i_3\ddot{\theta}_y+i_4\ddot{v}_o^*+i_5\ddot{\theta}_y^*\\
\delta\theta_z:&\quad \frac{\partial S_x}{\partial x}+\frac{\partial S_y}{\partial y}-N_z=i_2\ddot{w}_o+i_3\ddot{\theta}_z\\
\delta u_o^*:&\quad \frac{\partial N_x^*}{\partial x}+\frac{\partial N_{xy}^*}{\partial y}-2S_x=i_3\ddot{u}_o+i_4\ddot{\theta}_x+i_5\ddot{u}_o^*+i_6\ddot{\theta}_x^*\\
\delta v_o^*:&\quad \frac{\partial N_y^*}{\partial y}+\frac{\partial N_{xy}^*}{\partial x}-2S_y=i_3\ddot{v}_o+i_4\ddot{\theta}_y+i_5\ddot{v}_o^*+i_6\ddot{\theta}_y^*\\
\delta\theta_x^*:&\quad \frac{\partial M_x^*}{\partial x}+\frac{\partial M_{xy}^*}{\partial y}-3Q_x^*=i_4\ddot{u}_o+i_5\ddot{\theta}_x+i_6\ddot{u}_o^*+i_7\ddot{\theta}_x^*\\
\delta\theta_y^*:&\quad \frac{\partial M_y^*}{\partial y}+\frac{\partial M_{xy}^*}{\partial x}-3Q_y^*=i_4\ddot{v}_o+i_5\ddot{\theta}_y+i_6\ddot{v}_o^*+i_7\ddot{\theta}_y^*
\end{aligned}
\tag{A.4}
$$

Table D.5
Model-5 'HOSNT10M'.

Disp.	u_0	v_0	w_0	θ_x	θ_y	θ_z	u_0^*	v_0^*	θ_x^*	θ_y^*
$[\mathbf{M}]_{10\times10}$	1	2	3	4	5	6	7	8	9	10
1	i_1	0	0	i_2	0	0	i_3	0	i_4	0
2	0	i_1	0	0	i_2	0	0	i_3	0	i_4
3	0	0	i_1	0	0	i_2	0	0	0	0
4	i_2	0	0	i_3	0	0	i_4	0	i_5	0
5	0	i_2	0	0	i_3	0	0	i_4	0	i_5
6	0	0	i_2	0	0	i_3	0	0	0	0
7	i_3	0	0	i_4	0	0	i_5	0	i_6	0
8	0	i_3	0	0	i_4	0	0	i_5	0	i_6
9	i_4	0	0	i_5	0	0	i_6	0	i_7	0
10	0	i_4	0	0	i_5	0	0	i_6	0	i_7

Table D.6
Model-6 'HOST9'.

Disp.	u_0	v_0	w_0	θ_x	θ_y	u_0^*	v_0^*	θ_x^*	θ_y^*
$[\mathbf{M}]_{9\times9}$	1	2	3	4	5	6	7	8	9
1	i_1	0	0	i_2	0	i_3	0	i_4	0
2	0	i_1	0	0	i_2	0	i_3	0	i_4
3	0	0	i_1	0	0	0	0	0	0
4	i_2	0	0	i_3	0	i_4	0	i_5	0
5	0	i_2	0	0	i_3	0	i_4	0	i_5
6	i_3	0	0	i_4	0	i_5	0	i_6	0
7	0	i_3	0	0	i_4	0	i_5	0	i_6
8	i_4	0	0	i_5	0	i_6	0	i_7	0
9	0	i_4	0	0	i_5	0	i_6	0	i_7

Table D.7
Model-7 'FOST'.

Disp.	u_0	v_0	w_0	θ_x	θ_y
$[\mathbf{M}]_{5\times5}$	1	2	3	4	5
1	i_1	0	0	i_2	0
2	0	i_1	0	0	i_2
3	0	0	i_1	0	0
4	i_2	0	0	i_3	0
5	0	i_2	0	0	i_3

Table D.8
Model-8 'CPT'.

Disp	u_0	v_0	w_0
$[\mathbf{M}]_{3\times3}$	1	2	3
1	i_1	0	0
2	0	i_1	0
3	0	0	i_1

A.5. Model-6 'HOST9'

$$
\begin{aligned}
\delta u_o:&\quad \frac{\partial N_x}{\partial x}+\frac{\partial N_{xy}}{\partial y}=i_1\ddot{u}_o+i_2\ddot{\theta}_x+i_3\ddot{u}_o^*+i_4\ddot{\theta}_x^*\\
\delta v_o:&\quad \frac{\partial N_y}{\partial y}+\frac{\partial N_{xy}}{\partial x}=i_1\ddot{v}_o+i_2\ddot{\theta}_y+i_3\ddot{v}_o^*+i_4\ddot{\theta}_y^*\\
\delta w_o:&\quad \frac{\partial Q_x}{\partial x}+\frac{\partial Q_y}{\partial y}=i_1\ddot{w}_o\\
\delta\theta_x:&\quad \frac{\partial M_x}{\partial x}+\frac{\partial M_{xy}}{\partial y}-Q_x=i_2\ddot{u}_o+i_3\ddot{\theta}_x+i_4\ddot{u}_o^*+i_5\ddot{\theta}_x^*\\
\delta\theta_y:&\quad \frac{\partial M_y}{\partial y}+\frac{\partial M_{xy}}{\partial x}-Q_y=i_2\ddot{v}_o+i_3\ddot{\theta}_y+i_4\ddot{v}_o^*+i_5\ddot{\theta}_y^*\\
\delta u_o^*:&\quad \frac{\partial N_x^*}{\partial x}+\frac{\partial N_{xy}^*}{\partial y}-2S_x=i_3\ddot{u}_o+i_4\ddot{\theta}_x+i_5\ddot{u}_o^*+i_6\ddot{\theta}_x^*\\
\delta v_o^*:&\quad \frac{\partial N_y^*}{\partial y}+\frac{\partial N_{xy}^*}{\partial x}-2S_y=i_3\ddot{v}_o+i_4\ddot{\theta}_y+i_5\ddot{v}_o^*+i_6\ddot{\theta}_y^*\\
\delta\theta_x^*:&\quad \frac{\partial M_x^*}{\partial x}+\frac{\partial M_{xy}^*}{\partial y}-3Q_x^*=i_4\ddot{u}_o+i_5\ddot{\theta}_x+i_6\ddot{u}_o^*+i_7\ddot{\theta}_x^*\\
\delta\theta_y^*:&\quad \frac{\partial M_y^*}{\partial y}+\frac{\partial M_{xy}^*}{\partial x}-3Q_y^*=i_4\ddot{v}_o+i_5\ddot{\theta}_y+i_6\ddot{v}_o^*+i_7\ddot{\theta}_y^*
\end{aligned}
\tag{A.5}
$$

A.6. Model-7 'FOST' [29]

$$
\begin{aligned}
\delta u_o:&\quad \frac{\partial N_x}{\partial x}+\frac{\partial N_{xy}}{\partial y}=i_1\ddot{u}_o+i_2\ddot{\theta}_x\\
\delta v_o:&\quad \frac{\partial N_y}{\partial y}+\frac{\partial N_{xy}}{\partial x}=i_1\ddot{v}_o+i_2\ddot{\theta}_y\\
\delta w_o:&\quad \frac{\partial Q_x}{\partial x}+\frac{\partial Q_y}{\partial y}=i_1\ddot{w}_o\\
\delta\theta_x:&\quad \frac{\partial M_x}{\partial x}+\frac{\partial M_{xy}}{\partial y}-Q_x=i_2\ddot{u}_o+i_3\ddot{\theta}_x\\
\delta\theta_y:&\quad \frac{\partial M_y}{\partial y}+\frac{\partial M_{xy}}{\partial x}-Q_y=i_2\ddot{v}_o+i_3\ddot{\theta}_y
\end{aligned}
\tag{A.6}
$$

A.7. Model-8 'CPT' [30]

$$
\begin{aligned}
\delta u_o:&\quad \frac{\partial N_x}{\partial x}+\frac{\partial N_{xy}}{\partial y}=i_1\ddot{u}_o\\
\delta v_o:&\quad \frac{\partial N_y}{\partial y}+\frac{\partial N_{xy}}{\partial x}=i_1\ddot{v}_o\\
\delta w_o:&\quad \frac{\partial^2 M_x}{\partial x^2}+\frac{2\partial^2 M_{xy}}{\partial x\partial y}+\frac{\partial^2 M_y}{\partial y^2}=i_1\ddot{w}_o
\end{aligned}
\tag{A.7}
$$

Appendix B. Elements of the sub matrices of plate rigidity matrix in Eq. (11) for various displacement models

B.1. Model-1 'HOSNT12'

$$[\mathbf{A}]_{11\times11}=\begin{bmatrix} I_{11,0} & I_{12,0} & I_{11,2} & I_{12,2} & I_{13,0} & 3I_{13,2} & I_{11,1} & I_{12,1} & I_{11,3} & I_{12,3} & 2I_{13,1}\\ I_{12,0} & I_{22,0} & I_{12,2} & I_{22,2} & I_{23,0} & 3I_{23,2} & I_{12,1} & I_{22,1} & I_{12,3} & I_{22,3} & 2I_{23,1}\\ I_{11,2} & I_{12,2} & I_{11,4} & I_{12,4} & I_{13,2} & 3I_{13,4} & I_{11,3} & I_{12,3} & I_{11,5} & I_{12,5} & 2I_{13,3}\\ I_{12,2} & I_{22,2} & I_{12,4} & I_{22,4} & I_{23,2} & 3I_{23,4} & I_{12,3} & I_{22,3} & I_{12,5} & I_{22,5} & 2I_{23,3}\\ I_{13,0} & I_{23,0} & I_{13,2} & I_{23,2} & I_{33,0} & 3I_{33,2} & I_{13,1} & I_{23,1} & I_{13,3} & I_{23,3} & 2I_{33,1}\\ I_{13,2} & I_{23,2} & I_{13,4} & I_{23,4} & I_{33,2} & 3I_{33,4} & I_{13,3} & I_{23,3} & I_{13,5} & I_{23,5} & 2I_{33,3}\\ I_{11,1} & I_{12,1} & I_{11,3} & I_{12,3} & I_{13,1} & 3I_{13,3} & I_{11,2} & I_{12,2} & I_{11,4} & I_{12,4} & 2I_{13,2}\\ I_{12,1} & I_{22,1} & I_{12,3} & I_{22,3} & I_{23,1} & 3I_{23,3} & I_{12,2} & I_{22,2} & I_{12,4} & I_{22,4} & 2I_{23,2}\\ I_{11,3} & I_{12,3} & I_{11,5} & I_{12,5} & I_{13,3} & 3I_{13,5} & I_{11,4} & I_{12,4} & I_{11,6} & I_{12,6} & 2I_{13,4}\\ I_{12,3} & I_{22,3} & I_{12,5} & I_{22,5} & I_{23,3} & 3I_{23,5} & I_{12,4} & I_{22,4} & I_{12,6} & I_{22,6} & 2I_{23,4}\\ I_{13,1} & I_{23,1} & I_{13,3} & I_{23,3} & I_{33,1} & 3I_{33,3} & I_{13,2} & I_{23,2} & I_{13,4} & I_{23,4} & 2I_{33,2} \end{bmatrix} \tag{B.1}$$

$$[\mathbf{A}']_{11\times8}=\begin{bmatrix} I_{14,0} & I_{14,0} & I_{14,2} & I_{14,2} & I_{14,1} & I_{14,1} & I_{14,3} & I_{14,3}\\ I_{24,0} & I_{24,0} & I_{24,2} & I_{24,2} & I_{24,1} & I_{24,1} & I_{24,3} & I_{24,3}\\ I_{14,2} & I_{14,2} & I_{14,4} & I_{14,4} & I_{14,3} & I_{14,3} & I_{14,5} & I_{14,5}\\ I_{24,2} & I_{24,2} & I_{24,4} & I_{24,4} & I_{24,3} & I_{24,3} & I_{24,5} & I_{24,5}\\ I_{34,0} & I_{34,0} & I_{34,2} & I_{34,2} & I_{34,1} & I_{34,1} & I_{34,3} & I_{34,3}\\ I_{34,2} & I_{34,2} & I_{34,4} & I_{34,4} & I_{34,3} & I_{34,3} & I_{34,5} & I_{34,5}\\ I_{14,1} & I_{14,1} & I_{14,3} & I_{14,3} & I_{14,2} & I_{14,2} & I_{14,4} & I_{14,4}\\ I_{24,1} & I_{24,1} & I_{24,3} & I_{24,3} & I_{24,2} & I_{24,2} & I_{24,4} & I_{24,4}\\ I_{14,3} & I_{14,3} & I_{14,5} & I_{14,5} & I_{14,4} & I_{14,4} & I_{14,6} & I_{14,6}\\ I_{24,3} & I_{24,3} & I_{24,5} & I_{24,5} & I_{24,4} & I_{24,4} & I_{24,6} & I_{24,6}\\ I_{34,1} & I_{34,1} & I_{34,3} & I_{34,3} & I_{34,2} & I_{34,2} & I_{34,4} & I_{34,4} \end{bmatrix} \tag{B.2}$$

$$[\mathbf{B}']_{4\times11}=\begin{bmatrix} I_{14,0} & I_{24,0} & I_{14,2} & I_{24,2} & I_{34,0} & 3I_{34,2} & I_{14,1} & I_{24,1} & I_{14,3} & I_{24,3} & 2I_{34,1}\\ I_{14,2} & I_{24,2} & I_{14,4} & I_{24,4} & I_{34,2} & 3I_{34,4} & I_{14,3} & I_{24,3} & I_{14,5} & I_{24,5} & 2I_{34,3}\\ I_{14,1} & I_{24,1} & I_{14,3} & I_{24,3} & I_{34,1} & 3I_{34,3} & I_{14,2} & I_{24,2} & I_{14,4} & I_{24,4} & 2I_{34,2}\\ I_{14,3} & I_{24,3} & I_{14,5} & I_{24,5} & I_{34,3} & 3I_{34,5} & I_{14,4} & I_{24,4} & I_{14,6} & I_{24,6} & 2I_{34,4} \end{bmatrix} \tag{B.3}$$

$$[\mathbf{B}]_{4\times8}=\begin{bmatrix} I_{44,0} & I_{44,0} & I_{44,2} & I_{44,2} & I_{44,1} & I_{44,1} & I_{44,3} & I_{44,3}\\ I_{44,2} & I_{44,2} & I_{44,4} & I_{44,4} & I_{44,3} & I_{44,3} & I_{44,5} & I_{44,5}\\ I_{44,1} & I_{44,1} & I_{44,3} & I_{44,3} & I_{44,2} & I_{44,2} & I_{44,4} & I_{44,4}\\ I_{44,3} & I_{44,3} & I_{44,5} & I_{44,5} & I_{44,4} & I_{44,4} & I_{44,6} & I_{44,6} \end{bmatrix} \tag{B.4}$$

$$[\mathbf{D}]_{4\times7}=\begin{bmatrix} I_{66,0} & I_{66,0} & 3I_{66,2} & I_{66,2} & 2I_{66,1} & I_{66,1} & I_{66,3}\\ I_{66,2} & I_{66,2} & 3I_{66,4} & I_{66,4} & 2I_{66,3} & I_{66,3} & I_{66,5}\\ I_{66,1} & I_{66,1} & 3I_{66,3} & I_{66,3} & 2I_{66,2} & I_{66,2} & I_{66,4}\\ I_{66,3} & I_{66,3} & 3I_{66,5} & I_{66,5} & 2I_{66,4} & I_{66,4} & I_{66,6} \end{bmatrix} \tag{B.5}$$

$$[\mathbf{D}']_{4\times7}=\begin{bmatrix} I_{56,0} & I_{56,0} & 3I_{56,2} & I_{56,2} & 2I_{56,1} & I_{56,1} & I_{56,3}\\ I_{56,2} & I_{56,2} & 3I_{56,4} & I_{56,4} & 2I_{56,3} & I_{56,3} & I_{56,5}\\ I_{56,1} & I_{56,1} & 3I_{56,3} & I_{56,3} & 2I_{56,2} & I_{56,2} & I_{56,4}\\ I_{56,3} & I_{56,3} & 3I_{56,5} & I_{56,5} & 2I_{56,4} & I_{56,4} & I_{56,6} \end{bmatrix} \tag{B.6}$$

$$[\mathbf{E}']_{4\times7}=\begin{bmatrix} I_{56,0} & I_{56,0} & 3I_{56,2} & I_{56,2} & 2I_{56,1} & I_{56,1} & I_{56,3}\\ I_{56,2} & I_{56,2} & 3I_{56,4} & I_{56,4} & 2I_{56,3} & I_{56,3} & I_{56,5}\\ I_{56,1} & I_{56,1} & 3I_{56,3} & I_{56,3} & 2I_{56,2} & I_{56,2} & I_{56,4}\\ I_{56,3} & I_{56,3} & 3I_{56,5} & I_{56,5} & 2I_{56,4} & I_{56,4} & I_{56,6} \end{bmatrix} \tag{B.7}$$

$$[\mathbf{E}]_{4\times7}=\begin{bmatrix} I_{55,0} & I_{55,0} & 3I_{55,2} & I_{55,2} & 2I_{55,1} & I_{55,1} & I_{55,3}\\ I_{55,2} & I_{55,2} & 3I_{55,4} & I_{55,4} & 2I_{55,3} & I_{55,3} & I_{55,5}\\ I_{55,1} & I_{55,1} & 3I_{55,3} & I_{55,3} & 2I_{55,2} & I_{55,2} & I_{55,4}\\ I_{55,3} & I_{55,3} & 3I_{55,5} & I_{55,5} & 2I_{55,4} & I_{55,4} & I_{55,6} \end{bmatrix} \tag{B.8}$$

B.2. Model-2 'HOSNT11'

$$[\mathbf{A}]_{11\times11}=\begin{bmatrix} I_{11,0} & I_{12,0} & I_{11,2} & I_{12,2} & I_{13,0} & 0 & I_{11,1} & I_{12,1} & I_{11,3} & I_{12,3} & 2I_{13,1}\\ I_{12,0} & I_{22,0} & I_{12,2} & I_{22,2} & I_{23,0} & 0 & I_{12,1} & I_{22,1} & I_{12,3} & I_{22,3} & 2I_{23,1}\\ I_{11,2} & I_{12,2} & I_{11,4} & I_{12,4} & I_{13,2} & 0 & I_{11,3} & I_{12,3} & I_{11,5} & I_{12,5} & 2I_{13,3}\\ I_{12,2} & I_{22,2} & I_{12,4} & I_{22,4} & I_{23,2} & 0 & I_{12,3} & I_{22,3} & I_{12,5} & I_{22,5} & 2I_{23,3}\\ I_{13,0} & I_{23,0} & I_{13,2} & I_{23,2} & I_{33,0} & 0 & I_{13,1} & I_{23,1} & I_{13,3} & I_{23,3} & 2I_{33,1}\\ I_{13,2} & I_{23,2} & I_{13,4} & I_{23,4} & I_{33,2} & 0 & I_{13,3} & I_{23,3} & I_{13,5} & I_{23,5} & 2I_{33,3}\\ I_{11,1} & I_{12,1} & I_{11,3} & I_{12,3} & I_{13,1} & 0 & I_{11,2} & I_{12,2} & I_{11,4} & I_{12,4} & 2I_{13,2}\\ I_{12,1} & I_{22,1} & I_{12,3} & I_{22,3} & I_{23,1} & 0 & I_{12,2} & I_{22,2} & I_{12,4} & I_{22,4} & 2I_{23,2}\\ I_{11,3} & I_{12,3} & I_{11,5} & I_{12,5} & I_{13,3} & 0 & I_{11,4} & I_{12,4} & I_{11,6} & I_{12,6} & 2I_{13,4}\\ I_{12,3} & I_{22,3} & I_{12,5} & I_{22,5} & I_{23,3} & 0 & I_{12,4} & I_{22,4} & I_{12,6} & I_{22,6} & 2I_{23,4}\\ I_{13,1} & I_{23,1} & I_{13,3} & I_{23,3} & I_{33,1} & 0 & I_{13,2} & I_{23,2} & I_{13,4} & I_{23,4} & 2I_{33,2} \end{bmatrix} \tag{B.9}$$

$$[\mathbf{B}]_{4\times8}=\begin{bmatrix} I_{44,0} & I_{44,0} & I_{44,2} & I_{44,2} & I_{44,1} & I_{44,1} & I_{44,3} & I_{44,3}\\ I_{44,2} & I_{44,2} & I_{44,4} & I_{44,4} & I_{44,3} & I_{44,3} & I_{44,5} & I_{44,5}\\ I_{44,1} & I_{44,1} & I_{44,3} & I_{44,3} & I_{44,2} & I_{44,2} & I_{44,4} & I_{44,4}\\ I_{44,3} & I_{44,3} & I_{44,5} & I_{44,5} & I_{44,4} & I_{44,4} & I_{44,6} & I_{44,6} \end{bmatrix} \tag{B.10}$$

$$[\mathbf{D}]_{4\times7}=\begin{bmatrix} I_{66,0} & I_{66,0} & 3I_{66,2} & I_{66,2} & 2I_{66,1} & I_{66,1} & 0\\ I_{66,2} & I_{66,2} & 3I_{66,4} & I_{66,4} & 2I_{66,3} & I_{66,3} & 0\\ I_{66,1} & I_{66,1} & 3I_{66,3} & I_{66,3} & 2I_{66,2} & I_{66,2} & 0\\ I_{66,3} & I_{66,3} & 3I_{66,5} & I_{66,5} & 2I_{66,4} & I_{66,4} & 0 \end{bmatrix} \tag{B.11}$$

$$[\mathbf{E}]_{4\times7}=\begin{bmatrix} I_{55,0} & I_{55,0} & 3I_{55,2} & I_{55,2} & 2I_{55,1} & I_{55,1} & 0\\ I_{55,2} & I_{55,2} & 3I_{55,4} & I_{55,4} & 2I_{55,3} & I_{55,3} & 0\\ I_{55,1} & I_{55,1} & 3I_{55,3} & I_{55,3} & 2I_{55,2} & I_{55,2} & 0\\ I_{55,3} & I_{55,3} & 3I_{55,5} & I_{55,5} & 2I_{55,4} & I_{55,4} & 0 \end{bmatrix} \tag{B.12}$$

B.3. Model-3 'HOSNT11M'

$$[\mathbf{A}]_{11\times11}=\begin{bmatrix} I_{11,0} & I_{12,0} & I_{11,2} & I_{12,2} & I_{13,0} & 3I_{13,2} & I_{11,1} & I_{12,1} & I_{11,3} & I_{12,3} & 0\\ I_{12,0} & I_{22,0} & I_{12,2} & I_{22,2} & I_{23,0} & 3I_{23,2} & I_{12,1} & I_{22,1} & I_{12,3} & I_{22,3} & 0\\ I_{11,2} & I_{12,2} & I_{11,4} & I_{12,4} & I_{13,2} & 3I_{13,4} & I_{11,3} & I_{12,3} & I_{11,5} & I_{12,5} & 0\\ I_{12,2} & I_{22,2} & I_{12,4} & I_{22,4} & I_{23,2} & 3I_{23,4} & I_{12,3} & I_{22,3} & I_{12,5} & I_{22,5} & 0\\ I_{13,0} & I_{23,0} & I_{13,2} & I_{23,2} & I_{33,0} & 3I_{33,2} & I_{13,1} & I_{23,1} & I_{13,3} & I_{23,3} & 0\\ I_{13,2} & I_{23,2} & I_{13,4} & I_{23,4} & I_{33,2} & 3I_{33,4} & I_{13,3} & I_{23,3} & I_{13,5} & I_{23,5} & 0\\ I_{11,1} & I_{12,1} & I_{11,3} & I_{12,3} & I_{13,1} & 3I_{13,3} & I_{11,2} & I_{12,2} & I_{11,4} & I_{12,4} & 0\\ I_{12,1} & I_{22,1} & I_{12,3} & I_{22,3} & I_{23,1} & 3I_{23,3} & I_{12,2} & I_{22,2} & I_{12,4} & I_{22,4} & 0\\ I_{11,3} & I_{12,3} & I_{11,5} & I_{12,5} & I_{13,3} & 3I_{13,5} & I_{11,4} & I_{12,4} & I_{11,6} & I_{12,6} & 0\\ I_{12,3} & I_{22,3} & I_{12,5} & I_{22,5} & I_{23,3} & 3I_{23,5} & I_{12,4} & I_{22,4} & I_{12,6} & I_{22,6} & 0\\ I_{13,1} & I_{23,1} & I_{13,3} & I_{23,3} & I_{33,1} & 3I_{33,3} & I_{13,2} & I_{23,2} & I_{13,4} & I_{23,4} & 0 \end{bmatrix} \tag{B.13}$$

$$[\mathbf{A}']_{11\times8}=\begin{bmatrix} I_{14,0} & I_{14,0} & I_{14,2} & I_{14,2} & I_{14,1} & I_{14,1} & I_{14,3} & I_{14,3}\\ I_{24,0} & I_{24,0} & I_{24,2} & I_{24,2} & I_{24,1} & I_{24,1} & I_{24,3} & I_{24,3}\\ I_{14,2} & I_{14,2} & I_{14,4} & I_{14,4} & I_{14,3} & I_{14,3} & I_{14,5} & I_{14,5}\\ I_{24,2} & I_{24,2} & I_{24,4} & I_{24,4} & I_{24,3} & I_{24,3} & I_{24,5} & I_{24,5}\\ I_{34,0} & I_{34,0} & I_{34,2} & I_{34,2} & I_{34,1} & I_{34,1} & I_{34,3} & I_{34,3}\\ I_{34,2} & I_{34,2} & I_{34,4} & I_{34,4} & I_{34,3} & I_{34,3} & I_{34,5} & I_{34,5}\\ I_{14,1} & I_{14,1} & I_{14,3} & I_{14,3} & I_{14,2} & I_{14,2} & I_{14,4} & I_{14,4}\\ I_{24,1} & I_{24,1} & I_{24,3} & I_{24,3} & I_{24,2} & I_{24,2} & I_{24,4} & I_{24,4}\\ I_{14,3} & I_{14,3} & I_{14,5} & I_{14,5} & I_{14,4} & I_{14,4} & I_{14,6} & I_{14,6}\\ I_{24,3} & I_{24,3} & I_{24,5} & I_{24,5} & I_{24,4} & I_{24,4} & I_{24,6} & I_{24,6}\\ I_{34,1} & I_{34,1} & I_{34,3} & I_{34,3} & I_{34,2} & I_{34,2} & I_{34,4} & I_{34,4} \end{bmatrix} \tag{B.14}$$

$$[\mathbf{B}']_{4\times11}=\begin{bmatrix} I_{14,0} & I_{24,0} & I_{14,2} & I_{24,2} & I_{34,0} & 3I_{34,2} & I_{14,1} & I_{24,1} & I_{14,3} & I_{24,3} & 0\\ I_{14,2} & I_{24,2} & I_{14,4} & I_{24,4} & I_{34,2} & 3I_{34,4} & I_{14,3} & I_{24,3} & I_{14,5} & I_{24,5} & 0\\ I_{14,1} & I_{24,1} & I_{14,3} & I_{24,3} & I_{34,1} & 3I_{34,3} & I_{14,2} & I_{24,2} & I_{14,4} & I_{24,4} & 0\\ I_{14,3} & I_{24,3} & I_{14,5} & I_{24,5} & I_{34,3} & 3I_{34,5} & I_{14,4} & I_{24,4} & I_{14,6} & I_{24,6} & 0 \end{bmatrix} \tag{B.15}$$

$$[\mathbf{B}]_{4\times8}=\begin{bmatrix} I_{44,0} & I_{44,0} & I_{44,2} & I_{44,2} & I_{44,1} & I_{44,1} & I_{44,3} & I_{44,3}\\ I_{44,2} & I_{44,2} & I_{44,4} & I_{44,4} & I_{44,3} & I_{44,3} & I_{44,5} & I_{44,5}\\ I_{44,1} & I_{44,1} & I_{44,3} & I_{44,3} & I_{44,2} & I_{44,2} & I_{44,4} & I_{44,4}\\ I_{44,3} & I_{44,3} & I_{44,5} & I_{44,5} & I_{44,4} & I_{44,4} & I_{44,6} & I_{44,6} \end{bmatrix} \tag{B.16}$$

$$[\mathbf{D}]_{4\times7}=\begin{bmatrix} I_{66,0} & I_{66,0} & 3I_{66,2} & 0 & 2I_{66,1} & I_{66,1} & I_{66,3}\\ I_{66,2} & I_{66,2} & 3I_{66,4} & 0 & 2I_{66,3} & I_{66,3} & I_{66,5}\\ I_{66,1} & I_{66,1} & 3I_{66,3} & 0 & 2I_{66,2} & I_{66,2} & I_{66,4}\\ I_{66,3} & I_{66,3} & 3I_{66,5} & 0 & 2I_{66,4} & I_{66,4} & I_{66,6} \end{bmatrix} \tag{B.17}$$

$$[\mathbf{D}']_{4\times7}=\begin{bmatrix} I_{56,0} & I_{56,0} & 3I_{56,2} & 0 & 2I_{56,1} & I_{56,1} & I_{56,3}\\ I_{56,2} & I_{56,2} & 3I_{56,4} & 0 & 2I_{56,3} & I_{56,3} & I_{56,5}\\ I_{56,1} & I_{56,1} & 3I_{56,3} & 0 & 2I_{56,2} & I_{56,2} & I_{56,4}\\ I_{56,3} & I_{56,3} & 3I_{56,5} & 0 & 2I_{56,4} & I_{56,4} & I_{56,6} \end{bmatrix} \tag{B.18}$$

$$[\mathbf{E}']_{4\times7}=\begin{bmatrix} I_{56,0} & I_{56,0} & 3I_{56,2} & 0 & 2I_{56,1} & I_{56,1} & I_{56,3}\\ I_{56,2} & I_{56,2} & 3I_{56,4} & 0 & 2I_{56,3} & I_{56,3} & I_{56,5}\\ I_{56,1} & I_{56,1} & 3I_{56,3} & 0 & 2I_{56,2} & I_{56,2} & I_{56,4}\\ I_{56,3} & I_{56,3} & 3I_{56,5} & 0 & 2I_{56,4} & I_{56,4} & I_{56,6} \end{bmatrix} \tag{B.19}$$

$$[\mathbf{E}]_{4\times7}=\begin{bmatrix} I_{55,0} & I_{55,0} & 3I_{55,2} & 0 & 2I_{55,1} & I_{55,1} & I_{55,3}\\ I_{55,2} & I_{55,2} & 3I_{55,4} & 0 & 2I_{55,3} & I_{55,3} & I_{55,5}\\ I_{55,1} & I_{55,1} & 3I_{55,3} & 0 & 2I_{55,2} & I_{55,2} & I_{55,4}\\ I_{55,3} & I_{55,3} & 3I_{55,5} & 0 & 2I_{55,4} & I_{55,4} & I_{55,6} \end{bmatrix} \tag{B.20}$$

B.4. Model-4 'HOSNT10B'

$$[\mathbf{A}]_{11\times11}=\begin{bmatrix} I_{11,0} & I_{12,0} & I_{11,2} & I_{12,2} & 0 & 0 & I_{11,1} & I_{12,1} & I_{11,3} & I_{12,3} & 2I_{13,1}\\ I_{12,0} & I_{22,0} & I_{12,2} & I_{22,2} & 0 & 0 & I_{12,1} & I_{22,1} & I_{12,3} & I_{22,3} & 2I_{23,1}\\ I_{11,2} & I_{12,2} & I_{11,4} & I_{12,4} & 0 & 0 & I_{11,3} & I_{12,3} & I_{11,5} & I_{12,5} & 2I_{13,3}\\ I_{12,2} & I_{22,2} & I_{12,4} & I_{22,4} & 0 & 0 & I_{12,3} & I_{22,3} & I_{12,5} & I_{22,5} & 2I_{23,3}\\ I_{13,0} & I_{23,0} & I_{13,2} & I_{23,2} & 0 & 0 & I_{13,1} & I_{23,1} & I_{13,3} & I_{23,3} & 2I_{33,1}\\ I_{13,2} & I_{23,2} & I_{13,4} & I_{23,4} & 0 & 0 & I_{13,3} & I_{23,3} & I_{13,5} & I_{23,5} & 2I_{33,3}\\ I_{11,1} & I_{12,1} & I_{11,3} & I_{12,3} & 0 & 0 & I_{11,2} & I_{12,2} & I_{11,4} & I_{12,4} & 2I_{13,2}\\ I_{12,1} & I_{22,1} & I_{12,3} & I_{22,3} & 0 & 0 & I_{12,2} & I_{22,2} & I_{12,4} & I_{22,4} & 2I_{23,2}\\ I_{11,3} & I_{12,3} & I_{11,5} & I_{12,5} & 0 & 0 & I_{11,4} & I_{12,4} & I_{11,6} & I_{12,6} & 2I_{13,4}\\ I_{12,3} & I_{22,3} & I_{12,5} & I_{22,5} & 0 & 0 & I_{12,4} & I_{22,4} & I_{12,6} & I_{22,6} & 2I_{23,4}\\ I_{13,1} & I_{23,1} & I_{13,3} & I_{23,3} & 0 & 0 & I_{13,2} & I_{23,2} & I_{13,4} & I_{23,4} & 2I_{33,2} \end{bmatrix} \tag{B.21}$$

$$[\mathbf{B}]_{4\times8}=\begin{bmatrix} I_{44,0} & I_{44,0} & I_{44,2} & I_{44,2} & I_{44,1} & I_{44,1} & I_{44,3} & I_{44,3}\\ I_{44,2} & I_{44,2} & I_{44,4} & I_{44,4} & I_{44,3} & I_{44,3} & I_{44,5} & I_{44,5}\\ I_{44,1} & I_{44,1} & I_{44,3} & I_{44,3} & I_{44,2} & I_{44,2} & I_{44,4} & I_{44,4}\\ I_{44,3} & I_{44,3} & I_{44,5} & I_{44,5} & I_{44,4} & I_{44,4} & I_{44,6} & I_{44,6} \end{bmatrix} \tag{B.22}$$

$$[\mathbf{D}]_{4\times7}=\begin{bmatrix} I_{66,0} & I_{66,0} & 3I_{66,2} & I_{66,2} & 2I_{66,1} & 0 & 0\\ I_{66,2} & I_{66,2} & 3I_{66,4} & I_{66,4} & 2I_{66,3} & 0 & 0\\ I_{66,1} & I_{66,1} & 3I_{66,3} & I_{66,3} & 2I_{66,2} & 0 & 0\\ I_{66,3} & I_{66,3} & 3I_{66,5} & I_{66,5} & 2I_{66,4} & 0 & 0 \end{bmatrix} \tag{B.23}$$

$$[\mathbf{E}]_{4\times7}=\begin{bmatrix} I_{55,0} & I_{55,0} & 3I_{55,2} & I_{55,2} & 2I_{55,1} & 0 & 0\\ I_{55,2} & I_{55,2} & 3I_{55,4} & I_{55,4} & 2I_{55,3} & 0 & 0\\ I_{55,1} & I_{55,1} & 3I_{55,3} & I_{55,3} & 2I_{55,2} & 0 & 0\\ I_{55,3} & I_{55,3} & 3I_{55,5} & I_{55,5} & 2I_{55,4} & 0 & 0 \end{bmatrix} \tag{B.24}$$

B.5. Model-5 'HOSNT10M'

$$[\mathbf{A}]_{11\times11}=\begin{bmatrix} I_{11,0} & I_{12,0} & I_{11,2} & I_{12,2} & I_{13,0} & 0 & I_{11,1} & I_{12,1} & I_{11,3} & I_{12,3} & 0\\ I_{12,0} & I_{22,0} & I_{12,2} & I_{22,2} & I_{23,0} & 0 & I_{12,1} & I_{22,1} & I_{12,3} & I_{22,3} & 0\\ I_{11,2} & I_{12,2} & I_{11,4} & I_{12,4} & I_{13,2} & 0 & I_{11,3} & I_{12,3} & I_{11,5} & I_{12,5} & 0\\ I_{12,2} & I_{22,2} & I_{12,4} & I_{22,4} & I_{23,2} & 0 & I_{12,3} & I_{22,3} & I_{12,5} & I_{22,5} & 0\\ I_{13,0} & I_{23,0} & I_{13,2} & I_{23,2} & I_{33,0} & 0 & I_{13,1} & I_{23,1} & I_{13,3} & I_{23,3} & 0\\ I_{13,2} & I_{23,2} & I_{13,4} & I_{23,4} & I_{33,2} & 0 & I_{13,3} & I_{23,3} & I_{13,5} & I_{23,5} & 0\\ I_{11,1} & I_{12,1} & I_{11,3} & I_{12,3} & I_{13,1} & 0 & I_{11,2} & I_{12,2} & I_{11,4} & I_{12,4} & 0\\ I_{12,1} & I_{22,1} & I_{12,3} & I_{22,3} & I_{23,1} & 0 & I_{12,2} & I_{22,2} & I_{12,4} & I_{22,4} & 0\\ I_{11,3} & I_{12,3} & I_{11,5} & I_{12,5} & I_{13,3} & 0 & I_{11,4} & I_{12,4} & I_{11,6} & I_{12,6} & 0\\ I_{12,3} & I_{22,3} & I_{12,5} & I_{22,5} & I_{23,3} & 0 & I_{12,4} & I_{22,4} & I_{12,6} & I_{22,6} & 0\\ I_{13,1} & I_{23,1} & I_{13,3} & I_{23,3} & I_{33,1} & 0 & I_{13,2} & I_{23,2} & I_{13,4} & I_{23,4} & 0 \end{bmatrix} \tag{B.25}$$

$$[\mathbf{B}]_{4\times8}=\begin{bmatrix} I_{44,0} & I_{44,0} & I_{44,2} & I_{44,2} & I_{44,1} & I_{44,1} & I_{44,3} & I_{44,3}\\ I_{44,2} & I_{44,2} & I_{44,4} & I_{44,4} & I_{44,3} & I_{44,3} & I_{44,5} & I_{44,5}\\ I_{44,1} & I_{44,1} & I_{44,3} & I_{44,3} & I_{44,2} & I_{44,2} & I_{44,4} & I_{44,4}\\ I_{44,3} & I_{44,3} & I_{44,5} & I_{44,5} & I_{44,4} & I_{44,4} & I_{44,6} & I_{44,6} \end{bmatrix} \tag{B.26}$$

$$[\mathbf{D}]_{4\times7}=\begin{bmatrix} I_{66,0} & I_{66,0} & 3I_{66,2} & 0 & 2I_{66,1} & I_{66,1} & 0\\ I_{66,2} & I_{66,2} & 3I_{66,4} & 0 & 2I_{66,3} & I_{66,3} & 0\\ I_{66,1} & I_{66,1} & 3I_{66,3} & 0 & 2I_{66,2} & I_{66,2} & 0\\ I_{66,3} & I_{66,3} & 3I_{66,5} & 0 & 2I_{66,4} & I_{66,4} & 0 \end{bmatrix} \tag{B.27}$$

$$[\mathbf{E}]_{4\times7}=\begin{bmatrix} I_{55,0} & I_{55,0} & 3I_{55,2} & 0 & 2I_{55,1} & I_{55,1} & 0\\ I_{55,2} & I_{55,2} & 3I_{55,4} & 0 & 2I_{55,3} & I_{55,3} & 0\\ I_{55,1} & I_{55,1} & 3I_{55,3} & 0 & 2I_{55,2} & I_{55,2} & 0\\ I_{55,3} & I_{55,3} & 3I_{55,5} & 0 & 2I_{55,4} & I_{55,4} & 0 \end{bmatrix} \tag{B.28}$$

B.6. Model-6 'HOST9'

$$[\mathbf{A}]_{11\times11}=\begin{bmatrix} I_{11,0} & I_{12,0} & I_{11,2} & I_{12,2} & 0 & 0 & I_{11,1} & I_{12,1} & I_{11,3} & I_{12,3} & 0\\ I_{12,0} & I_{22,0} & I_{12,2} & I_{22,2} & 0 & 0 & I_{12,1} & I_{22,1} & I_{12,3} & I_{22,3} & 0\\ I_{11,2} & I_{12,2} & I_{11,4} & I_{12,4} & 0 & 0 & I_{11,3} & I_{12,3} & I_{11,5} & I_{12,5} & 0\\ I_{12,2} & I_{22,2} & I_{12,4} & I_{22,4} & 0 & 0 & I_{12,3} & I_{22,3} & I_{12,5} & I_{22,5} & 0\\ I_{13,0} & I_{23,0} & I_{13,2} & I_{23,2} & 0 & 0 & I_{13,1} & I_{23,1} & I_{13,3} & I_{23,3} & 0\\ I_{13,2} & I_{23,2} & I_{13,4} & I_{23,4} & 0 & 0 & I_{13,3} & I_{23,3} & I_{13,5} & I_{23,5} & 0\\ I_{11,1} & I_{12,1} & I_{11,3} & I_{12,3} & 0 & 0 & I_{11,2} & I_{12,2} & I_{11,4} & I_{12,4} & 0\\ I_{12,1} & I_{22,1} & I_{12,3} & I_{22,3} & 0 & 0 & I_{12,2} & I_{22,2} & I_{12,4} & I_{22,4} & 0\\ I_{11,3} & I_{12,3} & I_{11,5} & I_{12,5} & 0 & 0 & I_{11,4} & I_{12,4} & I_{11,6} & I_{12,6} & 0\\ I_{12,3} & I_{22,3} & I_{12,5} & I_{22,5} & 0 & 0 & I_{12,4} & I_{22,4} & I_{12,6} & I_{22,6} & 0\\ I_{13,1} & I_{23,1} & I_{13,3} & I_{23,3} & 0 & 0 & I_{13,2} & I_{23,2} & I_{13,4} & I_{23,4} & 0 \end{bmatrix} \tag{B.29}$$

$$[\mathbf{B}]_{4\times 8}=\begin{bmatrix} I_{44,0} & I_{44,0} & I_{44,2} & I_{44,2} & I_{44,1} & I_{44,1} & I_{44,3} & I_{44,3}\\ I_{44,2} & I_{44,2} & I_{44,4} & I_{44,4} & I_{44,3} & I_{44,3} & I_{44,5} & I_{44,5}\\ I_{44,1} & I_{44,1} & I_{44,3} & I_{44,3} & I_{44,2} & I_{44,2} & I_{44,4} & I_{44,4}\\ I_{44,3} & I_{44,3} & I_{44,5} & I_{44,5} & I_{44,4} & I_{44,4} & I_{44,6} & I_{44,6}\end{bmatrix} \tag{B.30}$$

$$[\mathbf{D}]_{4\times 7}=\begin{bmatrix} I_{66,0} & I_{66,0} & 3I_{66,2} & 0 & 2I_{66,1} & 0 & 0\\ I_{66,2} & I_{66,2} & 3I_{66,4} & 0 & 2I_{66,3} & 0 & 0\\ I_{66,1} & I_{66,1} & 3I_{66,3} & 0 & 2I_{66,2} & 0 & 0\\ I_{66,3} & I_{66,3} & 3I_{66,5} & 0 & 2I_{66,4} & 0 & 0\end{bmatrix} \tag{B.31}$$

$$[\mathbf{E}]_{4\times 7}=\begin{bmatrix} I_{55,0} & I_{55,0} & 3I_{55,2} & 0 & 2I_{55,1} & 0 & 0\\ I_{55,2} & I_{55,2} & 3I_{55,4} & 0 & 2I_{55,3} & 0 & 0\\ I_{55,1} & I_{55,1} & 3I_{55,3} & 0 & 2I_{55,2} & 0 & 0\\ I_{55,3} & I_{55,3} & 3I_{55,5} & 0 & 2I_{55,4} & 0 & 0\end{bmatrix} \tag{B.32}$$

B.7. Model-7 'FOST'

$$\begin{Bmatrix} M_x\\ M_y\\ M_{xy}\\ N_x\\ N_y\\ N_{xy}\\ Q_x\\ Q_y\end{Bmatrix}_{8\times 1}=\begin{bmatrix} I_{11,1} & I_{12,1} & 0 & I_{11,2} & I_{12,2} & 0 & 0 & 0\\ I_{12,1} & I_{22,1} & 0 & I_{12,2} & I_{22,2} & 0 & 0 & 0\\ 0 & 0 & I_{33,1} & 0 & 0 & I_{33,2} & 0 & 0\\ I_{11,0} & I_{12,0} & 0 & I_{11,1} & I_{12,1} & 0 & 0 & 0\\ I_{12,0} & I_{22,0} & 0 & I_{12,1} & I_{22,1} & 0 & 0 & 0\\ 0 & 0 & I_{33,0} & 0 & 0 & I_{33,1} & 0 & 0\\ 0 & 0 & 0 & 0 & 0 & 0 & k_sI_{33,0} & 0\\ 0 & 0 & 0 & 0 & 0 & 0 & 0 & k_sI_{33,0}\end{bmatrix}_{8\times 8}\begin{Bmatrix} \frac{\partial u_0}{\partial x}\\ \frac{\partial v_0}{\partial y}\\ \frac{\partial u_0}{\partial y}+\frac{\partial v_0}{\partial x}\\ \frac{\partial \theta_x}{\partial x}\\ \frac{\partial \theta_y}{\partial y}\\ \frac{\partial \theta_x}{\partial y}+\frac{\partial \theta_y}{\partial x}\\ \theta_x+\frac{\partial w_0}{\partial x}\\ \theta_y+\frac{\partial w_0}{\partial y}\end{Bmatrix}_{8\times 1} \tag{B.33}$$

where k_s = Shear correction factor.

B.8. Model-8 'CPT'

$$\begin{Bmatrix} M_x\\ M_y\\ M_{xy}\\ N_x\\ N_y\\ N_{xy}\end{Bmatrix}_{6\times 1}=\begin{bmatrix} I_{11,1} & I_{12,1} & 0 & I_{11,2} & I_{12,2} & 0\\ I_{12,1} & I_{22,1} & 0 & I_{12,2} & I_{22,2} & 0\\ 0 & 0 & I_{33,1} & 0 & 0 & I_{33,2}\\ I_{11,0} & I_{12,0} & 0 & I_{11,1} & I_{12,1} & 0\\ I_{12,0} & I_{22,0} & 0 & I_{12,1} & I_{22,1} & 0\\ 0 & 0 & I_{33,0} & 0 & 0 & I_{33,1}\end{bmatrix}_{6\times 6}\begin{Bmatrix} \frac{\partial u_0}{\partial x}\\ \frac{\partial v_0}{\partial y}\\ \frac{\partial u_0}{\partial y}+\frac{\partial v_0}{\partial x}\\ -\frac{\partial^2 w_0}{\partial x^2}\\ -\frac{\partial^2 w_0}{\partial y^2}\\ -2\frac{\partial^2 w_0}{\partial x\partial y}\end{Bmatrix}_{6\times 1} \tag{B.34}$$

in which,

$$I_{ij,k}=\int_{-h/2}^{+h/2}Q_{ij}z^k dz \tag{B.35}$$

As structural reference axes (x,y,z) of the FG plate coincide with the principal material axes $(1,2,3)$ of the FG plate, thus;

$$\begin{aligned} &Q_{11}=C_{11}, Q_{12}=C_{12}, Q_{13}=C_{13}, Q_{22}=C_{22}, Q_{23}=C_{23}\\ &Q_{33}=C_{33}, Q_{44}=C_{44}, Q_{55}=C_{55}, Q_{66}=C_{66}\\ &Q_{14}=Q_{24}=Q_{34}=Q_{56}=0\end{aligned} \tag{B.36}$$

Appendix C. Elements of coefficient matrix [X] in Eq. (14) for various displacement models

See Tables C1–C8.

Appendix D. Elements of mass matrix [M] in Eq. (14) for various displacement models

See Tables D1–D8.

References

[1] Koizumi M. FGM activities in Japan. Composites: Part B 1997;28:1–4.
[2] Suresh S, Mortensen A. Fundamentals of functionally graded materials. 1st ed. London: IOM Communications; 1998.
[3] Birman V, Byrd LW. Modeling and analysis of functionally graded materials and structures. ASME Appl Mech Rev 2007;60:195–216.
[4] Jha DK, Kant Tarun, Singh RK. A critical review of recent research on functionally graded plates. Compos Struct 2013;96:833–49.
[5] Pagano NJ. Exact solutions for composite laminates in cylindrical bending. J Compos Mater 1969;3(3):398–411.
[6] Pagano NJ. Exact solutions for rectangular bidirectional composites and sandwich plates. J Compos Mater 1970;4(1):20–34.
[7] Srinivas S, Rao AK. Bending, vibration and buckling of simply supported thick orthotropic plates and laminates. Int J Solids Struct 1970;6:1463–81.
[8] Srinivas S, Joga Rao CV, Rao AK. An exact analysis for vibration of simply supported homogeneous and laminated thick rectangular plates. J Sound Vib 1970;12:187–99.
[9] Pandya BN, Kant T. Higher-order shear deformable theories for flexure of sandwich plates-finite element evaluations. Int J Solids Struct 1988;24(12):1267–86.
[10] Kant T, Manjunatha BS. On accurate estimation of transverse stresses in multilayer laminates. Comput Struct 1994;50(3):351–65.
[11] Reddy JN. Mechanics of laminated composite plates, theory and analysis. 1st ed. New York: CRC Press; 1997.
[12] Cheng ZQ, Batra RC. Exact correspondence between eigenvalues of membranes and functionally graded simply supported polygonal plates. J Sound Vib 2000;229:879–95.
[13] Kim Y-W. Temperature dependent vibration analysis of functionally graded rectangular plates. J Sound Vib 2005;284:531–49.
[14] Vel SS, Batra RC. Three-dimensional exact solution for the vibration of functionally graded rectangular plates. J Sound Vib 2004;272:703–30.
[15] Zenkour AM. A comprehensive analysis of functionally graded sandwich plates: part 2 – buckling and free vibration. Int J Solids Struct 2005;42:5243–58.
[16] Ferreira AJM, Batra RC, Roque CMC, Qian LF, Jorge RMN. Natural frequencies of functionally graded plates by a meshless method. Compos Struct 2006;75:593–600.
[17] Qian LF, Batra RC, Chen LM. Analysis of cylindrical bending thermoelastic deformations of functionally graded plates by a meshless local Petrov–Galerkin method. Comput Mech 2004;33:263–73.
[18] Prakash T, Ganapathi M. Asymmetric flexural vibration and thermoelastic stability of FGM circular plates using finite element method. Composites: Part B 2006;37:642–9.
[19] Bhangale RK, Ganesan N. Free vibration of simply supported functionally graded and layered magneto-electro-elastic plates by finite element method. J Sound Vib 2006;294:1016–38.
[20] Matsunaga H. Free vibration and stability of functionally graded plates according to a 2-D higher-order deformation theory. Compos Struct 2008;82:499–512.
[21] Ebrahimi F, Rastgoo A. An analytical study on the free vibration of smart circular thin FGM plate based on classical plate theory. Thin-Wall Struct 2008;46:1402–8.
[22] Liu DY, Wang CY, Chen WQ. Free vibration of FGM plates with in-plane material inhomogeneity. Compos Struct 2010;92:1047–51.
[23] Shahrjerdi A, Mustapha F, Bayat M, Sapuan SM, Zahari R, Shahzamanian MM. Natural frequency of F.G. rectangular plate by shear deformation theory. IOP Conf Ser: Mater Sci Eng 2011;17(1):1–6.
[24] Kumar JS, Reddy BS, Reddy CE, Reddy KVK. Higher order theory for free vibration analysis of functionally graded material plates. ARPN J Eng Appl Sci 2011;6:105–11.
[25] Benachour A, Tahar HD, Atmane HA, Tounsi A, Ahmed MS. A four variable refined plate theory for free vibrations of functionally graded plates with arbitrary gradient. Composites: Part B 2011;42:1386–94.
[26] Xiang S, Jin YX, Bi ZY, Jiang SX, Yang MS. A n-order shear deformation theory for free vibration of functionally graded and composite sandwich plates. Compos Struct 2011;93:2826–32.
[27] Neves AMA, Ferreira AJM, Carrera E, Roque CMC, Cinefra M, Jorge RMN, et al. A quasi-3D sinusoidal shear deformation theory for the static and free vibration analysis of functionally graded plates. Composites: Part B 2012;43:711–25.
[28] Neves AMA, Ferreira AJM, Carrera E, Roque CMC, Cinefra M, Jorge RMN, et al. A quasi-3D hyperbolic shear deformation theory for the static and free vibration analysis of functionally graded plates. Compos Struct 2012;94(5):1814–25.
[29] Whitney JM, Pagano NJ. Shear deformation in heterogeneous anisotropic plates. ASME J Appl Mech 1970;37:1031–6.
[30] Timoshenko SP, Woinowsky-Krieger S. Theory of plates and shells. 2nd edn. Singapore: McGraw-Hill; 1959.
[31] Timoshenko SP, Goodier JN. Theory of elasticity. 3rd international edn. Singapore: McGraw-Hill; 1970.

[32] Praveen GN, Reddy JN. Nonlinear transient thermoelastic analysis of functionlly graded ceramic-metal plates. Int J Solids Struct 1998;35:4457–71.
[33] Senthilnathan NR, Lim KH, Lee KH, Chow ST. Buckling of shear-deformable plates. AIAA J 1987;25:1268–71.
[34] Shimpi RP. Refined plate theory and its variants. AIAA J 2002;40:137–46.
[35] Shimpi RP, Patel HG. A two variable refined plate theory for orthotropic plate analysis. Int J Solids Struct 2006;43:6783–99.
[36] Reisman H, Lee YC. Forced motions of rectangular plates. Develop Theor Appl Mech 1969;4:3.
[37] Kant T, Reddy SK. Private communication; 2012.